ABSTRACT

Title of Document: SENSITIVITY ANALYSIS BASED APPROACHES FOR MITIGATING THE EFFECTS OF REDUCIBLE INTERVAL INPUT UNCERTAINTY ON SINGLE- AND MULTI-DISCIPLINARY SYSTEMS USING MULTI-OBJECTIVE OPTIMIZATION

Joshua M. Hamel, Doctor of Philosophy, 2010

Directed By: Shapour Azarm, Professor,
Department of Mechanical Engineering

Uncertainty is an unavoidable aspect of engineering systems and will often degrade system performance or perhaps even lead to system failure. As a result, uncertainty must be considered as a part of the design process for all real-world engineering systems. The presence of reducible uncertainty further complicates matters as designers must not only account for the degrading effects of uncertainty but must also determine what levels of uncertainty can be considered as acceptable. For these reasons, methods for determining and effectively mitigating the effects of uncertainty are necessary for solving engineering design problems. This dissertation presents several new methods for use in the design of engineering systems under interval input uncertainty. These new approaches were developed over the course of four interrelated research thrusts and focused on the overall goal of extending the current research in the area of sensitivity analysis based design under reducible interval uncertainty. The first research thrust focused on developing an

approach for determining optimal uncertainty reductions given multi-disciplinary engineering systems with multiple output functions at both the system and sub-system levels. The second research thrust extended the approach developed during the first thrust to use uncertainty reduction as a means for both reducing output variations and simultaneously ensuring engineering feasibility. The third research thrust looked at systems where uncertainty reduction alone is insufficient for ensuring feasibility and thus developed a sensitivity analysis approach that combined uncertainty reductions with small design adjustments in an effort to again reduce output variations and ensure feasibility. The fourth and final research thrust looked to relax many of the assumptions required by the first three research thrusts and developed a general sensitivity analysis inspired approach for determining optimal upper and lower bounds for reducible sources of input uncertainty. Multi-objective optimization techniques were used throughout this research to evaluate the tradeoffs between the benefits to be gained by mitigating uncertainty with the costs of making the design changes and/or uncertainty reductions required to reduce or eliminate the degrading effects of system uncertainty most effectively. The validity of the approaches developed were demonstrated using numerical and engineering example problems of varying complexity.

SENSITIVITY ANALYSIS BASED APPROACHES FOR MITIGATING THE EFFECTS OF REDUCIBLE INTERVAL INPUT UNCERTAINTY ON SINGLE- AND MULTI-DISCIPLINARY SYSTEMS USING MULTI-OBJECTIVE OPTIMIZATION

By

Joshua M. Hamel

Dissertation submitted to the Faculty of the Graduate School of the
University of Maryland, College Park, in partial fulfillment
of the requirements for the degree of
Doctor of Philosophy
2010

Advisory Committee:
Professor Shapour Azarm, Advisor and Chair
Professor P.K. Kannan, Dean's Representative
Professor Ali Mosleh
Associate Professor Linda Schmidt
Assistant Professor Byeng Dong Youn

To Jillian, for this would not have been possible without

your unwavering love and support.

ACKNOWLEDGEMENTS

I would like to thank my advisor Dr. Shapour Azarm, who had confidence in me when I did not think it was merited, who expertly applied pressure when necessary and who built me up when I needed it most. Through your example and timely advice you have taught me how to be a college professor and I hope to follow in your footsteps.

Thank you to my dissertation committee members, Dr. Kannan, Dr. Mosleh, Dr. Schmidt and Dr. Youn, for their support and wise comments throughout my studies.

A special thanks to Dr. Mian Li for all your help, guidance and advice throughout my doctoral studies. You are a gifted researcher and I have learned a great deal through our collaborations and our friendship.

I would also like to thank my colleagues at the U.S. Naval Academy, particularly Dr. Keith Lindler, CAPT Len Hamilton, CDR Joe Watkins, Rich Herron and Ethan Lust for their advice throughout my studies and for helping me to serve two masters.

Thank you to Nate Williams for introducing me to Dr. Azarm in the summer of 2007 and for encouraging me to take on this endeavor.

I would like to thank the Office of Naval Research for their partial support of this work through grant # N000140910035. Such support does not constitute an endorsement by the Office of Naval Research of the opinions expressed in this thesis.

I lastly would like to thank my family, particularly my wonderful wife Jillian, for standing by me throughout this process. I would not have embarked on this path without your blessing, I would probably have quit many times without your support and I would most likely have gone crazy without your love, perspective and encouragement.

TABLE OF CONTENTS

NOMENCLATURE

C	Input parameter control coefficient
$d_{L,k}$	Distance from anchor point to lower bound on p_k
$d_{U,k}$	Distance from anchor point to upper bound on p_k
D_{shell}	Shell diameter (heat exchanger problem)
E	Young's modulus (tube problem)
F	Load on tube (tube problem)
$\boldsymbol{f_A}^{(m)}$	m^{th} anchor point
f_i	i^{th} objective function
$f_{i,bad}$	Constant scaling factor on the i^{th} objective
$f_{i,good}$	Constant scaling factor on the i^{th} objective
$f_{i,max}$	Max value of the i^{th} objective on $p_{\text{L}} \le p_{\text{U}}$
$f_{i,min}$	Min value of the i^{th} objective on $p_{\text{L}} \le p_{\text{U}}$
g_j	j^{th} constraint function
$g_{j,max}$	Max value of the j^{th} constraint on $p_{\text{L}} \le p_{\text{U}}$
h	Tube height (tube problem)
I	Abbreviation for *Investment*, a cost metric
$\hat{I}$	Cost metric calculated via meta-models of analysis functions
I_p	Input uncertainty level control metric
id_{tube}	Internal tube diameter (heat exchanger problem)
L_{shell}	Shell length (heat exchanger problem)
M	Number of anchor points, $m = 1,\ldots,M$
$\dot{m}$	Mass flow rate (heat exchanger problem)
n_{tubes}	Number of tubes (heat exchanger problem)
o	Generic output function
$\boldsymbol{p_A}^{(m)}$	m^{th} anchor point
$p_{L,k}$	Specified lower bound on the k^{th} uncertain input parameter
$p_{lb,k}$	Extreme lower bound on the k^{th} uncertain input parameter
p_k	k^{th} input parameter
$p_{U,k}$	Upper bound on k^{th} uncertain input parameter
$p_{ub,k}$	Extreme upper bound on the k^{th} uncertain input parameter
$p_{v,k}$	Realization of uncertain p_k bounded by $p_{U,k}$ and $p_{L,k}$
$\dot{Q}$	Heat transfer rate (heat exchanger problem)
R	General output function variation(s) (Chapter 3)
R	Tube radius (tube problem in Chapters 5 and 6)

R_c	Combined objective and constraint function variation(s)
R_f	Objective function variation(s)
$\hat{R}_f$	Objective uncertainty calculated via meta-models of objective functions $\boldsymbol{f}$
R_g	Constraint function variation(s)
$\hat{R}_g$	Constraint uncertainty calculated via meta-models of constraint functions $\boldsymbol{g}$
SSi	Sub-system i in and multidisciplinary problem, $i = 0,1,2, \ldots, I$
s_{tubes}	Internal tube spacing (heat exchanger problem)
T	Temperature (heat exchanger problem)
t	Tube wall thickness (tube problem in Chapters 5 and 6)
t	Target variables (in Chapters 3 and 4)
V_f	Objective function variation metric
V_g	Constraint function variation metric
w	Weighting values in I_p and I metrics
x	Design variables
XX_0	Subscript denoting nominal solution (e.g. p_0, f_0, g_0)
XX_{Sh}	Subscript denoting shared parameter
y	Shared design variables
Y	Coupling function
α	Parameter uncertainty reduction vector
β	Parameter adjustment vector
Δf_i	Difference between $f_{i,max}$ and $f_{i,min}$
ΔP	Pressure drop (heat exchanger problem)
Δp_k	Uncertainty interval for the k^{th} parameter
δp_k	Maximum parameter adjustment value for the k^{th} parameter
ε	Designer selected limit(s) on RUID objective(s)
η	Maximum deviation of shared parameter values from target values
θ	Weighting values in *Investment* metric
σ_{max}	Maximum stress (tube problem)

LIST OF TABLES

LIST OF FIGURES

CHAPTER 1: INTRODUCTION

1.1 RESEARCH MOTIVATION

In recent years the design research community has become increasingly focused on solving the problems presented by uncertain input parameters to design methods and algorithms [Martin and Simpson, 2006; Moeller and Beer, 2008; Schueller and Jensen, 2008; Lee and Chen, 2009]. Design algorithms, such as design optimization, involve selecting (or determining) the physical parameters that define the characteristics of an engineering system [Deb, 2001; Arora, 2004; Aute and Azarm, 2006]. When dealing with any physical parameter there is always the possibility that the exact dimensions/characteristics of that parameter cannot be known with absolute certainty, regardless of how tightly a machining or fabrication tolerance can be controlled. As a result, uncertainty is an unavoidable aspect of any engineering system and may lead to poor system performance and/or unexpected system failure if not adequately accounted for during the design process [Jung and Lee, 2002; Li and Azarm, 2008]. However, understanding and mitigating the effects of uncertainty on the design of engineering systems is a complex problem, especially when faced with computationally expensive real world engineering design problems comprised of multiple engineering disciplines [Du and Chen, 2005; Chiralaksanakul and Mahadevan, 2007].

Figure 1.1 depicts just such a system. Clearly the design of a helicopter is a complex engineering challenge that involves designing many physically coupled systems, including the fuselage itself, the engines, and the flight control computer that communicates with the engines; just to name a few. Furthermore, designing these systems could involve numerous distinct computational models, such as a finite element

analysis (FEA) model to predict the behavior of the engine's turbine blades and a computational fluid dynamics (CFD) model to understand the properties of the flow of air through the engine. Clearly all these systems and sub-systems are highly coupled and any uncertainty in one system will invariably affect the design of the other coupled sub-systems or disciplines. There are many important questions about the effects of uncertainty on these types of systems that a designer would like to answer, such as: Which uncertain parameters have the greatest effect on the performance of the entire system? Which sub-systems are most important to the overall performance of the system? If the helicopter needs to be as light as possible with as much lifting force as possible, should the engines be designed better or should the fuselage itself be more carefully addressed? How much uncertainty in any given parameter of the helicopter's design should be considered acceptable? How best should limited uncertainty reduction and design adjustment resources be allocated during the design process in order to best mitigate the potentially damaging effects of system uncertainties? These are the types of questions the work presented in this dissertation has attempted to address.

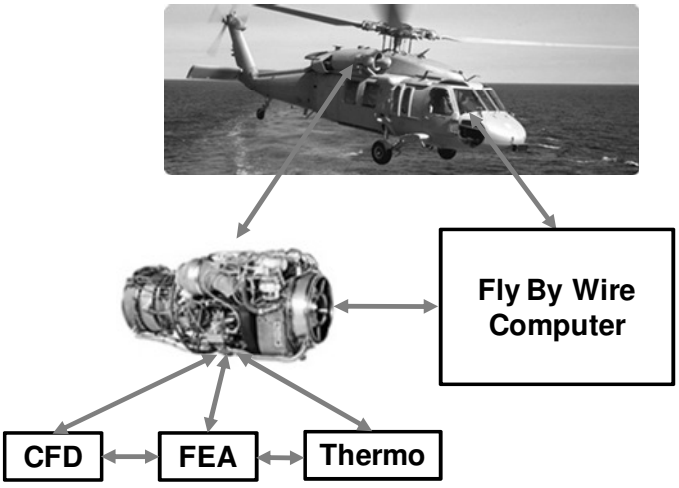

Figure 1.1: A Multi-Disciplinary System

1.2 RELEVANT RELATED RESEARCH: AN OVERVIEW

1.2.1 Uncertainty Overview

Generally speaking there are two different types of uncertainty in input parameters: irreducible and reducible [Guo and Du, 2007]. Irreducible uncertain parameters include any uncertain factor or parameter that a designer cannot control, influence, prescribe or reduce further, even if more information is obtained. A material property, such as density, is an example of an irreducible uncertain parameter due to the natural variations in the material. Reducible uncertainty on the other hand describes any uncertain parameter that a designer can control the level of uncertainty in through the specification of a tolerance, through the purchase of higher quality equipment, or through the collection of more statistical information. These two types of uncertainty can be quantified in one of three ways, either through probability distributions [Gunawan and Papalambros, 2007; Noh et al., 2008; Youn and Wang, 2008], through imprecise probabilities (e.g. [Mourelatos and Zhou, 2006; Zhou and Mourelatos, 2008]) or by simple upper and lower bounds (interval uncertainty) [Du, 2007; Wu and Rao, 2007; Li et al., 2009a]. At present, two distinct strategies have been used to manage input parameter uncertainty: robust design approaches [Beyer and Sendhoff, 2007] or Sensitivity Analysis (SA) approaches [Fiacco, 1983; Saltelli et al., 2000; Helton and Davis, 2003], both of which have their strengths and weaknesses.

1.2.2 Robust Approaches

Robust design approaches are most appropriate when uncertainty is irreducible and are excellent for ensuring the feasibility of an engineering system; thus preventing system failure due to uncertainty. It should be noted that robust approaches cannot be counted on to find that a desired preexisting design of interest for a system will be robust (or insensitive to uncertainty) and thus will most likely suggest alternate designs, which may not be something a designer is interested in for certain design problems. This is because robust approaches traditionally search over a wide range of potential designs in an effort to find the best design that is insensitive to the uncertainty in the system [Gunawan and Azarm, 2005; Lee, 2006]. For example, if the designer of the engines for the helicopter system shown in Figure 1.1 chose to use a robust approach to mitigate the effects of uncertainty, the key design parameters such as output horsepower and output shaft diameter will likely be changed in order to ensure insensitivity to uncertainty in order to accomplish that goal. More specific examples of robust methods are Robust Optimization (RO) [Yu and Ishii, 1998; Gu et. al, 2006; Du and Choi, 2006; Apley et al., 2006; Li and Azarm, 2008] and Reliability Based Design Optimization (RBDO) [Gunawan and Papalambros, 2006; Choi et al, 2008; Jung and Lee, 2008; Noh et al., 2008; Youn and Wang, 2008]. There are currently robust approaches specifically formulated for probabilistic uncertainty [e.g. Youn and Wang, 2008], imprecise probabilities [e.g. Zhou and Mourelatos, 2008] and interval uncertainty quantification [e.g. Li et al., 2007]. These approaches all treat input uncertainties as uncontrollable aspects of the system that must be designed around, which is why they are well-suited to systems where all sources of uncertainty can be safely assumed to be irreducible.

However, in many cases some uncertainty sources may very well be reducible and the presence of reducible uncertainty in a system design will undoubtedly present additional challenges. More often than not better machining processes, more expensive equipment and/or tighter tolerances could all reduce the uncertainty in a system and thus result in better system performance and a reduced potential for failure. Clearly all of these options for uncertainty reduction can and will increase the overall cost of the system design. For the system in Figure 1.1, the designer of the engines could select the best possible (and most expensive) thermocouples available on the market for use in monitoring engine temperatures as precisely as possible. However, would the resulting increased cost associated with those expensive thermocouples be necessary to achieving the overall goals and objectives of the system as a whole, or could those resources be better spent on some other aspect of the design? Designers would obviously like to know how best to spend limited resources, thus achieving the best possible performance of a system under uncertainty given the lowest possible cost, without the fear that money and resources have been wasted on over engineering non-critical sub-systems or parameters.

For the most part robust approaches in the literature are not able to assist designers faced with these types of decisions about reducible uncertainty. RBDO approaches have been developed that allow for the inclusion of additional statistical information should it become available as a means for considering reducible uncertainty [Gunawan and Papalambros, 2006; Youn and Wang, 2008]. Other approaches combine uncertainty reduction mechanisms with RBDO techniques, either through sequentially performing reliability-based design optimization followed by uncertainty reduction [Qu et al., 2003], or through simultaneously considering reliability and uncertainty reduction mechanisms

during the design process [Kale and Haftka, 2008]. There are also approaches presented in the literature that suggest treating the variance in an uncertain parameter as a factor to control within an RBDO algorithm provided a designer has a means for producing lower variance in input parameters [Benanzer et al., 2009]. However, the above approaches all require probabilistic information or imprecise probabilities for uncertainty quantification, which may be unavailable, undesirable or invalid when statistical information is not available or too expensive to obtain early in a design process.

1.2.3 Sensitivity Analysis Approaches

Sensitivity analysis (SA) based approaches are often better suited to finding opportunities for reducing any uncertainty levels in an engineering system design that are known to be reducible [Greenland, 2001; Acar et al., 2007; Wu and Rao, 2007; Li et al., 2009a]. This is because sensitivity analysis simply provides a designer with information relating output variation to input uncertainty. That information can then be used to drive uncertainty reduction decisions if desired. SA based approaches are also very useful when a designer is interested in the effects of uncertainty on a predetermined design of interest [Iman and Helton, 1988; Sobieszczanski-Sobieski, 1990]. If SA is used to analyze the design of the engine in Figure 1.1, the nominal values of the output power and shaft diameter are more likely to remain largely unchanged for a preexisting design of interest when using SA. This is because SA based approaches can provide a designer with information about the system that can be used to mitigate uncertainty in another manner. SA approaches can be classified as either local or global. Local SA approaches relate the variation in the outputs of a system to small uncertainty in the system inputs [Hamby, 1994; Frey and Patil, 2002; Kern et al., 2003], which is only valid for limited

levels of uncertainty. On the contrary, global SA approaches [Saltelli et al., 2008] account for the entire range of input uncertainty and determines the effects of input uncertainty on system outputs. Most of the SA approaches reported in the literature focus on probabilistic uncertainty quantification [e.g. Acar et al., 2007; Castillo et al., 2008; Du, 2008], in part because the acquisition of more data can often be used to reduce uncertainty in a probabilistic sense. However, some attempts have been made to apply SA based approaches to systems possessing interval uncertainty [Wu and Rao, 2007; Li et al., 2009a; Li et al., 2009b]. Sensitivity analysis techniques are ideally suited to relate system performance variation (and/or system failure) to input uncertainty. However, there are not many SA based approaches that can then also determine the design changes and/or uncertainty reductions required to improve the performance (or eliminate the possibility of failure) of a design under uncertainty, with Li's work being the only major exception [Li et al., 2009a, Li et al., 2009b].

1.2.4 Multi-Disciplinary Approaches

Much of the work done in this area of design under uncertainty has focused on single disciplinary engineering systems, including both robust approaches [Crespo et al., 2008] and SA approaches [Helton and Davis, 2003]. Furthermore, SA approaches capable of handling multiple system outputs are relatively rare in the literature [Barron and Schmidt, 1988; Zhang, 2003; Li et al., 2009a]. However, engineering systems of interest will possess multiple design goals (or objectives) and will most certainly be comprised of many different disciplines. As discussed above in the helicopter engine example, those multiple disciplines could be in the form of coupled computational models, such as an FEA model for a structure and a CFD model for analyzing the drag

forces on the structure. Alternately, the multiple disciplines could be in the form of geometrically coupled but distinct sub-systems of a greater engineering system, such as the motor and battery modules that comprise the design of a power tool which are to be designed by different teams possibly in different geographic locations.

1.3 RESEARCH FOCUS AND KEY ASSUMPTIONS

The work presented in this dissertation has sought to address many of the shortcomings of the current research in the area of design under uncertainty as described in the previous section. The overall goal of this work has been to provide designers with sensitivity analysis based algorithms for understanding and then optimally mitigating the effects of input uncertainty on single and multi-disciplinary engineering systems that are as computationally efficient as possible. In order to achieve this goal the research presented in this dissertation has focused on the following five key areas and their corresponding assumptions.

Sensitivity Analysis (SA): As described previously, SA based approaches are effective tools for better understanding the effects of uncertainty on a preexisting design. However, most SA based approaches currently in the literature are simply tools for gaining greater insight into the effects of uncertainty on an engineering system. As a result, it is then up to the designer how best to proceed using any newly gained insight. Much of the work presented in this dissertation combines SA with multi-objective optimization techniques to provide a designer both with greater insight into the effects of uncertainty and more importantly with options for how best to adjust any available degrees of freedom in the system to mitigate the effects of uncertainty. As such, much of the research presented in this dissertation has assumed that a preexisting design for an

engineering system of interest exists and is known to possess uncertain input parameters. Figure 1.2 depicts the general capability of SA, which is to relate output variations to input uncertainties.

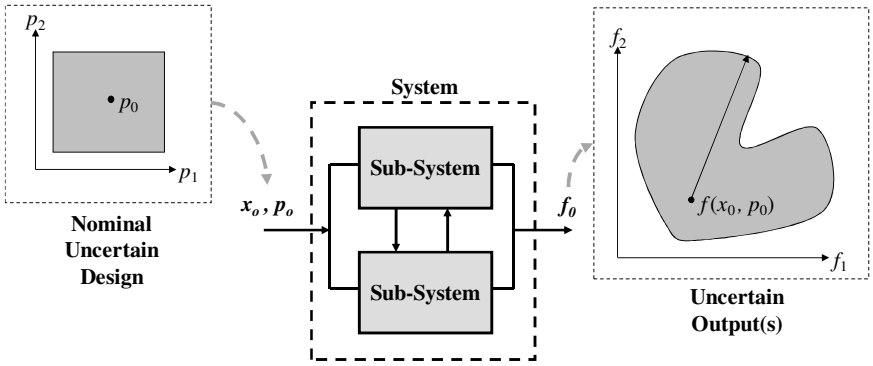

Figure 1.2: Sensitivity Analysis

Engineering Feasibility: Perhaps the most important effect of uncertainty that needs to be mitigated in any engineering design effort is the potential for system failure due to uncertainty. This concept of engineering failure when placed in the context of engineering optimization is also known as infeasibility. Previous work in the area of sensitivity analysis has focused on reducing variations in system outputs but there have only been limited efforts to address system failure specifically. This work has focused specifically on this key area in engineering design and how sensitivity analysis can be used to ensure engineering feasibility, in both single and multi-disciplinary systems.

Interval Uncertainty: While probability distributions are not always available for uncertain parameters (and obtaining such information is often quite expensive, if even possible), interval uncertainty levels are often much easier to determine and/or estimate. For this reason the sensitivity analysis based work presented in this dissertation has focused exclusively on interval uncertainty in an effort to be as general (and easy to

implement) as possible. Note that this work has focused on system input parameter uncertainty and does not specifically address any model uncertainty potentially associated with the analysis models of the system being analyzed.

Reducible Uncertainty: As previously discussed, the presence of reducible sources of input uncertainty presents a distinct challenge to engineering system designers. When uncertainty is potentially reducible a designer is forced to make decisions about the improvement in performance that can be obtained through uncertainty reduction while simultaneously taking into account the increased cost of further reducing uncertainty. The research presented in this dissertation attempts to provide system designers with multiple approaches for addressing this challenge in a systematic and automated fashion, thus making the process of design under reducible uncertainty a simpler task.

Algorithm Efficiency: For any design algorithm to be useful it must be very efficient as current computational models for engineering systems can take many hours to execute. In order to address this very real issue, all the work presented in this dissertation has attempted to increase the computational efficiency of the approaches developed through the use of surrogate approximation models wherever possible. Surrogate modeling, also widely known as meta-modeling, describes a set of techniques for using limited actual analysis data to approximate a complex computational model [e.g. Shan and Wang, 2008]. The work presented in this dissertation have used analysis data generated early in design procedures to build surrogate models that are then used during later steps to greatly reduce computational effort through the intelligent re-use of already obtained system information.

1.4 RESEARCH THRUSTS

To accomplish the overall goals of this dissertation research, four distinct research thrusts were pursued. Each thrust built on the work of the previous thrust by relaxing some previous assumptions and/or addressing issues that were ignored or avoided in previous thrusts. Only interval uncertainty was considered throughout the research and the interval uncertainty levels associated with each design under consideration were assumed to be reducible to some extent. Each of four research thrusts performed will be described briefly in the following paragraphs and then in detail later in this dissertation.

1.4.1 Thrust 1: Multi-Disciplinary Multi-Output Sensitivity Analysis

The first step in this dissertation research was to extend the work of Li et al. [2009a] to multi-disciplinary systems. As such, a sensitivity analysis based uncertainty reduction approach, called Multi-dIsciplinary Multi-Output Sensitivity Analysis (MIMOSA) was developed. This approach was developed for multi-disciplinary engineering systems decomposed into multiple sub-systems, where each sub-system analysis model has multiple uncertain inputs and multiple outputs. MIMOSA can determine: i) the sensitivity of system and sub-system outputs to input uncertainties at both system and sub-system levels, ii) the sensitivity of the system outputs to the variations from sub-system outputs, and iii) the optimal "investment" required to reduce uncertainty in inputs in order to obtain a maximum reduction in output variations at both the system and sub-system levels. A numerical and an engineering example with two and three sub-systems, respectively, were used to demonstrate the applicability of the MIMOSA approach. A portion of this research thrust was presented in Li et al., [2009b] and the details of this new approach will be presented in Chapter 3 of this dissertation.

The objective of this research thrust was to develop an approach for understanding and optimally mitigating the effects of reducible interval input uncertainty on multi-disciplinary, multi-output engineering systems.

1.4.2 Thrust 2: Multi-Disciplinary Combined Sensitivity Analysis

The goal of the second research thrust was to develop a sensitivity analysis method for determining where the appropriate uncertainty reduction opportunities exist in a preexisting multi-disciplinary system design in an effort to ensure the feasibility of all included sub-system designs. This approach builds on the work of the previous thrust, which did not consider engineering feasibility. Using the MIMOSA approach as a starting point, the Multi-dIsciplinary COmbined Sensitivity Analysis (MICOSA) approach was formulated to achieve both minimal output function variation at the system and sub-system levels (like MIMOSA), while simultaneously ensuring that both the overall system and all included sub-systems will be feasible in the presence of any retained uncertainty. MICOSA combines output function variation reduction with the equally important goal of preventing the possibility of engineering failure due to input uncertainty. This approach was applied to a notional multi-disciplinary unmanned underwater vehicle model to demonstrate its capabilities. The details of this approach are presented in Chapter 4.

The objective of the second research thrust was to extend the MIMOSA approach to also consider engineering feasibility, thus making it possible to use uncertainty reduction mechanisms as a means for both optimally reducing output function variations while simultaneously ensuring the feasibility of multi-disciplinary engineering systems.

1.4.3 Thrust 3: Design Improvement by Sensitivity Analysis

Uncertainty in the input parameters to an engineering system may not only degrade the system's performance, but may also cause failure or infeasibility, as was addressed in the second research thrust. However, MICOSA only uses uncertainty reduction mechanism as a means for achieving feasibility under uncertainty, which may not always be sufficient. The third research thrust addressed this limitation of MICOSA and focused on the development of a new sensitivity analysis based approach called Design Improvement by Sensitivity Analysis (DISA). DISA analyzes the interval uncertainty of input parameters and, using multi-objective optimization, determines an optimal combination of design improvements that will ensure a minimal variation in the objective functions of the system while also ensuring feasibility. The approach provides a designer with options for both uncertainty reduction and, more importantly, slight design adjustments (which will be defined in detail later in this dissertation). A two stage sequential framework is used that can employ either the original analysis functions, or meta-model approximations, to greatly increase the computational efficiency of the approach. This new approach has been applied to two engineering examples of varying difficulty to demonstrate its applicability and effectiveness. The results produced by these examples show the ability of the approach to ensure the feasibility of a preexisting design under interval uncertainty by effectively adjusting available degrees of freedom in the system without the need to completely redesign the system. A portion of this work was presented in Hamel et al. [2010] and the details of this research thrust are presented in Chapter 5 of this dissertation.

The objective of the third research thrust was to develop a sensitivity analysis based approach for optimally mitigating the effects of reducible interval input uncertainty on a preexisting candidate design that is capable of both engineering feasibility and minimal objective function variations at a minimal require cost through the use of uncertainty reduction mechanisms and small design adjustments.

1.4.4 Thrust 4: Reducible Uncertain Interval Design

Optimization under uncertainty can be a difficult and computationally expensive problem driven by the need to consider the degrading effects of system variations, as discussed earlier in this chapter. Sources of uncertainty that may be reducible in some fashion present a particular challenge because designers must determine how much uncertainty to accept in the final design. As previously discussed, many of the existing approaches for design under input uncertainty, such as MIMOSA and DISA for example, require potentially unavailable or unknown information about the uncertainty in a system's input parameters; such as probability distributions, nominal values or uncertain intervals. These requirements may force designers into arbitrary or even erroneous assumptions about a system's input uncertainty when attempting to estimate nominal values and/or uncertain intervals for example. These types of assumptions can be especially degrading during the early stages in a design process when limited system information is available. In an effort to address these challenges a new SA inspired design approach was developed that can produce optimal solutions in the form of upper and lower bounds (which specify uncertain intervals) for all input parameters to a system that possess reducible uncertainty. These solutions provide minimal variation in system objectives for a maximum allowed level of input uncertainty in a multi-objective sense

and furthermore guarantee as close to deterministic Pareto optimal performance as possible with respect to the uncertain parameters. The function calls required by this approach are dramatically reduced through the use of a kriging meta-model assisted multi-objective optimization technique performed in two stages. The capabilities of the approach are demonstrated through three example problems of varying complexity. This final research thrust seeks to relax many of the limiting assumptions of the MIMOSA, MICOSA and DISA approaches in an effort to provide designers with a general approach for the design of engineering system under reducible interval uncertainty. A portion of this work was presented in Hamel and Azarm [2010] and the details of this final research thrust are presented in Chapter 6 of this dissertation.

The objective of this fourth and final research thrust was to develop an sensitivity analysis inspired approach for the multi-objective optimal design of engineering systems under reducible interval input uncertain that is capable of determining the optimal upper and lower bounds for sources of reducible input uncertainty to an engineering system with as few required a priori assumptions as possible.

1.5 ORGANIZATION OF DISSERTATION

The research thrusts introduced in the previous section represent the major contributions of the work presented in this dissertation. As previously discussed the four research thrusts are interrelated and each thrust successively builds up on the work of the previous thrusts. Figure 1.3 below depicts the relationships between the four thrusts graphically.

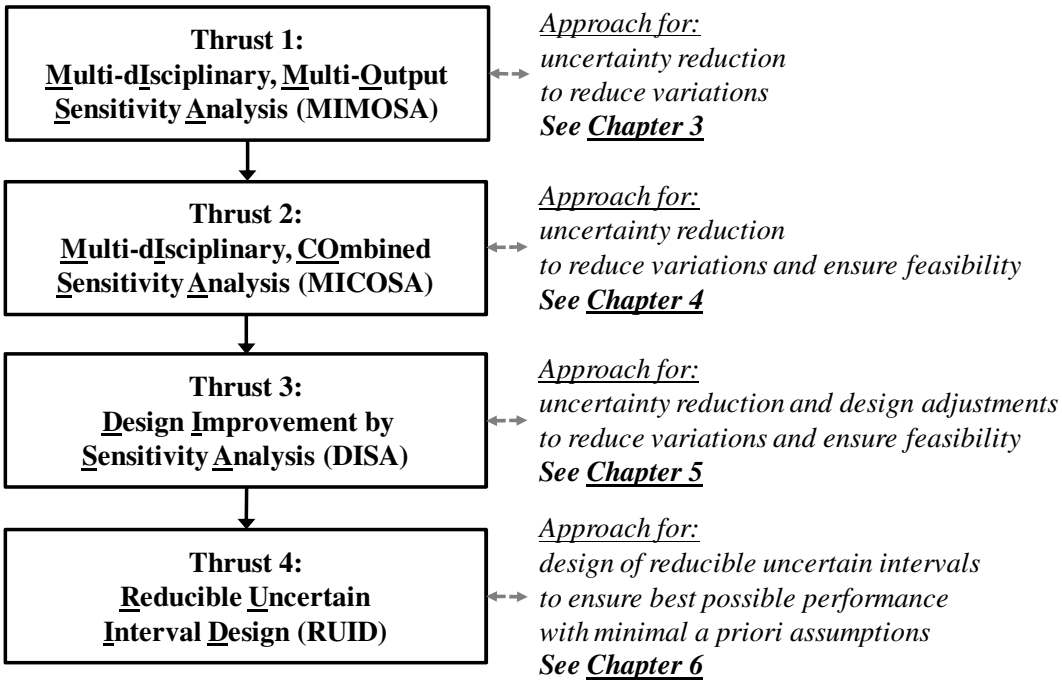

Figure 1.3: Organization of Research Thrusts

As can be seen in Figure 1.3, the new approach presented in each thrust is either more capable and/or requires less *a priori* information from the designer to produce similar results. For example, in the first research thrust a new approach for using uncertainty reduction to control the output variations in a multi-disciplinary system is presented. Then, the second thrust extends the approach presented in the first to also consider engineering feasibility, which was not considered previously. This progression resulted in a set of four new SA based approaches for the design of engineering systems under reducible interval uncertainty where each new approach presented addresses the weaknesses and/or limitations of the previously presented approaches.

The remainder of this dissertation will be organized as follows. Chapter 2 contains some relevant background definitions and terminology that will be used throughout this dissertation. Chapters 3 through 6 cover the details of the four main research thrusts.

Chapter 7 contains the relevant conclusions developed in each of the four research thrusts, an overview of the major contributions of this work and some potential directions for future research.

CHAPTER 2: BACKGROUND AND TERMINOLOGY

2.1 INTRODUCTION

In this chapter some general background information, definitions and terminology will be presented. These terms, equations and figures will be referred to throughout the dissertation.

2.2 MULTI-OBJECTIVE OPTIMIZATION

Multi-objective optimization involves solving the problem shown in Eqn. (2.1), where $\boldsymbol{f}$ describes a set of objective functions for a system which depend on a vector of design variables $\boldsymbol{x}$ and a vector of parameters $\boldsymbol{p}$, and limited by a set of constraint functions $\boldsymbol{g}$. If any of the constraint functions $\boldsymbol{g}$ in Eqn. (2.1) has a value greater than 0, the system is said to be infeasible. Typically Eqn. (2.1) would also contain a set of equality constraint functions as well, but these have been omitted in this work as most equality constraints will necessarily be violated under uncertainty.

$$\begin{aligned} &\min_{x} f_i(\boldsymbol{x}, \boldsymbol{p}) \quad i = 1,\ldots,I \\ &s.t. \\ &\quad g_j(\boldsymbol{x}, \boldsymbol{p}) \le 0 \quad j = 1,\ldots,J \end{aligned} \tag{2.1}$$

Traditionally the vector $\boldsymbol{x}$ describes factors that a designer can control while $\boldsymbol{p}$ is a vector of uncontrolled inputs. However, if the elements of both $\boldsymbol{x}$ and $\boldsymbol{p}$ are either known, in the form of a candidate design (as required by most SA procedures), or potentially controllable in some sense (because the parameter or its upper and/or lower bounds are selectable), then the system can be thought of as depending simply on a single vector of input parameters $\boldsymbol{p} = \{\boldsymbol{x}, \boldsymbol{p}\}$ (assuming $\boldsymbol{x}$ and $\boldsymbol{p}$ are row vectors) as shown in Eqn. (2.2). In most cases this input vector is bounded by extreme upper and lower bounds as shown.

From this point forward there will be no distinction between $\boldsymbol{x}$ and $\boldsymbol{p}$. All inputs to an analysis model will simply be referred to as parameters $\boldsymbol{p}$ as shown in Eqn. (2.2).

$$\begin{aligned} &\min_{\boldsymbol{p}} f_i(\boldsymbol{p}) \quad i = 1,...,I \\ &s.t. \\ &\quad g_j(\boldsymbol{p}) \le 0 \quad j = 1,...,J \\ &\quad \boldsymbol{p}_{lb} \le \boldsymbol{p} \le \boldsymbol{p}_{ub} \\ &\quad where \ \boldsymbol{p} = \{p_1,..., p_k,..., p_K\} \end{aligned} \tag{2.2}$$

From this point forward, a set of values for the vector $\boldsymbol{p}$ will be referred to as a design and evaluating the values for the actual functions $\boldsymbol{f}$ and $\boldsymbol{g}$ for a single design $\boldsymbol{p}$ will be referred to as a function call. Multi-objective optimization can be accomplish with many different techniques [Miettinen, 1999; Deb, 2001], but the work presented throughout this dissertation uses Multi-Objective Genetic Algorithms (MOGA) in order to accommodate mixed continuous-discrete input parameters and discontinuous output functions [Deb, 2001].

2.3 MULTI-DISCIPLINARY DESIGN OPTIMIZATION

When the analysis model or simulation model for an engineering system contains more than one coupled sub-system analysis models then the system is said to be multi-disciplinary and optimizing the design of such a system is called Multi-disciplinary Design Optimization (MDO). An MDO problem can be solved in an all-at-once (i.e., with all coupled sub-systems considered together in a single system) or a decomposed (i.e., with decoupled sub-systems) fashion. Some examples of MDO decomposition techniques include Concurrent Subspace Optimization (CSSO), Collaborative Optimization (CO) [Yi et al., 2007] and Analytical Target Cascading (ATC) [Kokkolaras

et al., 2006], all of which involve nesting sub-system optimizations within system level optimizers. The decomposed solution is more useful in that it allows a designer to consider and evaluate the performance of each sub-system individually. Figure 2.1 below shows the relationship between the all-at-once and decomposed MDO formulations using the Collaborative Optimization (CO) technique. The major difference between the two approaches in the figure is the addition of a new type of variables for the decomposed approach, target variables $\boldsymbol{t}$, at the system level, which serves as a target for the coupling variables $\boldsymbol{y}$ in each sub-system at the sub-system level. An additional set of constraints are also added in the decomposed approach to ensure that at the sub-system level each of the coupling variables $\boldsymbol{y}$ is equal to its target variable value. This technique was extended to multiple system objectives by Aute and Azarm [2006], and their approach is used throughout this dissertation when an MDO framework is required. Note that the subscript *sh* in Figure 2.1 denotes input at the system level shared by more than one of the sub-systems.

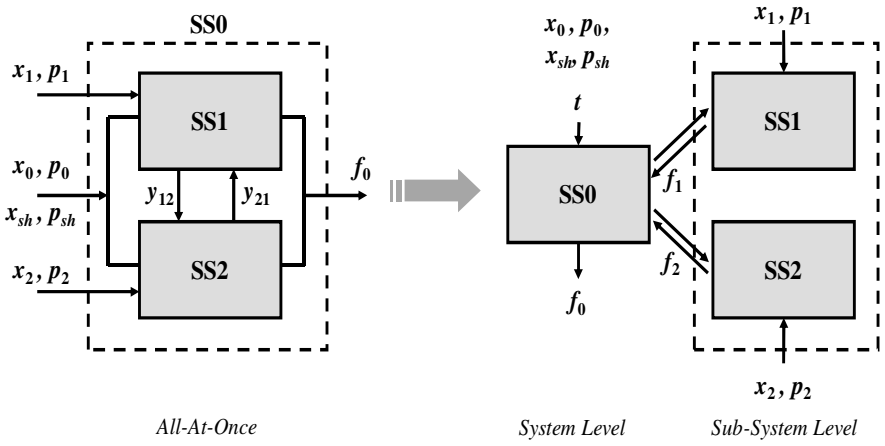

Figure 2.1: Decomposition of a Multi-Disciplinary System

2.4 CANDIDATE DESIGN

In order to perform sensitivity analysis the assumption is that the variables $\boldsymbol{p}$ in Eqn. (2.2) are already given in the form of a predetermined design. Thus hereafter in this dissertation the vector $\boldsymbol{p_0}$ is used to denote the nominal values for all inputs into a system for which a solution, or design, already exists. Furthermore this design $\boldsymbol{p}_0$ will be called a candidate design. As a result, the nominal objective and constraint functions values for a candidate design may be thought of simply as functions of the nominal values $\boldsymbol{p}_0$, which is a vector that contains both the predetermined design variable values and the parameter values from the original engineering design problem in Eqn. (2.1). The work presented in this dissertation focuses on how changes to the parameters contained in the vector $\boldsymbol{p}_0$, both in terms of nominal values and uncertainty level, affect the performance of the design described by the functions $\boldsymbol{f}_0$ and $\boldsymbol{g}_0$.

2.5 INPUT PARAMETER UNCERTAINTY

Interval uncertainty is considered in this work due to the ability of a designer to define uncertainty given limited information about parameters during the early stages of a design process. As stated earlier in this chapter, throughout this dissertation any input to a system analysis model will be considered a parameter. The interval uncertainty possessed by the k^{th} element of the vector of input parameters $\boldsymbol{p}$ is defined as Δp_k. For notational simplicity it is assumed that the Δp_k associated with any parameter is symmetric. In other words, the difference between the nominal parameter values $\boldsymbol{p}_0$ and the upper bounds on those parameters $\boldsymbol{p_U}$ is the same as the difference between the nominal values and the lower bounds $\boldsymbol{p_L}$, or for the k^{th} uncertain interval $\Delta p_k = | p_{0,k} - p_{U,k} | = | p_{0,k} - p_{L,k} |$. This assumption is not necessary though and asymmetric uncertainty levels can be dealt with

easily by considering two Δp values for each uncertain parameter $p_{0,k}$. In two dimensions the uncertainty quantified this way can be depicted as a rectangle in the parameter space for a problem, as shown in Figure 2.2. The parameter space can be thought of as the entire range of all possible parameter combinations for a given system. The uncertainty associated with the candidate design $\boldsymbol{p_0}$ is a subset of the parameter space, bounded by the interval $[\boldsymbol{p_0} - \boldsymbol{\Delta p}, \boldsymbol{p_0} + \boldsymbol{\Delta p}]$ (as originally defined by Moore [1966]).

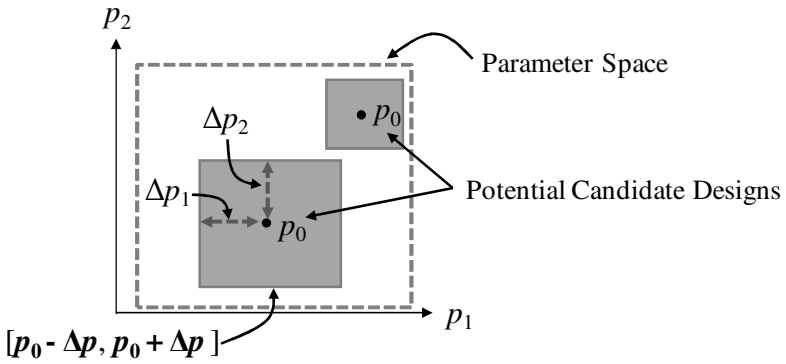

Figure 2.2: Parameter Space and Parameter Uncertainty

2.6 REDUCIBLE PARAMETER UNCERTAINTY

If the uncertainty in a set of parameters is reducible then, as proposed by Li et al. [2009a], reduction in that uncertainty can be quantified using a vector of uncertainty reduction scaling factors $\boldsymbol{\alpha} = \{\alpha_1,\ldots, \alpha_k,\ldots,\alpha_K\}$. For each reducible input uncertainty level Δp_k to a system, a scaling factor α_k is assigned. Each of the K elements of the vector $\boldsymbol{\alpha}$ is a number between 0 and 1. The values of $\boldsymbol{\alpha}$ and $\Delta\boldsymbol{p}$ work together to reduce the original uncertain intervals of $\boldsymbol{p}$ as shown in Figure 2.3. The new (smaller) uncertain region in the parameter space is calculated as the Hadamard product of the uncertainty reduction vector and the original vector of parameter uncertainties: $\boldsymbol{\alpha} \circ \boldsymbol{\Delta p} = \{\alpha_1\Delta p_1,\ldots, \alpha_k\Delta p_k,\ldots,\alpha_K\Delta p_K\}$. If the uncertainty level for a specific parameter cannot be reduced

completely, as is usually the case, a lower bound can be placed on the corresponding α_k value. Since the values for $\boldsymbol{\alpha}$ can be any value between 0 and 1, the uncertainty in any parameter $\boldsymbol{p}$ can be reduced to any subset of values on the original uncertain interval [$\boldsymbol{p_0 - \Delta p}$, $\boldsymbol{p_0 + \Delta p}$]. For instance, if uncertainty in p_1 is completely irreducible then α_1 should be limited to always be equal to 1; while if the uncertainty in p_1 can only be reduced by 50%, then α_1 is limited to a minimum value of 0.5. Additionally, if any of the available uncertainty reduction options for the parameter p_k are discrete choices, then the available α_k options can be limited to corresponding discrete values between 0 and 1. It should be noted that the work presented in this dissertation assumes that uncertain intervals are symmetric about the nominal values $\boldsymbol{p_0}$ and thus only one element of the uncertainty reduction vector $\boldsymbol{\alpha}$ is required for each reducible input parameter of interest. In the case of an asymmetric uncertainty about the nominal, an additional element should be added to the $\boldsymbol{\alpha}$ vector (increasing the size of the vector) for each input parameter with asymmetric uncertainty. When using these additional elements, one element of the $\boldsymbol{\alpha}$ vector controls the reduction in the upper bound of the uncertain interval for a parameter while the additional element controls the reduction in the lower bound. This modification increases the dimensionality of the $\boldsymbol{\alpha}$ vector, but also gives a designer greater control over uncertainty reduction decisions if necessary.

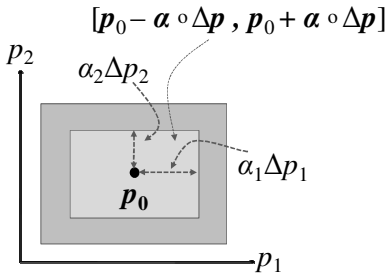

Figure 2.3: Parameter Uncertainty Reduction

If parameter uncertainty is reduced by decreasing the values for one or more elements in $\boldsymbol{\alpha}$, the range of output function variation will also inevitably be changed. This propagation of uncertainty from input parameters to output function values can be represented by a set of resulting uncertain objective and/or constraint function values. As discussed above, uncertainty propagation is a function of the nominal parameter values $\boldsymbol{p}_0$, the original uncertainty intervals $\Delta\boldsymbol{p}$, and the values of the uncertainty reduction vector $\boldsymbol{\alpha}$. Figure 2.4 depicts the impact that different uncertainty reduction values (denoted by decreasing $\boldsymbol{\alpha}$ values) could have on output objective function variations when nominal parameter values $\boldsymbol{p}_0$ remain unchanged.

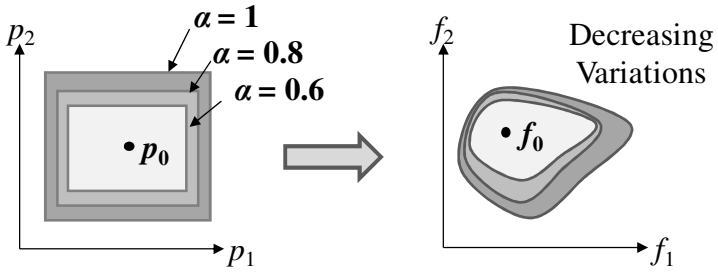

Figure 2.4: Parameter Uncertainty Mapping for Various α Values

2.7 UNCERTAINTY QUANTIFICATION METRICS

In order to effectively manage input uncertainty in an effort to improve output function performance (i.e., to reduce the variation in the outputs), it is necessary to measure and quantify objective and constraint function variations as a function of any uncertainty in the system's input parameters. In order to do this, Li et al.'s work [2009a] is extended in this dissertation to consider either objective functions $\boldsymbol{f}$, constraint functions $\boldsymbol{g}$, or both. If the variations in the objective functions are of interest, the metric used is call R_f, while the measure of constraint functions variations under uncertainty will

be called R_g. If both objectives and constraints are considered simultaneously their variations will be measured with a metric called R_c, while if the nature of the output functions (objectives or constraints) is not specified, a general metric called R will be used. Figure 2.5 below depicts two different notional R_f values for a notional bi-objective system. Similar figures could be drawn for R_g, R_c and/or R as needed.

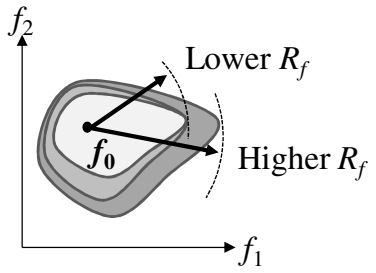

Figure 2.5: Graphical Depiction of R_f

Note in Figure 2.5 that R_f (or any output function variation for that matter) will always be a function of any changes to the nominal input parameters $\boldsymbol{p_0}$ and their associated uncertainty. For example, in the case of uncertainty reduction, R_f will be a function of the elements of the uncertainty reduction vector $\boldsymbol{\alpha}$ which describes the level of uncertainty reduction associated with a system design, as discussed in the previous subsection. This is depicted in Figure 2.5 by the light colored objective variation region having a smaller R_f than the larger darker colored region, which has a higher associated R_f value. In the subsequent discussions of each of the research thrusts the specific variation metrics used (i.e. R_f, R_g and/or R_c) will be defined more specifically as required.

2.8 INVESTMENT

As a measure of defining the cost of reducing uncertainty in input parameters the concept of *Investment* was developed by Li et al. [2009a]. The *Investment* metric is

essentially a notional function that correlates the amount of uncertainty associated with a candidate design to the "cost" required to produce that uncertainty level. The general concept of the *Investment* metric is presented for a two parameter system in Figure 2.6, which shows that a higher reduction in uncertainty from the nominal will require a greater *Investment* level.

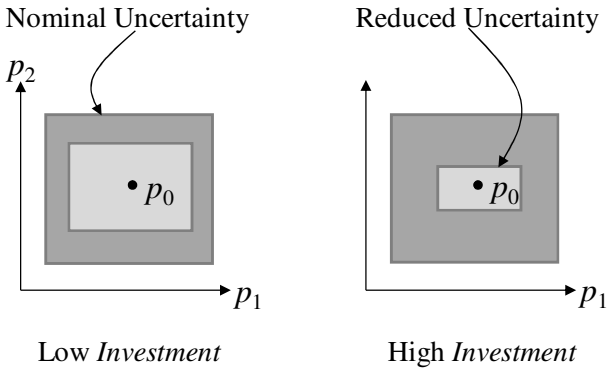

Figure 2.6: General Investment Concept

Various formulations of Li et al.'s [2009a] *Investment* metric are used throughout this work and the specific details of each formulation used will be presented in the appropriate chapters of this dissertation. The *Investment* metrics used in this work simply provides a means for quantifying uncertainty reduction costs in the absence of actual cost data and can be easily extended to include a function or set of functions that accurately quantify uncertainty reduction costs if available. Since the *Investment* metric quantifies the cost associated with uncertainty reduction, it is typically a function of the uncertainty reduction vector $\boldsymbol{\alpha}$. In some chapters of this dissertation the *Investment* metric is abbreviated by the single character *I* in the interest of simplicity.

2.9 MULTI-OBJECTIVE SENSITIVITY ANALYSIS (MOSA)

Much of the work presented in this dissertation is an extension of, or inspired by an approach developed by Li et al., [2009a] called multi-objective sensitivity analysis (MOSA), which is an uncertainty reduction technique. MOSA uses a bi-objective optimization problem to determine an optimal reduction in parameter uncertainty at a minimal cost, treating the uncertainty reduction vector as decision variables.

$$\begin{aligned} &\min_{\boldsymbol{\alpha}} \; R_f(\boldsymbol{\alpha}) \\ &\min_{\boldsymbol{\alpha}} \; Investment(\boldsymbol{\alpha}) \end{aligned} \tag{2.3}$$

Eqn. (2.3) can be solved using any multi-objective optimization technique; however, Li et al. [2009a] used genetic algorithms with much success. This formulation elegantly places objective function variation, R_f, in competition with the cost of producing variation reduction *Investment* (or *I* if the simplified notation for *Investment* is used), and produces a Pareto set of solutions for the designer to choose from based on available funds for uncertainty reduction and objective function performance needs. However, the MOSA approach is limited to single disciplinary systems. Furthermore, MOSA provides no assurance of feasibility under uncertainty, nor does it provide a means for achieving feasibility if necessary.

2.10 SURROGATE APPROXIMATION AND KRIGING

Surrogate approximation, also widely known as meta-modeling, describes a set of techniques for using limited actual analysis data (often selected via a design of experiments (DOE) technique) to approximate a complex computational model [e.g. Shan and Wang, 2008; Allaire and Willcox, 2008; Wang and Shan, 2007]. Once properly

verified using the underlying analysis model, a meta-model can be used in lieu of the actual analysis model in an optimization or sensitivity analysis algorithm to conserve computational effort. There are numerous techniques that can be used to approximate actual analysis data and one such particularly useful technique used in this work is a method borrowed from geostatistics called kriging [Martin and Simpson, 2005]. Kriging is well studied and none of the work presented in this dissertation attempts to improve kriging specifically, or meta-modeling in general, in any way. Rather this work simply uses the kriging technique as a means for increasing the computational efficiency of the various approaches presented in this dissertation. Kriging was selected over other approximation techniques for three distinct reasons: 1) the kriging algorithm ensures than any approximate function will honor all observed data points, 2) the kriging algorithm is well suited to high dimensional data sets, and 3) the kriging algorithm produces an estimate of the error for any interpolated point, information that can be used to correct the approximation regularly to ensure accuracy. It should be noted that meta-model accuracy is especially important in a sensitivity analysis context as inaccurate approximations could lead to errant sensitivity information. This issue will be specifically addressed when necessary throughout this dissertation.

CHAPTER 3: MULTI-DISCIPLINARY, MULTI-OUTPUT SENSITIVITY ANALYSIS (MIMOSA)

3.1 INTRODUCTION TO RESEARCH THRUST 1

The first research thrust of this dissertation involved the development of a new global sensitivity analysis approach. This new approach can be used for the sensitivity analysis of multiple sub-system multi-output analysis models in which the inputs to the analysis sub-systems have reducible uncertainty. This new approach is called Multi-dIsciplinary Multi-Output Sensitivity Analysis (MIMOSA). MIMOSA has several key properties and capabilities: a) it quantifies variation in multiple outputs in the system and/or each sub-system with respect to input interval uncertainty, considering multiple uncertain input parameters for a single design or a set of designs; b) it identifies the uncertain parameters, at the system and sub-system levels, which have the greatest effect on system output variations; and c) it does not require gradient information or probability density functions to quantify the uncertain parameters, rather it uses interval uncertainty which is more flexible and easier to obtain or estimate.

In the context of Multi-Disciplinary Optimization (MDO), there have been numerous approaches proposed in the literature for ensuring that optimal design solutions are insensitive to the uncertainty associated with the system's input parameters, mostly in the area of robust optimization (e.g., [Du and Chen, 2002 and 2005; Smith and Mahadevan, 2005; Kokkolaras et al., 2006; Padula et al., 2006; Gu et al., 2006; Chiralaksanakul and Mahadevan, 2007; Li and Azarm, 2008]). Those approaches, while valuable, do not address the possibility that in some cases the uncertainty in a system or its corresponding sub-systems could be reduced to some level, given enough investment,

and that reduction in uncertainty could in turn improve both the system's and its corresponding sub-systems' performance without the need for additional design optimization. This fact drives the need for a better understanding of the nature and effects of uncertainty in multi-disciplinary systems. Such knowledge would also lead to a better understanding of uncertainty, the relative importance of particular parameters and the opportunities to systematically apply limited resources in order to reduce the variations in a system's outputs optimally. Sensitivity Analysis (SA) techniques provide a particularly useful option for understanding the effect of uncertainty and the application of SA techniques to uncertainty reduction problems is fast becoming an area of interest in current research efforts.

The typical way that SA approaches are currently being used by designers is as methods for understanding the effects of system input uncertainty on system outputs [Iman and Helton, 1988; Saltelli et al., 2000]. The majority of the previous works in this particular application of SA have focused on systems where the uncertainty of input parameters has a presumed probabilistic distribution (e.g., [Saltelli et al., 2000; Chen et al., 2005]), or on systems where only one output at a time is considered (e.g., [Sobol, 2001; Helton and Davis, 2003]). Moreover, most of the current SA approaches are only applicable to single-disciplinary analysis-based engineering problems [Saltelli et al., 2000] as mentioned in Chapter 1. In contrast to these single-disciplinary methods, SA approaches that treat multi-disciplinary systems in a more flexible multiple sub-system fashion are obviously more attractive as they can determine the sensitivity of sub-system's outputs more flexibly and capture the interaction effects between sub-systems more accurately. Approaches addressing SA in a multi-disciplinary framework remain

rare in the literature and all of them require probabilistic distributions for uncertainty [Gu et al., 1998; Yin and Chen, 2008], or use gradient information of the function under consideration [Sobieszczanski-Sobieski, 1990; Sobieszczanski-Sobieski et al., 1991; Wehrhahn, 1991; Noor et al., 2000]. Moreover, in all the approaches currently in the literature, only one output is considered for each sub-system. However, almost all analysis models for engineering systems are multi-output in nature and probability distributions for uncertain inputs are not always known or valid (e.g., [Rao and Cao, 2002; Wu and Rao, 2007; Li and Azarm, 2008; Qiu et al., 2008]).

A single-disciplinary uncertainty reduction method, called Multi-Objective Sensitivity Analysis (MOSA), [Li et al., 2009a], was recently developed and the details of this approach are presented in Chapter 2. Much like GSA methods, the MOSA approach can determine the sensitivity of output variations to multiple input parameter uncertainty. However, as pointed out in Chapter 2, MOSA did not address the uncertainty reduction problem at each sub-system in a multi-disciplinary framework. Uncertainty in the input parameters of a multi-disciplinary engineering analysis system is not only unavoidable but also results in variations in the outputs at both the system and sub-system levels. Moreover, in a multi-disciplinary analysis model, uncertainty reduction in one parameter (or combination of parameters) may greatly improve the performance of one sub-system, but may have no effect, or perhaps even adverse effects on other coupled sub-systems. For this reason, it is necessary that SA techniques be extended to multi-disciplinary problems with multiple outputs in order to consider the complex relationships between input uncertainty and outputs of the analysis in each sub-system and across coupled sub-systems.

MIMOSA is capable of determining which sub-systems are most sensitive to input uncertainty and then can determine how limited resources should be applied to uncertainty reduction in order to obtain a maximum reduction in output variations at both the system and sub-system levels. The parameter uncertainty that MIMOSA is concerned with is assumed to be reducible and exists not only as input in each sub-system but also in the couplings between sub-systems. However, MIMOSA does not require probability distribution information for uncertainty characterization, but instead assumes that an uncertain interval is known for each uncertain parameter. In the MIMOSA approach, given the known interval uncertainty for input parameters in both the system and sub-system levels, a designer can identify parameters whose uncertainty should be reduced or, perhaps even eliminated, in order to achieve the desirable reduction in variation in the system's and it's corresponding sub-system's outputs simultaneously. In addition, the relative importance of each of the sub-systems can also be determined using the information produced by the MIMOSA approach. Two scalar metrics are used to quantify the amount of variation in outputs and the cost to the designer of reducing the uncertainty in the input parameters in both system and sub-system levels. A bi-objective SA problem is formulated in the system level problem and in each sub-system to minimize the variation in the corresponding system's outputs while simultaneously minimizing the investment required to produce the necessary reduction in the uncertainty of the system's parameters. A numerical example and an engineering design example, each having two or three sub-systems, respectively, are used to demonstrate the applicability of the MIMOSA approach.

The rest of this chapter is organized as follows. Some terminology and definitions used are described in Section 3.2. Details of the MIMOSA approach are presented in Section 3.3. Two examples, a numerical example having two sub-systems and an engineering example having three sub-systems, are presented in Section 3.4 to illustrate the applicability of the approach. Concluding remarks are presented in Section 3.5. A portion of this chapter was presented in Li et al. [2009b].

3.2 BACKGROUND AND TERMINOLOGY

3.2.1 Tolerance Region

The concept of a parameter uncertainty was first presented in Chapter 2 of this dissertation. The region of the parameter space bound by the uncertain input parameter intervals for a candidate design of a system can be called a Tolerance Region (TR). Figure 3.1 below depicts a TR for a notional two parameter system. Recall that the TR for an analysis model of a design quantifies the amount of uncertainty associated with the model's input parameters. These are not selectable values, but are instead a property of a design under consideration that is known to possess uncertain input parameters. As stated in Chapter 2, the parameter uncertainties considered in this work are assumed to be defined by intervals and are assumed to be reducible.

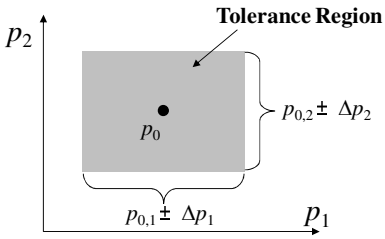

Figure 3.1: Tolerance Region

3.2.2 Uncertainty Reduction and Retained Tolerance Region (RTR)

The uncertainty reduction vector $\boldsymbol{\alpha} = \{\alpha_1,\ldots,\alpha_K\}$ was also first presented in Chapter 2. Recall that the elements of the $\boldsymbol{\alpha}$ vector are bound by 0 and 1, for $k = 1,\ldots, K$, one for each corresponding uncertain parameter. The term Retained Tolerance Region (RTR) is used to describe the reduced uncertain region of the parameter space defined as the portion of an original TR, determined by the $\boldsymbol{\alpha}$ vector and the original parameter uncertainty. Essentially, RTR can be any symmetric hyper-rectangle that is inside the original tolerance region centered at the nominal parameter values. Recall that the $\boldsymbol{\alpha}$ vector is a measure of the prescribed level of uncertainty reduction for the given uncertain parameters and is treated as a set of the decision variables and will be selected within the MIMOSA algorithm, not by the designer beforehand.

3.2.3 Reduced Output Sensitivity Region (ROSR)

Regardless of which type of uncertainty (irreducible or reducible) is considered, it is possible to map the effects of input parameter variation for one or more designs under consideration into the output space and then evaluate those effects on the resulting uncertainty, in a multi-output sense as described in Chapter 2. Given a known TR, which is characteristic of a given design and its associated uncertain parameters (the left side of Figure 3.2), the result of mapping that input uncertainty to the system outputs forms an Output Sensitivity Region (OSR) (the right side of Figure 3.2) for each design under consideration. Figure 3.2 assumes a two-input, two-output analysis model for several trial designs in the interest of visualization, but the concept is applicable to a problem of any size.

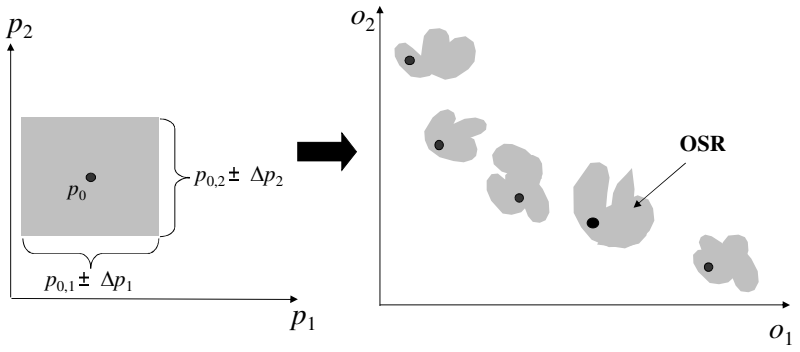

Figure 3.2: Mapping from the Tolerance Region to the OSR

For a trial design $\boldsymbol{x}_0$, the nominal values of the M analysis outputs are $\boldsymbol{o}(\boldsymbol{x}_0, \boldsymbol{p}_0) = \{o_1(\boldsymbol{x}_0, \boldsymbol{p}_0),\ldots, o_M(\boldsymbol{x}_0,\boldsymbol{p}_0)\}$. Output variations of $\boldsymbol{x}_0$ will be considered to be caused by the retained parameter variations $\boldsymbol{\alpha} \circ \Delta\boldsymbol{p}$ (as originally defined in Chapter 3) in Eqn. (3.1):

$$\begin{aligned} &\Delta\boldsymbol{o}(\boldsymbol{x}_0, \boldsymbol{p}) = \boldsymbol{o}(\boldsymbol{x}_0, \boldsymbol{p}) - \boldsymbol{o}(\boldsymbol{x}_0, \boldsymbol{p}_0) \\ &\textit{where} \\ &\quad \boldsymbol{p}_0 - \boldsymbol{\alpha} \circ \Delta\boldsymbol{p} \le \boldsymbol{p} \le \boldsymbol{p}_0 + \boldsymbol{\alpha} \circ \Delta\boldsymbol{p} \end{aligned} \tag{3.1}$$

Notice that the TR of parameters on the left of Figure 3.2 can lead to different OSRs for the designs represented in the output space on the right of Figure 3.2. This mapping of uncertain parameters can be quantified by measuring the distance of the largest deviation from the nominal output function values under the uncertain parameter intervals using a $\|.\|_\infty$ norm. This quantification was first presented in Chapter 2 and is here denoted by R, or the Reduced OSR (ROSR) for $\boldsymbol{x}_0$, the design under consideration for analysis, as shown in Eqn. (3.2). This R metric is a general metric (it does not differentiate between objective and constraint functions) since in the context of this work the output functions under consideration may be either objectives, constraints or both.

$$R(\boldsymbol{\alpha}) = \max_{p} \left\| \frac{\Delta \boldsymbol{o}(\boldsymbol{p})}{\Delta \boldsymbol{o}_0} \right\|_\infty$$

where

$$\Delta \boldsymbol{o}(\boldsymbol{p}) = \boldsymbol{o}(\boldsymbol{x}_0, \boldsymbol{p}) - \boldsymbol{o}(\boldsymbol{x}_0, \boldsymbol{p}_0)$$

$$\boldsymbol{p}_0 - \boldsymbol{\alpha} \circ \Delta \boldsymbol{p} \le \boldsymbol{p} \le \boldsymbol{p}_0 + \boldsymbol{\alpha} \circ \Delta \boldsymbol{p} \tag{3.2}$$

In Eqn. (3.2), $\Delta \boldsymbol{o}_0$ is the Acceptable Output Variation Region (AOVR) for the M outputs. The AOVR value is specified by the designer and then the variation in those outputs is normalized by the corresponding AOVR values. The value of the AOVR is usually assumed by the designer who has good knowledge about the system or a clear requirement on the acceptable variation range of the system performance. Given an AOVR, it is required that the variation in the outputs to be less than the AOVR. As a result, R should be less than or equal to 1 for the acceptable variation for the outputs obtained from the analysis of a design $\boldsymbol{x}_0$. If an AOVR is not available or not desired, R can still be normalized instead by using the nominal output values. Normalization in Eqn. (3.2) is usually necessary depending on the applications, especially for the engineering analysis problems that have multiple outputs with different units or orders of magnitude.

As shown in Figure 3.3, a measure of output variation R can be reduced (for multiple designs, as shown) by reducing the RTR for a given set of input parameters as, R is a function of the corresponding $\boldsymbol{\alpha}$ vector values for the system (or sub-system) of interest. This is concept was presented conceptually in Chapter 2.

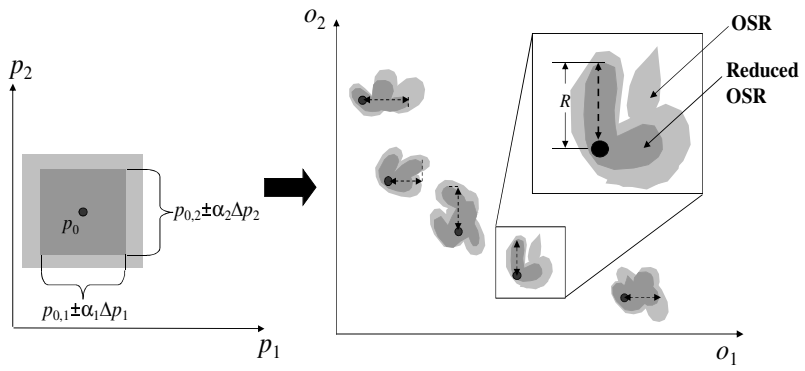

Figure 3.3: Mapping from RTR to Reduced OSR (ROSR) with variation *R*

3.2.4 Correlation Coefficient Matrix (CC)

CC is a matrix of correlation coefficients, calculated for a matrix whose rows are observed data of variables under consideration and whose columns are the variables. The $(i, j)^{th}$ element of the matrix *CC* is defined as shown in Eqn. (3.3), where $C(i, j)$ is the covariance value between variable *i* and variable *j*.

$$CC(i, j) = \frac{C(i, j)}{\sqrt{C(i,i)C(j, j)}} \tag{3.3}$$

3.2.5 Investment

The *Investment* metric, presented conceptually in Chapter 2, is essentially a notional function that correlates the amount of uncertainty to the "cost" required to produce that uncertainty reduction, and can be used in the absence of actual cost data or functions for an engineering analysis model. For this research thrust, the *Investment* metric used is the formulation first presented by Li et al. [2009a]. It is simply defined as the normalized representation of how much in terms of both perimeter and area (or volume) the uncertain region in the parameter space for a set of parameters is reduced as a function of the $\boldsymbol{\alpha}$ vector values, as detailed in Eqn. (3.4):

$$Investment = \theta_1 \left(\frac{K - \sum_{i}^{K} \alpha_k}{K} \right) + \theta_2 \left(1 - \prod_{i}^{K} \alpha_k \right), \; i = 1, \ldots, K \tag{3.4}$$

In Eqn. (3.4) the quantities $\mathbf{\Sigma}\alpha_k$ and $\mathbf{\Pi}\alpha_k$represent the hyper-perimeter and hyper-volume, respectively, of the uncertainty retained in the parameter space after the uncertainty is normalized by $\Delta \boldsymbol{p}$. The θ values can be selected and aligned according to the designer's preferences on the hyper-perimeter or the hyper-volume. In the work presented in this chapter it is assumed that $\theta_1 = \theta_2 = 0.5$, meaning that both the volume and perimeter metrics have equal weights for reduction. The hyper-perimeter included in Eqn. (3.4) indicates that the investment used to reduce uncertainty is linear to the amount of uncertainty in each parameter and identical for all parameters unless a weighting scheme is employed. Additionally, the hyper-volume included in Eqn. (3.4) describes that the investment is proportional to the product of uncertainty reduction for all parameters, which accounts for the total volume of uncertainty reduction given a set of $\boldsymbol{\alpha}$ values. It can be seen from Eqn. (3.4) that as the uncertainty reduction vector elements go to 0, *Investment* goes to 1 indicating that a maximum possible effort is required to eliminate all the uncertainty in the input parameters, while as all α_k values go to 1, *Investment* tends to 0 meaning no resources are required to reduce the input uncertainty. Clearly *Investment* and *R* are competing metrics as smaller output variation levels will always require greater cost. It should be noted that if any real utility or cost function associated with parameter uncertainty reductions is available for specific applications, such as a known dollar value required per unit of machining tolerance improvement for a geometric dimension, it can be easily incorporated into Eqn. (3.4).

3.2.6 Multi-Disciplinary Multi-Output Analysis System

Eqn. (3.5) and Figure 3.4 depict a typical multi-disciplinary multi-output system decomposed into three coupled sub-systems that share some design variables and input parameters, respectively represented as $\boldsymbol{x}_{sh}$ and $\boldsymbol{p}_{sh}$, along with their local sub-system variables and parameters $\boldsymbol{x}_i$ and $\boldsymbol{p}_i$, i = 1, 2, 3. The sub-system's outputs can be single or multiple and are used to resolve the system level outputs. In Eqn. (3.5), $\boldsymbol{y}_{ij}$ represents a coupling variable vector: Outputs from sub-system i (SSi) and inputs to sub-system j (SSj). The vector $\boldsymbol{x}_i$ and $\boldsymbol{o}_i$ are SSi's design variables and outputs, respectively. The vector $\boldsymbol{Y}_i$ in Eqn. (3.5) represents the functions that are used to calculate the coupling variables $\boldsymbol{y}_{ij}$. Parameters $\boldsymbol{p}_i$ represent the local uncertain parameters that have interval uncertainty. The entire system outputs can be represented by the vector $\boldsymbol{o}_0$, which can be assumed to be functions of shared design variables, parameters, and local (sub-system) outputs, respectively,

Given the shared and local design variables $\boldsymbol{x}_{sh}$ and $\boldsymbol{x}_i$, which specify the candidate design(s), the variations in the system and sub-system outputs are dependent on the uncertain input parameters and coupling variables.

$$\begin{aligned} &\boldsymbol{o}_i = \boldsymbol{O}(\boldsymbol{x}_{sh}, \boldsymbol{p}_{sh}, \boldsymbol{x}_i, \boldsymbol{p}_i, \boldsymbol{y}_{ji}) \\ &\textit{where} \\ &\quad \boldsymbol{y}_{ij} = \boldsymbol{Y}_i(\boldsymbol{x}_{sh}, \boldsymbol{p}_{sh}, \boldsymbol{x}_i, \boldsymbol{p}_i, \boldsymbol{y}_{ji}) \quad i = 1, 2, 3 \end{aligned} \tag{3.5}$$

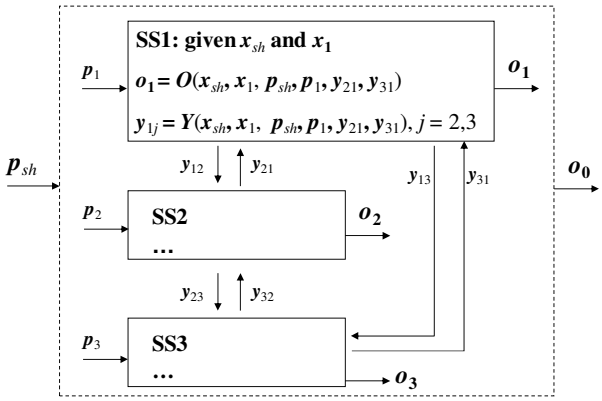

Figure 3.4: A Multi-Disciplinary System with Three Sub-Systems

One typical method to hierarchically decouple a fully (two-way) coupled multi-output multi-disciplinary system is to introduce a new set of variables at the system level, indicated in Figure 3.5 as $\boldsymbol{t}$, which represent target values, one for each of the coupling variables that connect the sub-systems [e.g., Aute and Azarm, 2006]. Each sub-system (SSi) uses the target variables to perform local calculations and obtain all local output values (i.e., $\boldsymbol{o}_i$, and $\boldsymbol{y}_{ij}$). The collaborative consistency of the system is maintained by enforcing a consistency constraint in each sub-system. This consistency constraint requires that the value of each element of $\boldsymbol{y}_{ij}$ converges to its corresponding target value in $\boldsymbol{t}_{ij}$ in the deterministic case. These new variables, $\boldsymbol{t}$, are considered as design variables to be given along with the shared design variables $\boldsymbol{x}_{sh}$, at the system level (SS0).

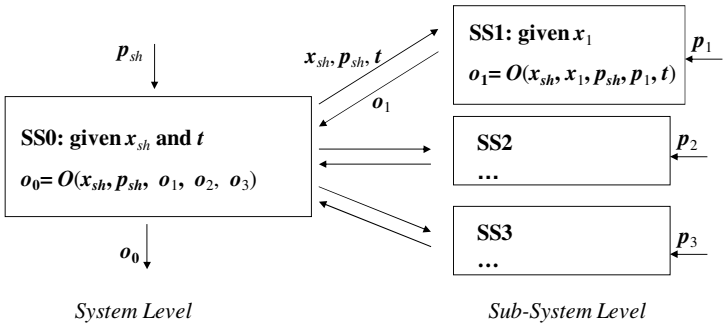

Figure 3.5: Multi-Output Multi-Disciplinary System in a Decomposed Framework

3.3 MIMOSA APPROACH

In this section the specifics of the MIMOSA approach are presented. The issue as to how to ensure the collaborative consistency of a multi-disciplinary system under uncertainty is addressed in Subsection 3.3.1. The formulation of the MIMOSA approach is outlined in Subsection 3.3.2. The detailed steps of MIMOSA are presented in Subsection 3.3.3.

3.3.1 Collaborative Consistency of MIMOSA

As mentioned previously, in order to decouple the multiple sub-systems that make up a multi-disciplinary system and maintain the collaborative consistency of the system, a target variable for each coupling variable must be introduced at the system level and then used in each sub-system. However, when uncertainty is considered in the system the collaborative consistency of the system is not straightforward and deserves more attention [Li and Azarm, 2008]. A multi-disciplinary system is said to possess collaborative consistency when all sub-systems achieve the same value for each coupling variable within the system's decomposed framework, thus ensuring that all sub-systems will work together consistently to define a design.

When considering the sub-system couplings shown in Figure 3.4, the propagation of uncertainty implies that outputs from one sub-system are not only affected by the uncertainty from this sub-system's parameters but also by the uncertainty in coupling variables. With the introduction of interval uncertainty in parameters, the collaborative consistency constraint can no longer be satisfied since the uncertainty in the input parameters $\boldsymbol{p}_i$ of SSi leads to a range rather than a single value for each component in the

coupling variables $\boldsymbol{y}_{ij}$. The collaborative consistency constraint in SSi cannot force a range of output values for each coupling variable $\boldsymbol{y}_{ij}$ to converge to a single target value of $\boldsymbol{t}_{ij}$. As a result, a system and corresponding sub-systems could become inconsistent due to a mismatch between the output range of each coupling variable and the deterministic value of each target variable. To resolve this mismatch the target variables $\boldsymbol{t}$ must be able to tolerate the resulting variation ranges in the coupling variables $\boldsymbol{y}$. In other words, to accept the variation in the coupling variables $\boldsymbol{y}$, target variables $\boldsymbol{t}$ should have an associated tolerance range. Given a candidate design, as long as the established tolerance range of $\boldsymbol{t}_{ij}$ encloses the resultant variation in $\boldsymbol{y}_{ij}$ for the system, the variations in coupling variables $\boldsymbol{y}_{ij}$ can be absorbed by a local uncertainty associated with the targets $\boldsymbol{t}_{ij}$ for SSj, ensuring that the system will remain collaboratively consistent.

To accommodate the propagation of uncertainty, it is necessary to ensure that the selected tolerance regions associated with the target variables are large enough to enclose the expected variations in the corresponding coupling variables in order to maintain the feasibility of the entire system. This tension between uncertainty reduction and collaborative consistency is resolved in the MIMOSA approach by adding a new collaborative consistency constraint under uncertainty in each sub-system. In order for this new constraint to function properly and have the desired result of ensuring the overall system consistency, all target variables which are a part of the collaborative consistency constraints are considered to have interval uncertainty at the system level and have corresponding $\boldsymbol{\alpha}$ vector values selected to control the associated uncertainty. Using this method, as long as the resultant variation in the coupling variables output from each sub-system is less than the retained uncertainty in the target variables passed down from the

system level, the collaborative consistency among sub-systems will be ensured (see the next subsection for a detailed formulation). The selection on the original TR of the target variabls are dependend on the designer's opinion or specific requirments on couplings.

3.3.2 Formulation of MIMOSA

For simplicity, the formulation of the MIMOSA approach will be presented as applied to a single candidate design, but extending this approach to multiple candidate designs is straightforward to accomplish (see [Li et al., 2009a]). The MIMOSA approach, as shown in Figure 3.6 consists of performing a two-objective optimization problem for SA at the system level and for each sub-system in a decomposed framework. The SA optimization problem is used to determine the best R and *Investment* attainable as a function of the $\boldsymbol{\alpha}$ vector elements for uncertain parameters $\boldsymbol{p}$ and the target variables $\boldsymbol{t}$. This is conducted at the system level and in each of the sub-systems being considered in a bi-level fashion. The formulation assumes that the designer already has obtained a candidate design (or designs) in which input parameters have reducible interval uncertainty.

At the system level (SS0), the variables are the vector $\boldsymbol{\alpha}_{SS0}$, which includes $\boldsymbol{\alpha}_{sh}$ and $\boldsymbol{\alpha}_{t}$ for $\boldsymbol{p}_{sh}$ and $\boldsymbol{t}$, respectively. The two objectives of the SA optimization at the system level are 1) to minimize *Investment* and 2) to minimize the variation in the system level design outputs represented as R_{SS0}, as shown in Eqn. (3.6). Here, R_{SS0} at the system level is defined as the $\|.\|_{\infty}$ norm of the variation in the corresponding system outputs.

$$
\begin{aligned}
&\min_{\alpha_{SS0}} \quad R_{SS0} = \left\| \Delta \boldsymbol{o}_{SS0} \right\|_{\infty} \\
&\min_{\alpha_{SS0}} \quad Investment_{SS0} \\
&\textit{where} \\
&\quad \Delta \boldsymbol{o}_{SS0} = \boldsymbol{o}_0(\boldsymbol{x}_0, \boldsymbol{p}) - \boldsymbol{o}_0(\boldsymbol{x}_0, \boldsymbol{p}_0) \\
&\quad \boldsymbol{p}_0 - \boldsymbol{\alpha}_{SS0} \circ \Delta \boldsymbol{p} \le \boldsymbol{p} \le \boldsymbol{p}_0 + \boldsymbol{\alpha}_{SS0} \circ \Delta \boldsymbol{p} \\
&\quad \boldsymbol{\alpha}_{SS0} = \{ \alpha_{sh}, \alpha_t \}
\end{aligned}
\tag{3.6}
$$

In Eqn. (3.6), $\Delta \boldsymbol{o}_{SS0}$ is the variation in SS0's outputs. If the outputs in SS0 have different units or different orders of magnitude with respect to each other, the normalization of the variation in the system level's (SS0) outputs is necessary. The most obvious choice is to normalize $\Delta \boldsymbol{o}_{SS0}$ by the nominal output values for a candidate design under consideration.

The formulation of the sub-system SA problem is very similar to the system level, with the key addition of the need to ensure collaborative consistency of the design under uncertainty. To do this consistency check under uncertainty, in each sub-system level optimization problem, SSi, the quantity η_C is defined as the maximum $\|\cdot\|_\infty$ distance from the coupling variable $\boldsymbol{y}_{ij}$ to the nominal target variable $\boldsymbol{t}_{ij,0}$, as shown in Eqn. (3.7a). As long as this distance is within the optimizer-specified retained tolerance region $\boldsymbol{\alpha} \circ \Delta \boldsymbol{t}_{ij,0}$ for target variables, the variation in the coupling variable is acceptable.

$$
\eta_{C_i} = \max_{\boldsymbol{p}, \boldsymbol{t}} \left\| C_i \right\|_{\infty}, \; i = 1, \; 2, \; 3 \tag{3.7a}
$$

Eqn. (3.7b) below details the value C_i, used in Eqn. (3.7a), which quantifies the difference between $\boldsymbol{y}_{ij}$ and the nominal value of $\boldsymbol{t}_{ij}$, normalized by the RTR of $\boldsymbol{t}_{ij}$. Recall that $\boldsymbol{\alpha} \circ \Delta \boldsymbol{t}_{ij}$ is the retained tolerance region for target variables $\boldsymbol{t}_{ij}$, in which $\boldsymbol{\alpha}$ is determined by the system level optimizer and sent to SSi from SS0:

$$
\begin{aligned}
& C_i = \frac{\boldsymbol{y}_{ij}(\boldsymbol{x}, \boldsymbol{p}, \boldsymbol{t}_{ji}) - \boldsymbol{t}_{ij,0}}{\boldsymbol{\alpha} \circ \Delta \boldsymbol{t}_{ij}}, \; j \neq i \\
& \boldsymbol{p}_0 - \boldsymbol{\alpha} \circ \Delta \boldsymbol{p} \leq \boldsymbol{p} \leq \boldsymbol{p}_0 + \boldsymbol{\alpha} \circ \Delta \boldsymbol{p} \\
& \boldsymbol{t}_{ji,0} - \boldsymbol{\alpha} \circ \Delta \boldsymbol{t}_{ji} \leq \boldsymbol{t}_{ji} \leq \boldsymbol{t}_{ji,0} + \boldsymbol{\alpha} \circ \Delta \boldsymbol{t}_{ji} \\
& \boldsymbol{p} = \{\boldsymbol{p}_{sh}, \boldsymbol{p}_t\}, \; \boldsymbol{\alpha} = \{\boldsymbol{\alpha}_{SS0}, \boldsymbol{\alpha}_i\}
\end{aligned}
\tag{3.7b}
$$

For the SA problem in sub-system i (SSi), the decision variables are the uncertainty reduction vector $\boldsymbol{\alpha}_i$ for the local uncertainty parameters $\boldsymbol{p}_i$. The two objectives for each sub-system are again to minimize $Investment_{SSi}$ while simultaneously minimizing the maximum of either the output variation at the local sub-system level R_{SSi}, or the variation in coupling variables, η_{Ci} in SSi. In Eqn. (3.8), R_{SSi} is again a measure of the variation in the sub-system's outputs, here normalized by the corresponding sub-system's AOVR $\Delta \boldsymbol{o}_{0,i}$, which is the presumed acceptable variation for the sub-system's outputs. This optimization problem is subject to two constraints as shown in Eqn. (3.8), including: 1) the variation in the SSi's original outputs must be enclosed by the designated AOVR of SSi; and 2) the variation in coupling variables must be less than the retained tolerance region of target variables (determined in SS0). These constraints must be satisfied in all sub-systems in order to maintain the consistency of the system under uncertainty. Thus the SA optimization problem formulation in SSi is as follows:

$$
\begin{aligned}
&\min_{\boldsymbol{\alpha}_i} \quad \max\left(R_{\mathrm{SS}i}, \eta_{C_i}\right) \\
&\min_{\boldsymbol{\alpha}_i} \quad Investment_{\mathrm{SS}i} \\
&s.t. \\
&\quad \max\left(R_{\mathrm{SS}i}, \eta_{C_i}\right) \le \mathbf{1} \\
&\quad R_{\mathrm{SS}i} = \max_{\boldsymbol{p}, \boldsymbol{t}_{ji}} \left\| \frac{\Delta \boldsymbol{o}_i(\boldsymbol{p})}{\Delta \boldsymbol{o}_{\mathbf{0},i}} \right\|_\infty, \quad \eta_{C_i} = \max_{\boldsymbol{p}, \boldsymbol{t}_{ji}} \left\| C_i \right\|_\infty \\
&where \\
&\quad C_i = \frac{\boldsymbol{y}_{ij}(\boldsymbol{x}_0, \boldsymbol{p}, \boldsymbol{t}_{ji}) - \boldsymbol{t}_{ij,0}}{\boldsymbol{\alpha} \circ \Delta \boldsymbol{t}_{ij}}, j \ne i \\
&\quad \Delta \boldsymbol{o}_i(\boldsymbol{p}) = \boldsymbol{o}_i(\boldsymbol{x}_0, \boldsymbol{p}) - \boldsymbol{o}_i(\boldsymbol{x}_0, \boldsymbol{p}_0) \\
&\quad \boldsymbol{p}_0 - \boldsymbol{\alpha} \circ \Delta \boldsymbol{p} \le \boldsymbol{p} \le \boldsymbol{p}_0 + \boldsymbol{\alpha} \circ \Delta \boldsymbol{p} \\
&\quad \boldsymbol{t}_{ji,0} - \boldsymbol{\alpha} \circ \Delta \boldsymbol{t}_{ji} \le \boldsymbol{t}_{ji} \le \boldsymbol{t}_{ji,0} + \boldsymbol{\alpha} \circ \Delta \boldsymbol{t}_{ji} \\
&\quad \boldsymbol{p} = \{\boldsymbol{p}_{sh}, \boldsymbol{p}_i\}, \boldsymbol{\alpha} = \{\boldsymbol{\alpha}_{\mathrm{SS0}}, \boldsymbol{\alpha}_i\}
\end{aligned}
\tag{3.8}
$$

The MIMOSA formulation is also shown in Figure 3.6 at both system and sub-system levels.

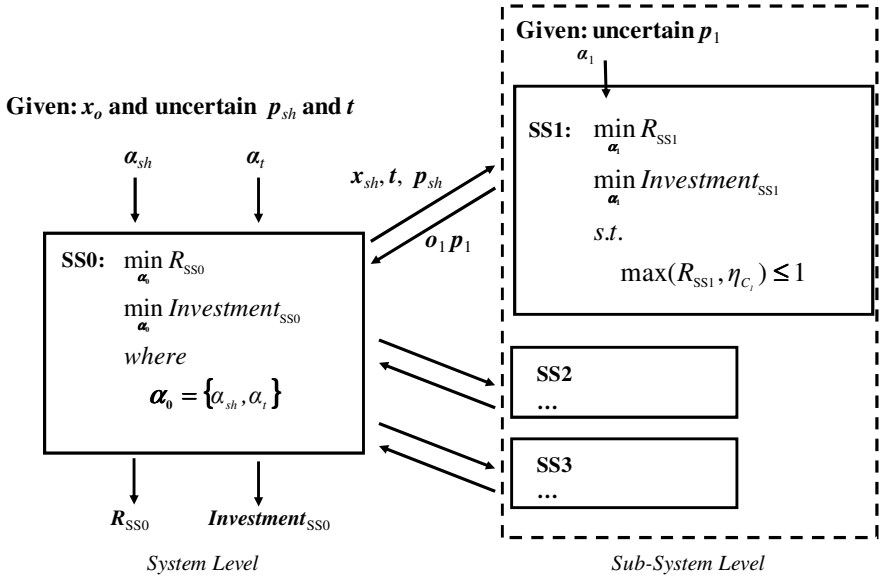

Figure 3.6: MIMOSA Formulation

A simplified formulation of MIMOSA at the sub-system level is also provided as shown in Eqn. (3.9), for the cases where a designer does not know or specify an AOVR for the sub-system outputs. In this regard, as long as the overall system is collaboratively

consistent by enforcing the constraint on η_{Ci} in Eqn. (3.9), the solution found will be acceptable. In this simplified formulation, normalization of R_{SSi} is still necessary in order to handle the possibility of different units or orders of magnitude in the sub-system outputs, and is accomplished by using the nominal output values. However, the value of R_{SSi} is usually much less than the value of η_{Ci} in this formulation and as a result the first objective of the SA problem for each sub-system should only minimize R_{SSi} alone. In Section 3.4, Eqn. (3.8) and Eqn. (3.9) will be used in the numerical and engineering example, respectively.

$$
\begin{aligned}
&\min_{\boldsymbol{\alpha}_i} \quad R_{SSi} \\
&\min_{\boldsymbol{\alpha}_i} \quad Investment_{SSi} \\
&s.t. \\
&\quad \eta_{C_i} \le 1 \\
&\quad R_{SSi} = \max_{\boldsymbol{p},\boldsymbol{t}_{ji}} \left\| \frac{\Delta \boldsymbol{o}_i(\boldsymbol{p})}{\boldsymbol{o}_i(\boldsymbol{x}_0, \boldsymbol{p}_0)} \right\|_\infty, \quad \eta_{C_i} = \max_{\boldsymbol{p},\boldsymbol{t}_{ji}} \left\| C_i \right\|_\infty \\
&where \\
&\quad C_i = \frac{\boldsymbol{y}_{ij}(\boldsymbol{x}_0, \boldsymbol{p}, \boldsymbol{t}_{ji}) - \boldsymbol{t}_{ij,0}}{\boldsymbol{\alpha} \circ \Delta \boldsymbol{t}_{ij}}, j \ne i \\
&\quad \Delta \boldsymbol{o}_i(\boldsymbol{p}) = \boldsymbol{o}_i(\boldsymbol{x}_0, \boldsymbol{p}) - \boldsymbol{o}_i(\boldsymbol{x}_0, \boldsymbol{p}_0) \\
&\quad \boldsymbol{p}_0 - \boldsymbol{\alpha} \circ \Delta \boldsymbol{p} \le \boldsymbol{p} \le \boldsymbol{p}_0 + \boldsymbol{\alpha} \circ \Delta \boldsymbol{p} \\
&\quad \boldsymbol{t}_{ji,0} - \boldsymbol{\alpha} \circ \Delta \boldsymbol{t}_{ji} \le \boldsymbol{t}_{ji} \le \boldsymbol{t}_{ji,0} + \boldsymbol{\alpha} \circ \Delta \boldsymbol{t}_{ji} \\
&\quad \boldsymbol{p} = \{\boldsymbol{p}_{sh}, \boldsymbol{p}_i\}, \boldsymbol{\alpha} = \{\boldsymbol{\alpha}_{SS0}, \boldsymbol{\alpha}_i\}
\end{aligned}
\tag{3.9}
$$

Notice first that in Eqn. (3.6) for SS0 and Eqn. (3.8) (or Eqn. (3.9)) for SS*i*, no additional information on the input-output relation from the analysis models is required. The analysis models in SS0 and SS*i* are treated like black-boxes and can be any kind of functions or computer simulations as long as the input and output values are provided. In addition, if one α_k value in the uncertainty reduction vector is intentionally fixed to be zero and all other elements to be one, one parameter is essentially "left out" and the

corresponding R_{SSi} value can be calculated. By repeating this for each parameter (or combination of parameters), the quantitative comparison on the importance of the parameter(s) can be obtained as using a traditional "leave one out" GSA method. However, the MIMOSA approach is more capable in that it allows every α_k value not only to be zero or one but also any value between them, optimally determined by the approach. In this regard, all uncertain input parameters in one sub-system can vary within the RTR specified by the $\boldsymbol{\alpha}$ vector and can affect the variation in sub-system outputs simultaneously. Thus, not only the main effect of each parameter, but also the interaction effects of those parameters are considered in this approach within the optimal uncertainty ranges. The individual importance of each parameter can also be determined from the resulting optimal solutions to Eqns. (3.6) and (3.8) as discussed later in Section 3.4. Due to the system properties considered by the MIMOSA approach, e.g., multi-input, multi-output, black-box analysis models, and most importantly, variable uncertainty ranges (i.e., not just zero or one for $\boldsymbol{\alpha}$ values), the MIMOSA approach is capable of providing more information about a system than produced by the other existing multi-disciplinary GSA approaches reviewed in Section 3.1.

3.3.3 Steps of MIMOSA

In order to perform the MIMOSA approach described above, an algorithm was developed and a step-by-step description of that algorithm follows. All system and sub-system SA problem optimizations are accomplished using evolutionary algorithms or more specifically using the Multi-Objective Genetic Algorithm (MOGA) [Deb, 2001]. The usage of MOGA to solve the system or sub-system level problems is not required and other multi-objective optimization approaches could also be applied, if applicable

and desired. However, MOGA is used in this approach because of its flexibility in finding all Pareto solutions simultaneously, its ability to handle non-linear and non-differentiable output functions with both continuous and/or discrete variables, and its ease in incorporating "black-box" type simulations. These properties are very common in the real engineering applications that are the target problems of this approach. However, MOGA is not the only choice of optimization solvers for use in this approach. The decomposed SA optimization formulation is solved using a multi-objective multi-disciplinary optimization technique [Aute and Azarm, 2006] as previously mentioned. The MIMOSA steps are as follows:

Step 1: Select a candidate design alternative (or a trial design), $\boldsymbol{x}_0$, whose sensitivity analysis is to be studied.

Step 2: Select which input parameters are to be studied, and then determine the interval uncertainty for those parameters, specifying the original TR, $\boldsymbol{p} = [\boldsymbol{p}_0 + \Delta\boldsymbol{p},\ \boldsymbol{p}_0 - \Delta\boldsymbol{p}]$ for all parameters at the system and sub-system levels.

Step 3: Select the original TR for target values $\boldsymbol{t} = [\boldsymbol{t}_0 + \Delta\boldsymbol{t},\ \boldsymbol{t}_0 - \Delta\boldsymbol{t}]$ at the system level.

Step 4: Initialize the optimization problem at the system level (SS0) as in Eqn. (3.6), given the system level design $\boldsymbol{x}_{sh}$ and original TR for $\boldsymbol{p}_{sh}$, and $\boldsymbol{t}$.

Step 5: Select the initial values for $\boldsymbol{\alpha}_{SS0}$ at the system level for each element in $\boldsymbol{p}_{sh}$ and $\boldsymbol{t}$, and use $\boldsymbol{\alpha}_{SS0}$ to calculate $Investment_{SS0}$.

Step 5: Send the system design variables, nominal shared parameters, nominal target values, and system level $\boldsymbol{\alpha}_{SS0}$ values to each sub-system level SA problem.

Step 6: Simultaneously initialize the SA approach in each sub-system level problem (SSi), given the $\boldsymbol{x}_{sh}$, $\boldsymbol{\alpha}_{SS0,}$ $\boldsymbol{p}_{sh}$, and $\boldsymbol{t}$ values from SS0 along with sub-system variables and parameters, including initial $\boldsymbol{\alpha}_i$ values for the sub-system level uncertain parameters.

Step 7: Determine the optimal $\boldsymbol{\alpha}_i$ to the optimization problem in Eqn. (3.8) (or Eqn. (3.9)) for each sub-system using MOGA, considering the variation in sub-system's outputs (i.e., the variation in outputs and/or coupling variables) and *Investment* as the objectives, while ensuring the collaborative consistency constraint and/or AOVR constraint.

Step 8: Return optimal output values and local optimal uncertainty reduction vector $\boldsymbol{\alpha}_i$ to the system level (SS0) from the sub-systems. If more than one local optimal solution $\boldsymbol{\alpha}_i$ is identified, some selection strategy should be used to select one local optimal solution for each sub-system. In this work, two selection strategies have been used: the optimal solution from the SSi's Pareto with the maximum and minimum R_{SSi} value will be selected as the sub-system's single optimal solution in the numerical example and the engineering example in Section 3.4, respectively, and will be returned back to SS0. Other appropriate strategies for selecting a single solution from the sub-system Pareto are also acceptable.

Step 9: Analyze system level R vs. *Investment* Pareto optimal solutions to Eqn. (3.6) for uncertainty reduction vector, $\boldsymbol{\alpha}_{SS0}$.

Step 10: Check stopping criteria of the system level SA problem. If stopping criteria are satisfied, stop the algorithm; otherwise generate a new set of candidates of uncertainty reduction vector $\boldsymbol{\alpha}_{SS0}$ at the system level from the optimizer, go to *Step 5*, and repeat sub-system level optimizations.

The stopping criteria used is a pre-specified maximum number of iterations (which is large enough to ensure convergence), plus an additional complementary stopping criterion that further requires that a sufficient number of Pareto solutions are produced during several successive generations. In other words, when the number of Pareto solutions is more than some pre-specified percentage of the population size and when it becomes steady (e.g., the number of Pareto solutions is more than "40% population size", for several generations), it can be concluded that the algorithm has converged. Compared to single-disciplinary SA approaches, the computational effort in this new MIMOSA approach will be larger due to the bi-level nature of the problem and will increase further when the number of sub-systems considered is increased, since a SA optimization problem (as shown in Eqn. (3.8)) must be solved for each sub-system considered. If the number of function calls in SS0 in Eqn. (3.6) is N_{SS0} and the number of function calls in each sub-system is N_{SSi} and the number of function calls to evaluate R_{SSi} in each sub-system is N_R, then the total number of function calls in MIMOSA is $O[N_{SS0} \times \text{NumSS}(N_{SSi} \times N_R)]$, where NumSS is the number of sub-systems. The computational cost of MIMOSA may increase when the number of sub-systems and/or the number of system inputs are increased.

3.4 EXAMPLES AND RESULTS

In this section, a numerical example and an engineering example are presented to demonstrate the applicability of the MIMOSA approach. Eqns. (3.8) and (3.9), as well as different selection strategies discussed above in Step 8 of Subsection 3.3.3, are used in those two examples, respectively, for the sub-system level SA problems.

3.4.1 Numerical Example

A two-output, bi-level numerical example is adapted from a previously presented bi-level MDO problem with two coupled sub-systems [Li and Azarm, 2008]. The two-output formulation for this problem in a single-disciplinary (or all-at-once) formulation is given in Eqn. (3.10). There are three design variables: $\boldsymbol{x} = \{x_1, x_2, x_3\}$, two output functions: $\boldsymbol{o} = \{o_1, o_2\}$.

$$\begin{aligned} o_1 &= x_2^{\,2} + x_3 + y_1 + e^{-y_2} \\ o_2 &= x_1 + \sqrt{x_2} + (y_2^{\,2} - y_1^{\,3})/10^4 + 150 \end{aligned} \tag{3.10}$$

The two coupling variables are y_1 and y_2 which make the two sub-systems fully coupled:

$$\begin{aligned} y_1 &= \boldsymbol{Y}_1(\boldsymbol{x}, y_2) = x_1^{\,2} + x_2 - 0.2y_2 \\ y_2 &= \boldsymbol{Y}_2(\boldsymbol{x}, y_1) = x_1 + x_3 + \sqrt{y_1} \end{aligned} \tag{3.11}$$

The above all-at-once formulation is converted into a system level and two sub-system level SA problems. Between these two sub-systems SSi, i =1 and 2, there are two coupling variables $\boldsymbol{y} = \{y_1, y_2\}$. In each sub-problem, there are two outputs in addition to the coupling variable. The decomposed formulation for this problem is as follows.

In SS0, $\boldsymbol{x}_{sh}$ includes only one design variable x_1 and the vector of target variables $\boldsymbol{t}$ includes two target variables t_1 and t_2 corresponding to the two coupling variables y_1 and y_2. Thus $\boldsymbol{x}_{sh} = \{x_1\}$, $\boldsymbol{t}_{12} = \{t_1\}$ and $\boldsymbol{t}_{21} = \{t_2\}$. Each output in SS0 is the summation of the corresponding outputs of two sub-systems as shown in Eqn. (3.12), where $o_{i,j}$, i, j =1 and 2, is j^{th} output in SSi and calculated from Eqn. (3.13) and Eqn. (3.14) below:

$$\begin{aligned} o_{0,1} &= o_{1,1} + o_{2,1} = y_1 + x_2^{\,2} + x_3 + e^{-y_2} \\ o_{0,2} &= o_{1,2} + o_{2,2} = -y_1^{\,3}/10^4 + 150 + \sqrt{x_2} + y_2^{\,2}/10^4 + x_1 \end{aligned} \tag{3.12}$$

SS1 has the local design variable: $\boldsymbol{x}_1 = \{x_2\}$, and the local copy of the target variable for t_2, i.e., t_2^1. The two outputs of SS1 plus the coupling variable y_1 are given in Eqn. (3.13):

$$\begin{aligned} o_{1,1} &= x_2^{\,2} + y_1 \\ o_{1,2} &= \sqrt{x_2} - y_1^{\,3}/10^4 + 150 \\ y_1 &= x_1^{\,2} + x_2 - 0.2t_2^1 \end{aligned} \tag{3.13}$$

Similarly, SS2 has the local design variable $\boldsymbol{x}_2 = \{x_3\}$ and the local copy of the target variable for t_1, i.e., t_1^2. The two outputs of SS2 plus the coupling variable y_2 are given in Eqn. (3.14):

$$\begin{aligned} o_{2,1} &= x_3 + e^{-y_2} \\ o_{2,2} &= x_1 + y_2^{\,2}/10^4 \\ y_2 &= x_1 + x_3 + \sqrt{t_1^2} \end{aligned} \tag{3.14}$$

The interval uncertainty is assumed in input variables x_1, x_2 and x_3, within ±6% from nominal. The AOVR for the outputs $\boldsymbol{o}_1$ and $\boldsymbol{o}_2$ in SS1 and SS2 is ±5 units from their nominal. The original TR for the target variables is: $\{\Delta t_1, \Delta t_2\} = \{\pm 4, \pm 3\}$ units from their nominal. The candidate design alternative selected is $\boldsymbol{x}_0$: $\{x_1, x_2, x_3, t_1, t_2\}$ = {-5.478, 0.035, 0.410, 30.262, 0.448}. The variables at the system level are $\boldsymbol{\alpha}_{SS0} = \{\alpha_{x_1}, \alpha_{t_1}, \alpha_{t_2}\}$. Here it is assume that not all of the uncertainties in the system can be completely reduced for each parameter, so α_{t_1} and $\alpha_{t_2}$are assumed to be in the ranges [0.3, 1] and [0, 1], respectively. At the sub-system level, the design variable in SS1 and SS2 are $\boldsymbol{\alpha}_1 = \{\alpha_{x_2}\}$ and $\boldsymbol{\alpha}_2 \equiv \{\alpha_{x_3}\}$ which are in the range [0, 1]. The MIMOSA formulation of this example for SS0, SS1 and SS2 is shown in Figure 3.7. The Pareto solutions are shown in Figure 3.8.

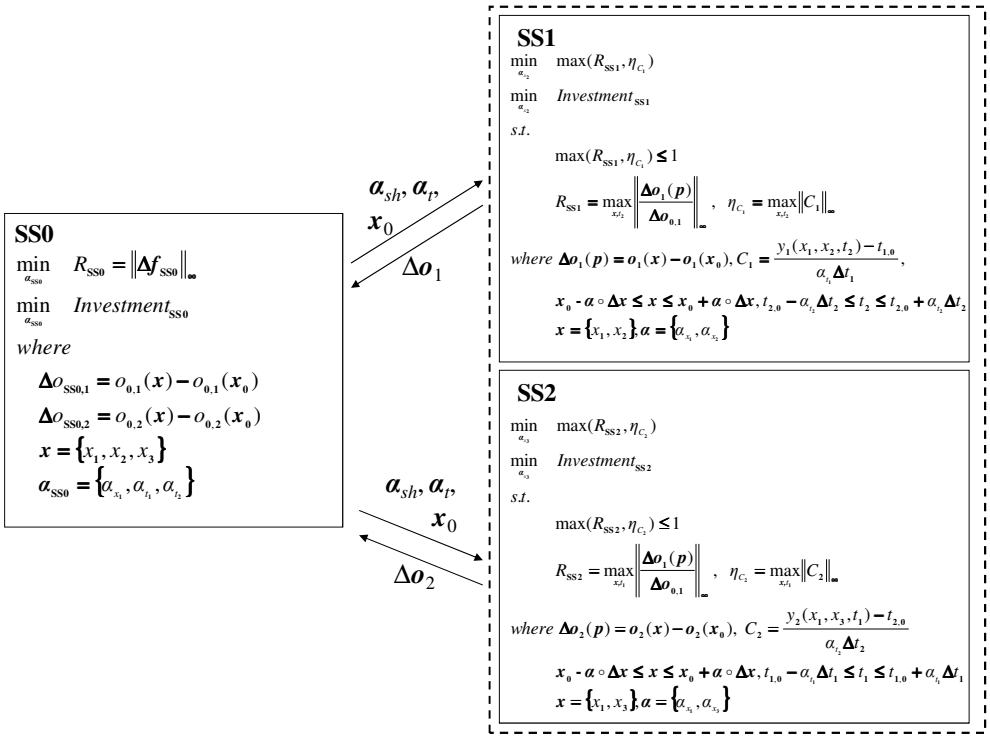

Figure 3.7: Numerical Example: The MIMOSA Formulation

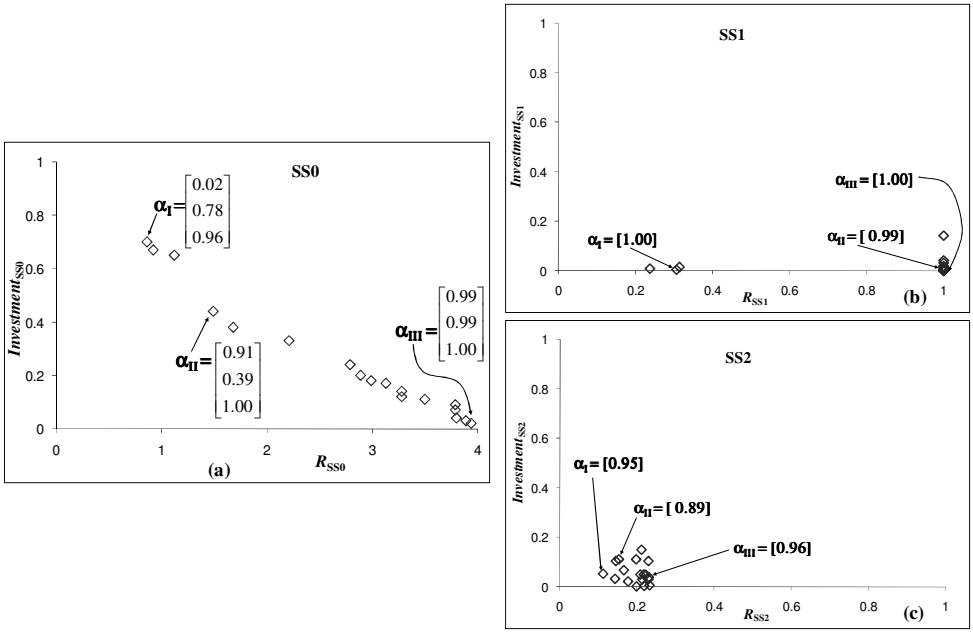

Figure 3.8: Numerical Example: Pareto Solutions at (a) SS0, (b) SS1 and (c) SS2

In this example, the optimal solution from the SS*i*'s Pareto with the maximum R_{SSi} value is selected as the sub-system's single optimal solution and is sent back to SS0. This

selection strategy is used in the cases that the designers in the sub-systems prefer the optimal $\boldsymbol{\alpha}_i$ with the minimum investment as long as the AOVR and consistency constraints are satisfied.

The obtained Pareto solutions with three typical $\boldsymbol{\alpha}$ solutions at the system and sub-system levels using the formulation in Eqn. (3.8) are shown in Figure 3.8 as well as in Table 3.1. The trade-off between the *Investment* and variation in SS0's outputs, R_{SS0} are clear. R_{SS0} (the variation in SS0) is decreasing with the increasing of *Investment*. As shown in Table 3.1, $\boldsymbol{\alpha}_{III}$ = {0.99 0.99 1} gives almost the original uncertainty, which represents the maximum uncertainty in the input parameters. $R_{SS0}(\boldsymbol{\alpha}_{III})$ is approximately 4% of the nominal output values of SS0, which is almost the biggest variation observed in SS0. When the RTR is reduced to $\boldsymbol{\alpha}_{II}$ = {0.91 0.39 1}, $R_{SS0}(\boldsymbol{\alpha}_{II})$ is reduced to 1.5% of the nominal output values. If the *RTR* is further reduced to $\boldsymbol{\alpha}_{I}$ (i.e., {0.02 0.78 0.96}), $R_{SS0}(\boldsymbol{\alpha}_{I})$ is only about 0.9% of the nominal output values, which is the smallest variation observed in SS0 for this problem. The corresponding sub-system values are shown in the chapter appendix. Clearly, as *Investment* values are increasing in this procedure, the amount of uncertainty in input parameters and outputs is eliminated, as shown in Table 3.1. The details of sub-system solutions corresponding to Figure 3.8 are shown in Table 3.2.

Table 3.1: Typical $\boldsymbol{\alpha}$ Solutions, *Investment* vs. R_{SS0}

	x_1	t_1	t_2	R_{SS0} (% of nominal)	*Investment*
α_I	0.02	0.78	0.96	0.86%	70%
α_{II}	0.91	0.39	1.00	1.49%	44%
α_{III}	0.99	0.99	1.00	3.94%	2%

Table 3.2: Detailed Values for Pareto Solutions in Figure 3.8

(a) SS1

Solution #	α_{x_2}	$\max\{R_{SS2}, \eta_{C_1}\}$	$Investment_{SS1}$	η_{C_1}	$\Delta o_{1,1}$	$\Delta o_{1,2}$
1: α_I	0.996	0.306	0.004	0.306	0.648	0.165
2	0.992	0.237	0.008	0.237	0.628	0.16
3	0.985	0.314	0.015	0.314	0.839	0.214
4: α_{II}	0.99	1	0.01	1	1.273	0.329
5	0.959	1	0.041	1	1.444	0.373
6	0.996	1	0.004	1	1.969	0.494
7	1	1	0	1	2.302	0.569
8	0.996	1	0.004	1	2.625	0.646
9	0.982	1	0.018	1	2.717	0.662
10	0.859	1	0.141	1	2.849	0.699
11	0.998	1	0.002	1	3	0.728
12	0.998	1	0.002	1	3	0.735
13	0.984	1	0.016	1	3.215	0.779
14	0.998	1	0.002	1	3.5	0.834
15	1	1	0	1	3.5	0.838
16	1	1	0	1	3.5	0.84
17	0.969	1	0.031	1	3.591	0.851
18: α_{III}	1	1	0	1	3.637	0.865

(b) SS2

Solution #	α_{x_3}	$\max\{R_{SS2}, \eta_{C_2}\}$	$Investment_{SS2}$	η_{C_2}	$\Delta o_{2,1}$	$\Delta o_{2,2}$
1:α_I	0.948	0.112	0.052	0.112	0.217	0.006
2	0.896	0.145	0.104	0.145	0.29	0.006
3	0.968	0.143	0.032	0.143	0.281	0.026
4:α_{II}	0.889	0.153	0.111	0.153	0.216	0.299
5	0.933	0.166	0.067	0.166	0.231	0.324
6	0.979	0.177	0.021	0.177	0.239	0.3
7	0.999	0.199	0.001	0.199	0.49	0.324
8	0.889	0.198	0.111	0.198	0.266	0.314
9	0.951	0.209	0.049	0.209	0.273	0.327
10	0.951	0.218	0.049	0.218	0.277	0.328
11	0.971	0.214	0.029	0.214	0.278	0.32
12	0.85	0.212	0.15	0.212	0.283	0.327
13	0.97	0.23	0.03	0.23	0.287	0.328
14	0.952	0.223	0.048	0.223	0.291	0.314
15	0.997	0.219	0.003	0.219	0.287	0.302
16	0.896	0.23	0.104	0.23	0.296	0.327
17	0.995	0.233	0.005	0.233	0.297	0.327
18:α_{III}	0.962	0.231	0.038	0.231	0.299	0.327

In order to identify the relative importance of each uncertain parameter, a correlation plot of α_1, α_2, R and *Investment* for all Pareto $\boldsymbol{\alpha}$ solutions in Figure 3.8 is given in Figure 3.9. To clearly illustrate the correlation among obtained solutions in Figure 3.8, correlation coefficient matrix values were calculated as defined in Section 3.2, for $\boldsymbol{\alpha}$, R, and *Investment* and are reported in Table 3.3. It can be shown from Figure 3.9 and Table 3.3 that among x_1, t_1, and t_2, the variable x_1 has the strongest correlation to the variation in SS0's outputs and *Investment*.

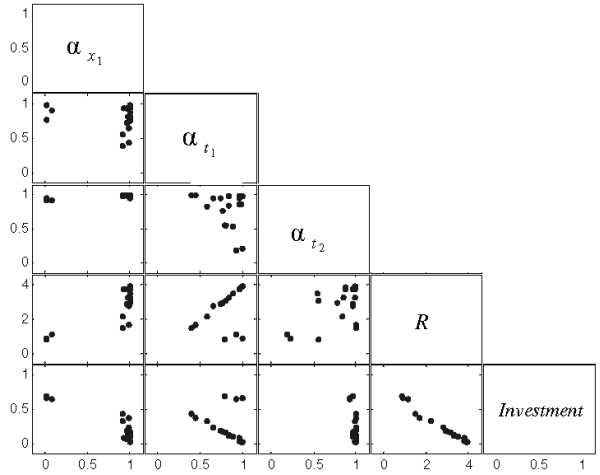

Figure 3.9: Numerical Example: Plots of Correlations among $\boldsymbol{\alpha}$, *Investment* and *R*

Table 3.3: Correlation Coefficient Matrix of Pareto solutions at System Level

Correlation Coefficient	α_{x_1}	α_{t_1}	α_{t_2}	R	*Investment*
α_{x_1}	1	-	-	-	-
α_{t_1}	-0.20	1	-	-	-
α_{t_2}	0.79	-0.33	1	-	-
R	0.78	0.45	0.54	1	-0.98
Investment	-0.87	-0.29	-0.64	-0.98	1

Several interesting observations can be concluded from Figure 3.8 and Table 3.2: i) The variations in all the sub-system level outputs and couplings are less than the specified AOVR and RTR of the target variables in each sub-system, but the variation in SS1 is

larger than the variation in SS2 as shown in Figures 3.8(b) and 3.8(c), showing that SS1 is more sensitive to the uncertainty; ii) Since the approach selects the optimal solution from SS's Pareto with the minimum *Investment*, $\boldsymbol{\alpha}$ solutions from SS1 and SS2 are both large and near to 1, meaning only small amount of uncertainty need to be reduced in x_2 and x_3; iii) The variations in SS1's outputs are much larger than those in SS2's outputs, making it clear that the uncertainty in SS1 has a much greater effect on the variation in the system level outputs and since the variation in SS2's outputs is always much less than 1, the AOVR (±5) for outputs in SS2 might be overestimated; iv) In both SS1 and SS2, the variation in the couplings (compared to their outputs) contributes significantly to each sub-system output variations; however, η_{C_2} in SS2 is much smaller than 1 while most η_{C_1} values are equal to 1 (i.e., the consistency constraint is active in SS1), meaning that the uncertainty propagated from SS2 to SS1 through the coupling variable t_2 has a greater effect than the variation propagated to SS2 in t_1. All those observations can help the designers revise the settings of AOVR and TR of the target variable and provide insights to understanding the uncertainty effects on this bi-level multi-disciplinary problem.

3.4.2 Engineering Example

To further demonstrate the capabilities of MIMOSA approach, a battery-powered right angle grinder model was chosen for its multi-disciplinary nature and its combination of continuous and discrete parameters. This angle grinder model was developed based on an all-at-once model first presented by Williams et al., [2008]. Here, Williams' model is decomposed into two coupled sub-system and a new battery sub-system is added, producing a bi-level multi-disciplinary system with three fully coupled sub-systems. Figure 3.10 depicts a graphical overview of this new angle grinder model. The grinder

system analysis models are collections of closed form equations, look-up tables and conditional functions used to described the various performance and constraint functions of the system as functions of geometric and performance parameters. Although the grinder model contains no complex analyses, such as finite element analysis, the system and sub-system analysis models are treated as "black-box" functions considering only inputs and outputs, which mirrors many engineering analysis models. The inclusion of more complex analysis examples would not change the MIMOSA approach beyond an obvious increase in the required computational effort.

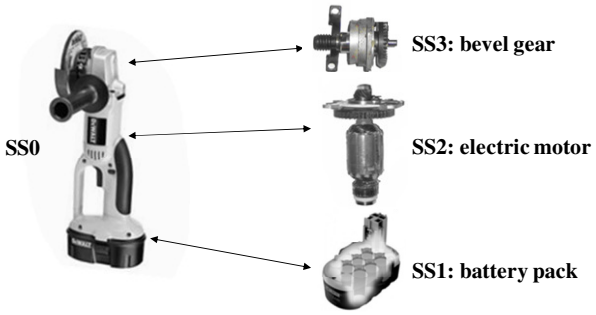

Figure 3.10: Engineering Example: Right Angle Grinder

The overall grinder system model (SS0) consists of three sub-systems which define the design of the three main physical components of the power tool: a battery pack model (SS1), an electric motor model (SS2) and a bevel gear assembly (SS3). The design of each of the three sub-systems, as shown in Figure 3.11, is accomplished through the use of various equations that describe the physics, performance and geometry of the specific sub-system. Additionally, each of the grinder's three sub-systems is connected to other sub-systems through coupling variables. For these reasons, this model provides a good platform for demonstrating the MIMOSA approach. Each of the sub-systems is briefly described in the following paragraphs.

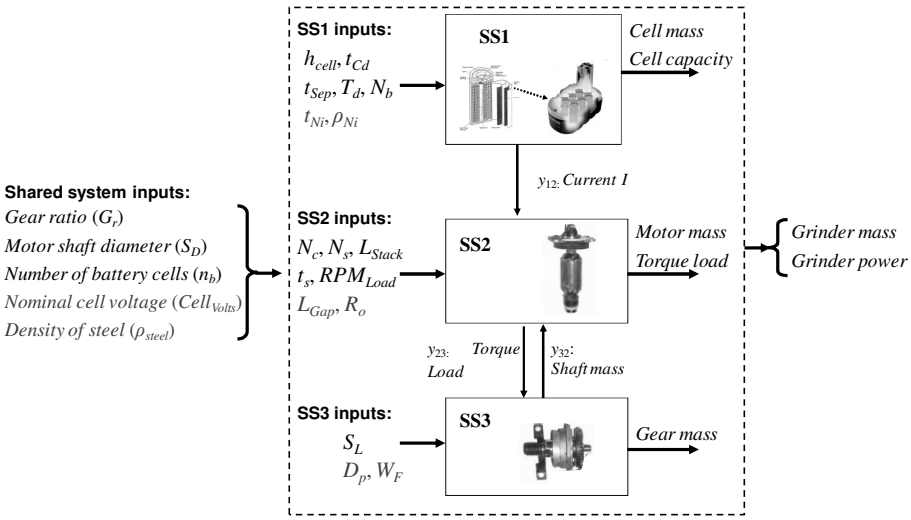

Figure 3.11: Design Variables, Couplings, and Outputs in Grinder Example

As shown in Figure 3.11, at the system level, there are three design variables that are used by more than one sub-system. These are gear ratio (G_r), motor shaft diameter (S_D), and number of battery cells in the battery pack (n_b), in which n_b is an integer variable. The overall system design outputs of interest are the total grinder mass and the total grinder power. Each sub-system has its own design variables and local outputs, as shown in Figure 3.11. More importantly, there are three coupling variables that connect three sub-systems: current (I) from SS1 to SS2, torque load from SS2 to SS3 and shaft mass from SS3 to SS2. In order to decompose the system into a decomposed framework, three target variables are introduced in SS0, one for each coupling. Thus, SS0 has six design variables in total. Two SS0's parameters have interval uncertainty in this example, as shown in Table 3.4. The design variables, parameters, and outputs of SS0 and each sub-system are detailed in the first column to the third column, respectively, in Table 3.4 to Table 3.7, where a bold font is used to highlight the design variables or parameters which have interval uncertainty in SS0 and each sub-system. As discussed earlier in Section 3.3, the target variables must have an original tolerance region and a retained

tolerance region controlled by their $\boldsymbol{\alpha}$ vector values. Additionally the outputs of interest in each sub-system have also been bolded and will necessarily have resulting variation.

Each sub-system has its own design variables and parameters. For this study two parameters or design variables for each sub-system are assumed to have interval uncertainty, so there are two α_k values established in each sub-system to control the possible uncertainty level reduction. Each sub-system also has two outputs of interest, selected from their analysis outputs, except SS3 (Bevel Gear) which has only one output due to the relatively simple nature of the model. Table 3.4 through Table 3.7 outlines the specifics of the 4 models that comprise the right angle grinder system.

Table 3.4: Grinder System (SS0)

Grinder Variables:	Grinder Parameters:	Grinder Outputs (Units):
Number of battery cells (n_b)	External components mass (m_{ext})	**Grinder mass (lbs)**
Gear ratio (G_r)	**Cell voltage ($Cell_{Volts}$)**	Grinder RPMs (rpm)
Motor shaft diameter (S_D)	**Density of steel (ρ_{steel})**	Grinder current (A)
Target Torque load		**Grinder power (W)**
Target Shaft Mass		Grinder duration (hr)
Target Current		Grinder grirth (in)

Table 3.5: Battery Sub-System (SS1)

Battery Variables:	Battery Parameters:	Battery Outputs (Units):
Battery cell height (h_{cell})	NiCd cell voltage (V_{cell})	**Battery cell mass (lbs)**
Ni reactant sheet thickness (t_{Ni})	**Density of Nickel (ρ_{Ni})**	**Battery cell capacity (Ah)**
Cd reactant sheet thickness (t_{Cd})	Density of Cadmium(ρ_{Cd})	Grinder voltage (V)
Separator sheet thickness (t_{Sep})	Density of Separator (ρ_{Sep})	Battery pack mass (lbs)
cell discharge time(T_d)	Density of cell wall material (ρ_{cw})	
Battery cell coil turns (N_b) - integer	Battery cell wall thickness (cwt)	

Table 3.6: Electric Motor Sub-System (SS2)

Motor Variables	Motor Parameters	Motor Outputs (Units)
Motor armature wire turns (N_c)	Density of steel (ρ_{steel})	**Motor mass (lbs)**
Stator armature wire turns (N_s)	Shear strength of steel (τ_{steel})	Motor girth (in)
Stator outer radius (R_o)	Demsity of copper (ρ_{Cu})	Motor RPM (rpm)
Stator thickness (t_S)	20 awg wire resistivity (R_w)	**Torque load (ft-lbs)**
Gap length (L_{Gap})	20 awg wire cross-section area (A_w)	
Stack length (L_{Stack})	Brush loss factor (α_{Brush})	
Grinder RPMs – loaded (RPM_{Load})	Permeability of free space (μ_O)	
	Permeability of steel (μ_{Steel})	

Table 3.7: Bevel Gear Sub-System (SS3)

Gear Variables:	Gear Parameters:	Gear Outputs (Units):
Motor shaft length (S_L)	Pressure angle (θ_P)	**Gear mass (lbs)**
Pinion pitch diameter (D_p)	**Face width (W_F)**	
	Gear elasticity factor (Z_e)	
	Amplification factor (K_a)	
	Load distribution factor (K_m)	
	Geometric factor (G_F)	
	Density of steel (ρ_{steel})	
	Arbor Mass (m_A)	
	Commutator Mass (m_C)	
	Pinion Shaft Mass (m_{PS})	

In this engineering example, it is assumed that the designer does not have a specified AOVR for SS0 or sub-systems and would like to understand the effects of input uncertainty on any possible variation ranges for the outputs at both system and sub-system levels. In this regard all output variations are normalized to their nominal output values and the MIMOSA formulation in Eqn. (3.9) is used for each sub-system. A grinder design was obtained to serve as the nominal or candidate solution using the the collaborative optimization approach of Aute and Azarm [2006]. Using this candidate design, a set of MIMOSA Pareto solutions is obtained using Eqn. (3.6) and Eqn. (3.9) at the system and sub-system levels with three typical solutions as shown in Figure 3.12. Different from the numerical example, the optimal $\boldsymbol{\alpha}_i$ solution with the minimum R_{SSi} is selected from SSi's Pareto in this engineering example and used to calculate the outputs

of the SA problem in SS0. The R_{SS0} is shown as a percentage of the nominal output function values. $\boldsymbol{\alpha} = \{\alpha_1, \alpha_2, \alpha_3, \alpha_4, \alpha_5\}$ is the uncertainty reduction vector corresponding for {target current, target torque load, target shaft mass, cell volts, density of steel}, as shown in bold in Table 3.4. The trade-off between *Investment* and the variation in SS0's outputs R_{SS0} are clearly shown in Figure 3.12. Figure 3.13 shows the correlation plot figures for five $\boldsymbol{\alpha}$ vector elements along with R_{SS0} and $Investment_{SS0}$ for all Pareto $\boldsymbol{\alpha}$ solutions shown in Figure 3.12. The correlation coefficient values for all Pareto $\boldsymbol{\alpha}$ solutions in Figure 3.12 are also given in Table 3.8.

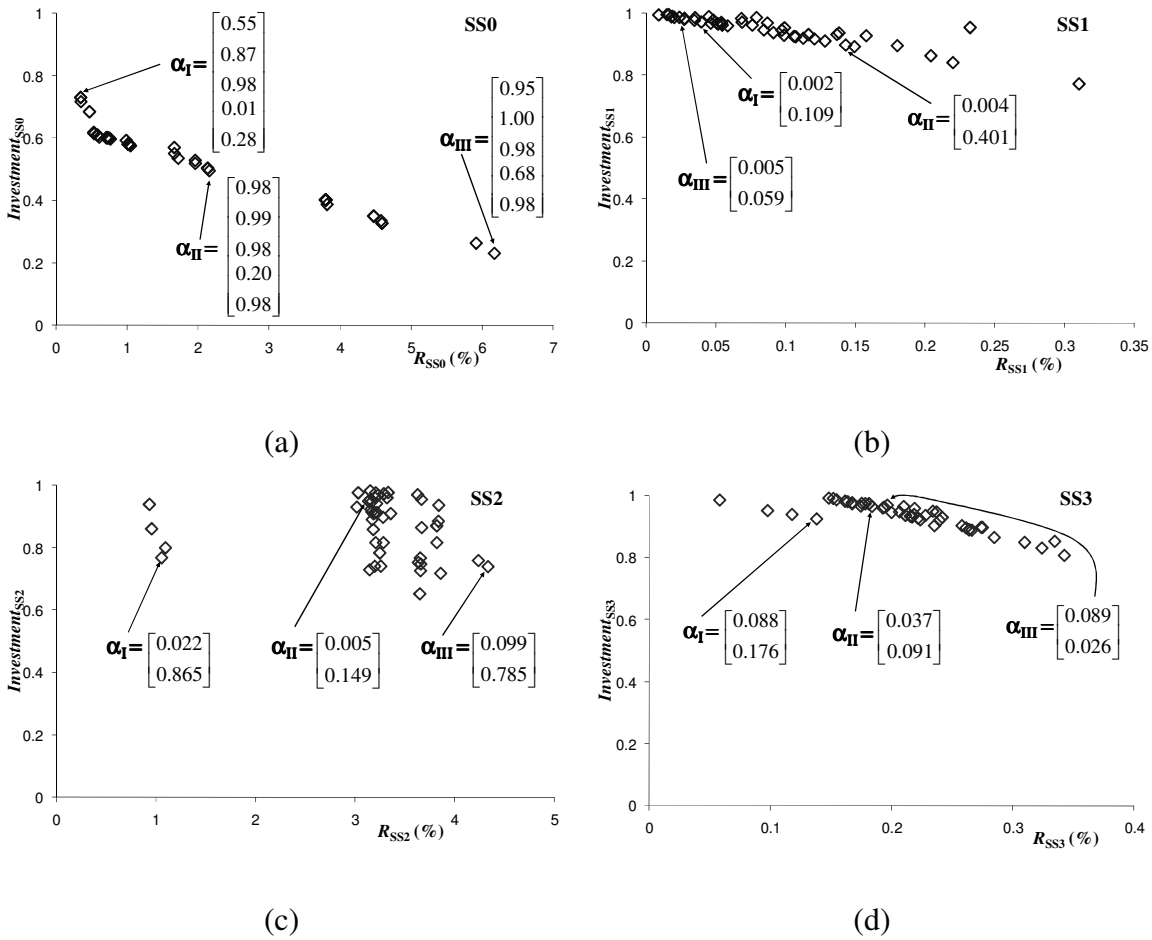

Figure 3.12: Grinder Design: Pareto Solutions for System and Sub-System Levels: (a) SS0, (b) SS1, (c) SS2, and (d) SS3

As shown in Figure 3.12(a), with the obtained largest uncertainty intervals ($\boldsymbol{\alpha}_{III}$ = {0.95 1.00 0.98 0.68 0.98}), the variations in SS0's outputs are about 6.2% of their nominal values. With more uncertainty being reduced (i.e., $\boldsymbol{\alpha}_{I}$ = {0.55 0.87 0.98 0.01 0.28}), the R_{SS0} can be reduced to around 0.3% of the nominal value.

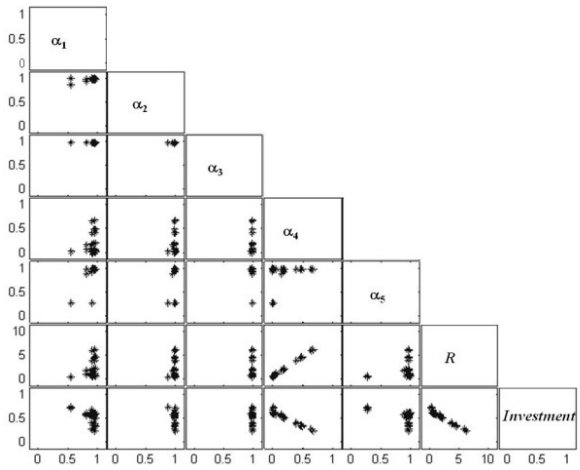

Figure 3.13: Grinder Design: Plots of Correlations among α_1 Investment and R

As clearly shown in Figure 3.13 and Table 3.8 (in the grey cells), among those five uncertain parameters, $Cell_{volts}$ (α_4) has the strongest, while target shaft mass has the weakest, correlation to the system output variation. Other three uncertain parameters are in the middle. In this regard, more investment should be used to reduce the uncertainty in the cell volts and the uncertainty in the current for the battery part (the second strongest correlated to R_{SS0}), which is consistent with expectations since the voltage and output current of the battery can significantly affect the performance of the grinder.

Table 3.8: Correlation Coefficient Matrix of Pareto Solutions at System Level

Correlation Coefficient	α_1	α_2	α_3	α_4	α_5	R	*Investment*
α_1	1	-	-	-	-	-	-
α_2	0.75	1	-	-	-	-	-
α_3	-0.18	-0.05	1	-	-	-	-
α_4	0.31	0.23	0.25	1	-	-	-
α_5	0.82	0.64	-0.19	0.29	1	-	-
R	0.34	0.25	0.24	1	0.32	1	-0.98
Investment	-0.51	-0.39	-0.19	-0.97	-0.50	-0.98	1

For the sake of brevity detailed solutions from each of the sub-systems are not given here. However, some additional observations are made in this example. Since a single optimal solution that possesses the minimum R_{SSi} from each sub-system's Pareto is selected for use in the corresponding SS0 solution, the *Investment* required by all three sub-systems are relatively large, as shown in Figure 3.12(b) to 3.12(d). It is also observed that although all three sub-systems have comparable variations in their mass values, after normalizing them by their nominal values, the normalized variation in SS2's outputs (Figure 3.12(c)) is considerably larger than the variation in SS1 and SS3 (Figure 3.12(b) and 3.12(d)). This shows that SS2 is more sensitive to the input uncertainty in this grinder model. The variations in the coupling variables are always less than the RTR of the target variables due to the consistency constraint. Moreover, at the sub-system level, three uncertain parameters, the nickel reactant sheet thickness in SS1, the stator outer radius in SS2, and the pinion pitch diameter in SS3, compared to another uncertainty parameter in the corresponding sub-system, are more strongly correlated to the output variations in their sub-systems. They have been underlined through Table 3.3 to Table 3.6. More investment should be spent on reducing uncertainty in those three parameters. This is an interesting finding recalling that in the current algorithm from the sub-system level the

uncertainty reduction vector ($\boldsymbol{\alpha}$) values are selected in order to produce the greatest reduction in sub-system output variation (minimum R without regard for *Investment*). In the case of the battery sub-system, this choice clearly demonstrates that controlling the nickel reactant sheet thickness parameter is far more important than controlling the density of the nickel used to ensure the performance of the battery sub-system. Figure 3.14 is a plot of the corresponding $\boldsymbol{\alpha}$ values for t_{Ni} and ρ_{Ni} from SS1 for all Pareto solutions at the system level shown in Figure 3.12. As can be seen on the figure, the uncertainty reduction value (α_k) for t_{Ni} is much smaller than the corresponding uncertainty reduction value for ρ_{Ni}, which indicates that in order to produce optimal variation reduction in the outputs for the battery sub-system, the uncertainty in the geometric parameter must be much more tightly controlled.

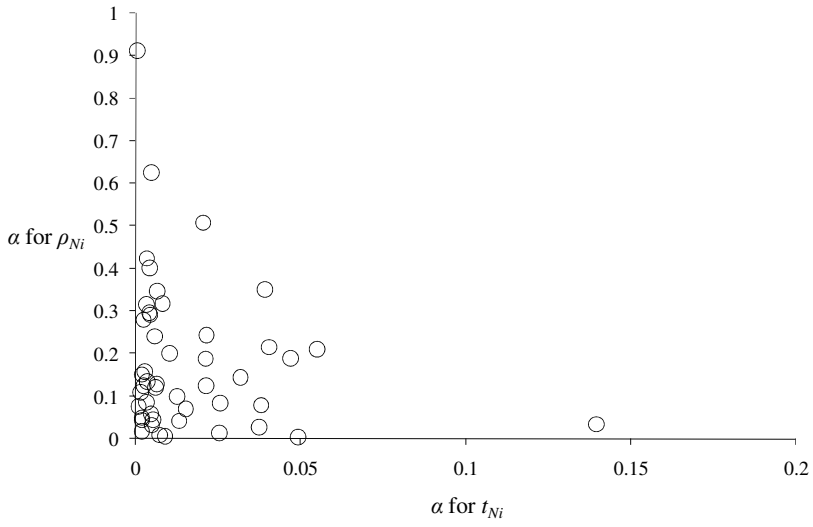

Figure 3.14: $\boldsymbol{\alpha}$ Values of t_{Ni} and ρ_{Ni} for Pareto Solutions at System Level

Based on the data presented, in order to optimally reduce the variation in the outputs at the system and sub-system levels, the designer of this right angle grinder should reduce the uncertainty mainly in the four parameters (or design variables) which are underlined through Table 3.4 to Table 3.7. The results shown here, while clearly

based on the grinder model used for this example, highlight the greater capability of the MIMOSA approach to efficiently identify the most important uncertain parameters in a complex model during the conceptual phase of design. This discussion is merely an example of the type of data that could be extracted from each of the other sub-systems and how it might be analyzed.

3.5 SUMMARY OF RESEARCH THRUST 1

In this chapter a new global SA method, called MIMOSA, is presented. MIMOSA has the ability to analyze the effects of uncertainty on system and sub-system performance for fully coupled multi-output multi-disciplinary problems in which uncertainty exists not only in parameters in each sub-system but also in the sub-system couplings. Given multiple interval uncertainties for parameters at the system and sub-system levels, MIMOSA can optimally identify how much the investment is necessary to optimally reduce uncertainty in input parameters in order to ensure a desired level of variation in the system and sub-systems' output values, considering a single design or a set of designs. Two metrics, *R* and *Investment*, have been used in the SA problems in SS0 and sub-systems to quantify the variation in multiple system and/or sub-system outputs and the cost used to reduce the input uncertainty. MIMOSA can also efficiently determine the relative importance among uncertain parameters in the system and sub-systems in terms of uncertainty reduction. Sub-systems' relative importance, in terms of their contribution to the entire system performance variation, can also be analyzed using this new approach. MIMOSA is a global SA approach which uses interval uncertainty to quantify the uncertainty instead of gradient information or probability density functions. Because MIMOSA is accomplished by using the MOGA as its optimization solver, it is

capable of handling both continuous and discrete design variables and/or parameters. Finally, MIMOSA is flexible enough to be able to handle various designer preferences, including the limits on parameter uncertainty reduction levels, different acceptable output variation levels, and different selection strategies if applicable.

The applicability and capabilities of the MIMOSA approach have been demonstrated using a numerical and an engineering example, both of which have multiple fully coupled sub-systems. The numerical example had two outputs in each of two sub-systems while the engineering example includes three sub-systems and has mixed continuous-discrete design variables. From the results obtained in these two examples, the trade-off between the investment used to reduce the uncertainty levels in the input parameters and the variations in the system outputs are clearly demonstrated. Both examples show the ability of MIMOSA to optimally determine the best uses of limited investment available for uncertainty reduction in the attempt to improve system performance in terms of reducing output variations. The correlation between uncertain parameters and the variations in the system and sub-system outputs are easily determined based on the obtained Pareto solutions for R vs. *Investment*. Both examples specifically present how the MIMOSA approach can identify the sub-system in a decomposed multi-sub-system problem that is the most sensitive to the uncertainty and has the greatest effect on the system level performance under uncertainty. The engineering example also demonstrates how MIMOSA is capable of isolating parameters whose uncertainty greatly influence system and sub-system outputs in contrast to those who do not. The importance of parameters in each of the sub-systems of the angle grinder has been identified as well.

The MIMOSA approach presented is adaptable to many different types of engineering problems and thus has a wide range of applications not specifically addressed in this research thrust. As a result of this flexibility, the MIMOSA approach is an excellent tool for clearly understanding and optimally eliminating the wide-spread effects of uncertainty in many different engineering design efforts based on designer preferences, limitations and/or goals. For instance, *Investment* could be further defined to include a real cost function associated with specific uncertainty reductions, and that cost function needs not be the same for all uncertain parameters within a problem (e.g., [Acar et al., 2007] and [Kale and Haftka, 2008]). MIMOSA could also be used to ignore (redundant) design parameters or outputs from the design process that are unimportant or already insensitive to uncertainty in favor of using valuable computational resources for the more important or more critical design aspects, thus simplifying a complicated problem down to a more manageable size consisting of more relevant issues.

The MIMOSA approach is clearly quite capable and very useful given the correct system properties, such as a preexisting candidate design and input uncertainty that is reducible about known nominal parameter values. However, as stated in Chapter 1, MIMOSA does not consider engineering feasibility which is a critical element of many engineering design challenges. The work presented in the next chapter attempts to address this shortcoming.

CHAPTER 4: MULTI-DISCIPLINARY COMBINED SENSITIVITY ANALYSIS (MICOSA)

4.1 INTRODUCTION TO RESEARCH THRUST 2

The goal of the second research thrust was quite simply to extend the MIMOSA approach of Chapter 3 to multi-disciplinary systems that may include infeasibility under uncertainty. The MIMOSA algorithm presented in Chapter 3 provides a multi-disciplinary SA framework, but it does not acknowledge the possibility for infeasibility due to the input parameter uncertainty in an engineering system. Just because a system's objectives, for example, are insensitive to the variation in its input parameters does not mean that the feasibility of the system is necessarily ensured under uncertainty. Furthermore it may at times be more important for the feasibility of a design to be insensitive to uncertainty than for the design be optimal in an objective sense. The ability to use uncertainty reduction to improve the performance of a system under uncertainty is a powerful tool. However, there is a very real possibility for uncertainty to lead to failure (infeasibility) at either the system level or sub-system level of a multi-disciplinary system. The work presented in this is chapter is a simple but necessary modification to the MIMOSA approach presented in previous chapter which makes it possible to use uncertainty reduction to also ensure engineering feasibility in addition to producing reduced output function variations. This new approach is called Multi-dIsciplinary, multi-objective COmbined Sensitivity Analysis (MICOSA); with the word "combined" chosen to indicate that this approach considers the effects of both objective and constraint function variations in a combined fashion.

4.2 BACKGROUND AND TERMINOLOGY

This section contains some relevant background and terminology used throughout the rest of this chapter.

4.2.1 MIMOSA Review

As previously stated, the MICOSA approach is a direct extension of the MIMOSA approach presented in Chapter 3. The MICOSA approach uses the same framework and is based on the same assumptions as the MIMOSA approach. All of the relevant details of the MIMOSA approach can be found in the preceding chapter.

4.2.2 Objective and Constraint Function Variation Metrics

In the previous chapter, the output functions analyzed by MIMOSA could be either objectives, constraints, or both, and the formulation of the approach made no distinction. As a result, in order to extend MIMOSA to also consider engineering feasibility a distinction between objectives and constraints is necessary. Eqn. (4.1) adapts the formulation for R presented in Chapter 3 for objective function(s) only, while Eqn. (4.2) adapts the R formulation for constraint function(s) only. Recall that the R metric presented in the previous chapter is a function of the $\boldsymbol{\alpha}$ vector, which is a measure of uncertainty reduction for the K input parameters to a system. In Eqns. (4.1) and (4.2) the vector $\boldsymbol{p}_v$ is established, which represents a single realization of the uncertain values $\boldsymbol{p}$ bounded by the retained uncertain interval $[\boldsymbol{p}_0 - \boldsymbol{\alpha} \circ \Delta\boldsymbol{p}, \boldsymbol{p}_0 + \boldsymbol{\alpha} \circ \Delta\boldsymbol{p}]$. This vector will be used throughout this chapter (and later on in the dissertation) as a decision variable when attempting to quantify the effect of input uncertainty.

$$R_f(\boldsymbol{\alpha}) = \max_{p_v} \left\| \Delta f_i(\boldsymbol{\alpha}) \right\|_2$$

$$\text{where} \quad \Delta f_i(\boldsymbol{\alpha}) = \frac{f_i(\boldsymbol{p}_v) - f_{0,i}}{f_{0,i}} \; i = 1,\ldots,\ I \tag{4.1}$$

$$(\boldsymbol{p}_0 - \boldsymbol{\alpha} \circ \Delta \boldsymbol{p}) \le \boldsymbol{p}_v \le (\boldsymbol{p}_0 + \boldsymbol{\alpha} \circ \Delta \boldsymbol{p})$$

$$R_g(\boldsymbol{\alpha}) = \max_{p_v} \left\| \Delta g_j(\boldsymbol{\alpha}) \right\|_\infty$$

$$\text{where} \quad \Delta g_j(\boldsymbol{\alpha}) = \left\{ \begin{array}{cc} \dfrac{g_j(\boldsymbol{p}_v) - g_{0,j}}{\left| g_{0,j} \right|} & \text{if } g_j(\boldsymbol{p}_v) > g_{0,j} \\ \mathbf{0} & \text{otherwise} \end{array} \right\} \; j = 1,\ldots,\ I \tag{4.2}$$

$$(\boldsymbol{p}_0 - \boldsymbol{\alpha} \circ \Delta \boldsymbol{p}) \le \boldsymbol{p}_v \le (\boldsymbol{p}_0 + \boldsymbol{\alpha} \circ \Delta \boldsymbol{p})$$

It should be noted that the value for R_g will be greater than 1 for an infeasible level of input uncertainty based on the formulation of Eqn. (4.2). This capability is important because it makes it possible to easily detect when a particular combination of input uncertainties will lead to potential engineering infeasibility.

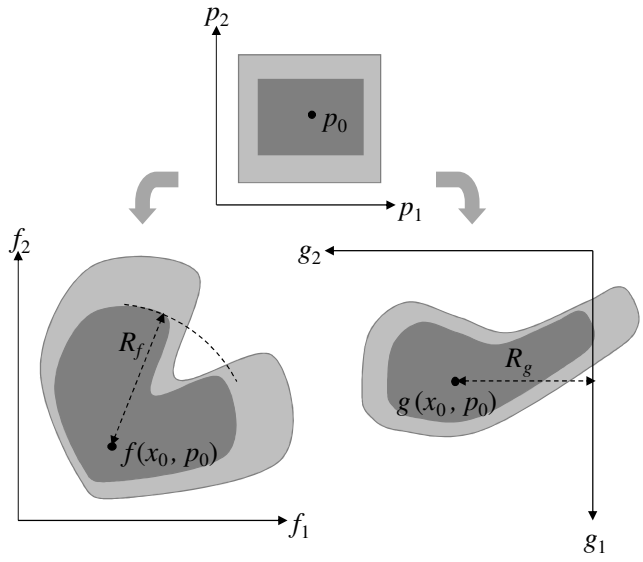

Figure 4.1: Effects of Reduced Uncertainty on Objectives and Constraints

Figure 4.1 depicts R_f and R_g graphically given input parameter uncertainty. Note that uncertainty in $\boldsymbol{p}$ will lead to uncertainty in $\boldsymbol{f}$ and $\boldsymbol{g}$, as discussed in Chapter 2. Note that for the light grey (larger) uncertain region, the value for g_2 is greater than 0 indicating

infeasibility, while the darker grey uncertain region ensures that all possible outcomes of $\boldsymbol{p}$ will result in all constraint functions (g_1 and g_2) being less than 0 and thus feasible. Refer to the discussion on multi-objective optimization in Chapter 2 for details on the violation of constraint functions within the context of optimal design.

4.2.3 Combined Output Variation Metric

To simultaneously consider both objective and constraint function variations, the following new metric, called R_c, is presented. This metric simply compares the resulting R_f and R_g values for a given level of input uncertainty and select the larger value. This formulation makes it possible for R_c to reflect the system performance measure, either objective function variation(s) or constraint function variation(s), that is more important for a given level of input uncertainty as specified by $\boldsymbol{\alpha}$. This metric will be used as an objective function in the MICOSA formulation which will be presented later in this chapter.

$$R_C = \max\left(R_f, R_g\right) \tag{4.3}$$

4.3 MICOSA FORMULATION

In order to account for the shortcoming of the MIMOSA approach previously discussed, the following extension was developed. This extension, called MICOSA, seeks to use uncertainty reduction as a means for improving the objective performance of a multi-disciplinary system design, while simultaneously ensuring the feasibility of the system under uncertainty. The MICOSA algorithm includes two changes from the MIMOSA formulation presented in the last chapter. First, the first objective function of the MICOSA formulation is changed to minimize R_c, vice R as was used in the previous

chapter. Recall that R_c is a function of R_f and R_g, which are given in Eqns. (4.1) and (4.2) respectively. Using R_c the MICOSA algorithm seeks to reduce variations in either the objective or constraint function(s) at the system and sub-system levels, whichever are greater given the current levels of input uncertainty. The second change is the inclusion of a constraint that R_g at both the system and sub-system levels must be less than or equal to 1. Using the formation for R_g provided in Eqn. (4.2), a value of R_g less than or equal to 1 will indicate a feasible system as previously discussed, assuming the nominal (deterministic) design is feasible. Eqn. (4.4a) provides this new MICOSA formulation, which is applicable to a single disciplinary system or any sub-system (SS*i*) within a multi-disciplinary framework. If Eqn. (4.4a) is used to analyze a single disciplinary system, the name of the approach is shorted to Combined Sensitivity Analysis (COSA) for simplicity. In this chapter the *Investment* metric has been abbreviated with the letter *I* only, but the formulation used is identical to that provided for *Investment* in Chapter 3.

$$\begin{aligned} &\min R_{C,SSi} \\ &\min I_{SSi} \\ &s.t. \quad R_{g,SSi} \le 1 \\ &where \quad R_{C,SSi} = \max(R_{f,SSi}, R_{g,SSi}) \end{aligned} \tag{4.4a}$$

For demonstration purposes, an unconstrained formulation of the COSA algorithm is provided in Eqn. (4.4b). Notice that Eqn. (4.4b) is identical to Eqn. (4.4a) except for the lack of the constraint on the value of R_g. This formulation is provided for comparison purposes and will be used to show that the formulation in Eqn. (4.4a) is necessary to achieve the stated goals of this research thrust, namely to ensure feasibility of the engineering system under uncertainty.

$$\begin{aligned} &\min R_{C,SSi} \\ &\min I_{SSi} \\ &where \quad R_{C,SSi} = \max(R_{f,SSi}, R_{g,SSi}) \end{aligned} \tag{4.4b}$$

MICOSA requires simply employing the MIMOSA framework with the new COSA formulation at the system and sub-system levels, as shown in Figure 4.2. The steps and procedures for employing the MICOSA approach are identical to that of MIMOSA as presented in the previous chapter. The only changes are those detailed above with regard to the new objective function R_c and the inclusion of the R_g constraint at the system and sub-system levels.

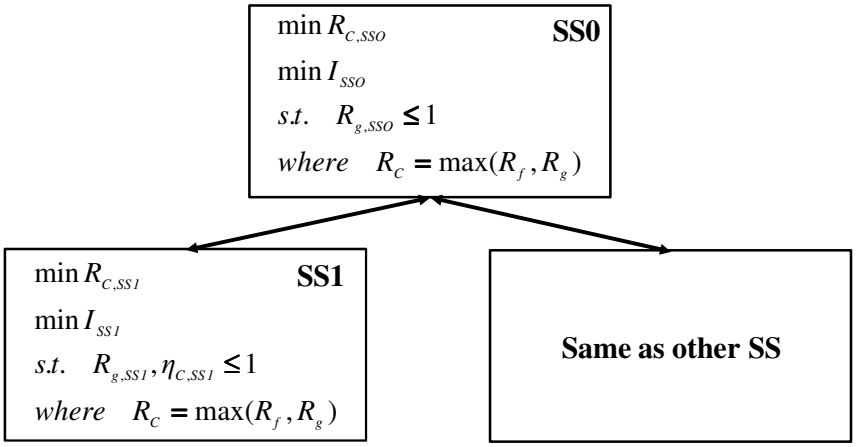

Figure 4.2: MICOSA Framework

4.4 EXAMPLES AND RESULTS

In an effort to demonstrate the capabilities of the approach, the MICOSA approach was applied to two examples, a single disciplinary propulsor model and a multi-disciplinary unmanned underwater vehicle (UUV) model. The single disciplinary model demonstrates the ability of the approach to ensure the feasibility of the system through uncertainty reduction. The multi-disciplinary example then demonstrates the ability of the approach to handle more complex system models within a decomposed framework.

4.4.1 Single Disciplinary Propulsor Example

To verify the COSA algorithm, the approach was used to analyze a candidate design for an undersea vehicle propulsor. The propulsor system analysis model is a set of meta-models fitted to a set of CFD data for a notional propulsor provided to the University of Maryland by the Naval Surface Warfare Center as part of active research collaborations. Figure 4.3 depicts this example problem. This figure contains several pieces of information required for employing COSA, including: the underlying optimization problem (e.g. maximizing propulsor efficiency and minimizing propulsor noise), the parameter values for the candidate design of interest (e.g. OD = 8.11 inches) and the nominal uncertainty levels (e.g. 1% of nominal for the outer diameter parameter value of 8.11 inches) for each of the input parameters.

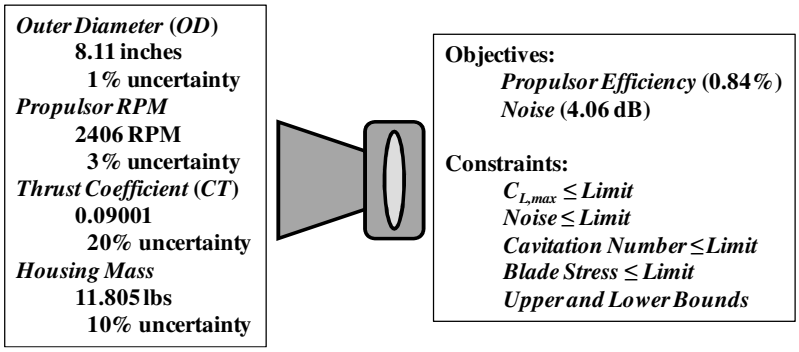

Figure 4.3: UUV Propulsor Model

Using the single disciplinary COSA algorithm the above problem was solved twice and the results are presented in Figure 4.4, once using the constrained formulation provided in Eqn. (4.4a) and once using the unconstrained formulation provided in Eqn. (4.4b). The Pareto frontiers provided on the left side of Figure 4.4 show the expected tradeoff between R_c and I. Of particular interest is the demonstrated need for the R_g constraint. As seen in the two solutions highlighted by the dashed circle on both sides of

the figure, the R_c and I values for the constrained and unconstrained solutions are similar (left side figure), but upon further examination the constrained solution is feasible (R_g < 1) and the unconstrained solution is infeasible (R_g > 1) as seen on the right side plot, which is not a Pareto frontier but rather a plot of R_g vs I for comparison purposes.

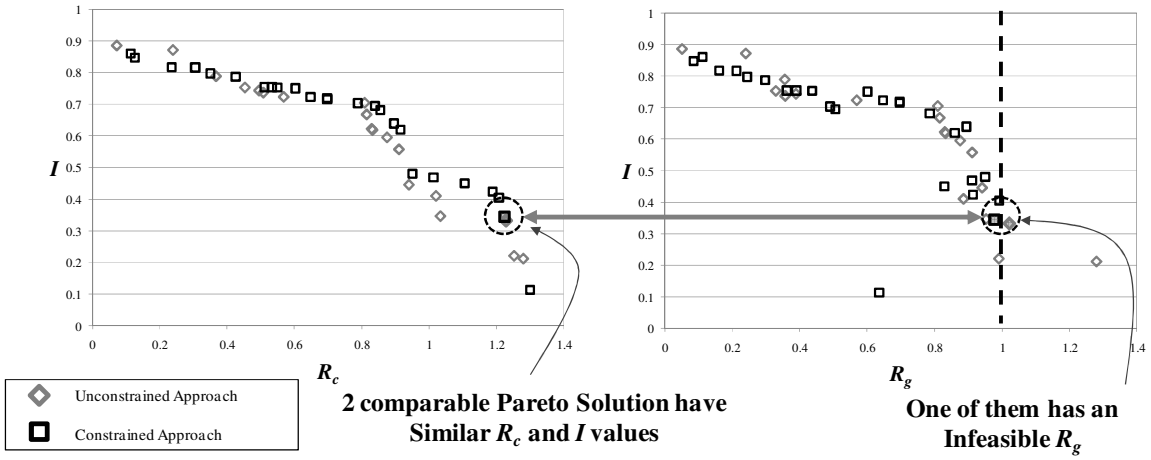

Figure 4.4: Combined Sensitivity Analysis Results for Propulsor Design

These two solutions differ in terms of how the reduced variation (R_c) is produced. Figure 4.5 depicts the uncertainty bands for each of the four parameters considered in the example, comparing the nominal uncertainty (black bands on the left side of each plot), the retained uncertainty in the unconstrained case (hollow grey bands in the middle of each plot) and the retained uncertainty in the constrained formulation (hollow black bands on the right of each plot), which is the actual COSA approach. In the unconstrained case the uncertainty in the housing mass is greatly reduced because this reduces the variation the propulsor mass (one of the objective functions for the original problem) more significantly. However, the uncertainty in the RPM value must have a greater effect on feasibility for the propulsor system and thus, when feasibility is considered in the constrained approach, the uncertainty in the RPM is reduced further while the housing mass parameter retains more of its original uncertainty. Table 4.1

contains the numerical $\boldsymbol{\alpha}$ values for the four parameters discussed above (and shown in Figure 4.5) for completeness.

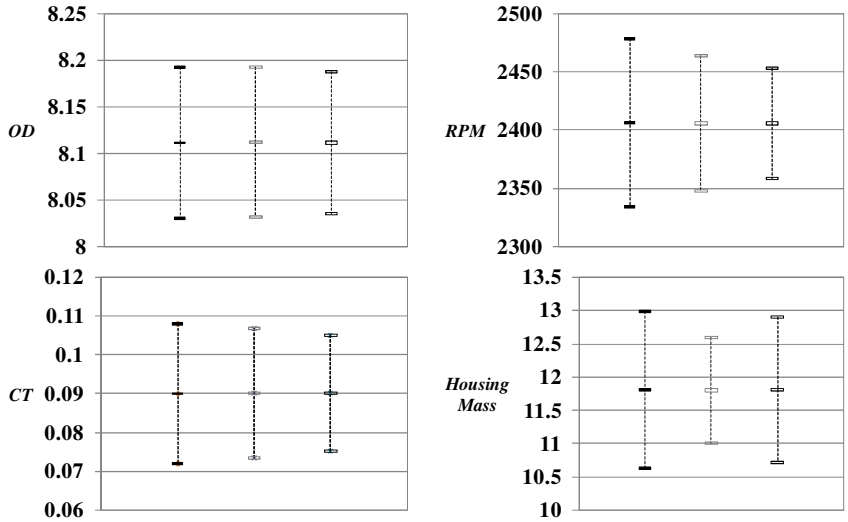

Figure 4.5: Comparison of Highlighted COSA Solutions

Table 4.1: Uncertainty Reduction Vector Values for Figure 4.5 Solutions

α values:	OD	RPM	CT	Housing
Unconstrained	0.992	0.800	0.921	0.671
Constrained	0.940	0.656	0.830	0.927

4.4.2 Multi-Disciplinary UUV Example

The MICOSA approach was also applied to a complex multi-disciplinary system model. The model chosen was an unmanned underwater vehicle (UUV) model comprised of 5 sub-systems. This model was developed using open literature sources [Hamel et al. 2009]. For this application only the system level model and two of the sub-system models were assumed to possess uncertainty. Figure 4.6 depicts the analysis system diagram, the system and sub-system candidate design nominal values for all uncertain inputs, the uncertainty associated the input parameters and the underlying design optimization problem for each of the systems to be analyzed. Much of the details

of this model are omitted in the interest of brevity, as the complete system model consists of over a hundred input parameters and numerous outputs. The system given in Figure 4.6 was analyzed using the MICOSA formulation and the system level results along with a sample of the sub-system level results obtained are provided in Figure 4.7. It should be noted that sub-system results presents are associated with just one of the Pareto solution in the system level solution set. As with the MIMOSA approach, a complete set of Pareto solutions are produced at the sub-system level for each solution point generated at the system level and the vast majority of the sub-system solutions are not presented in this dissertation in the interest of brevity.

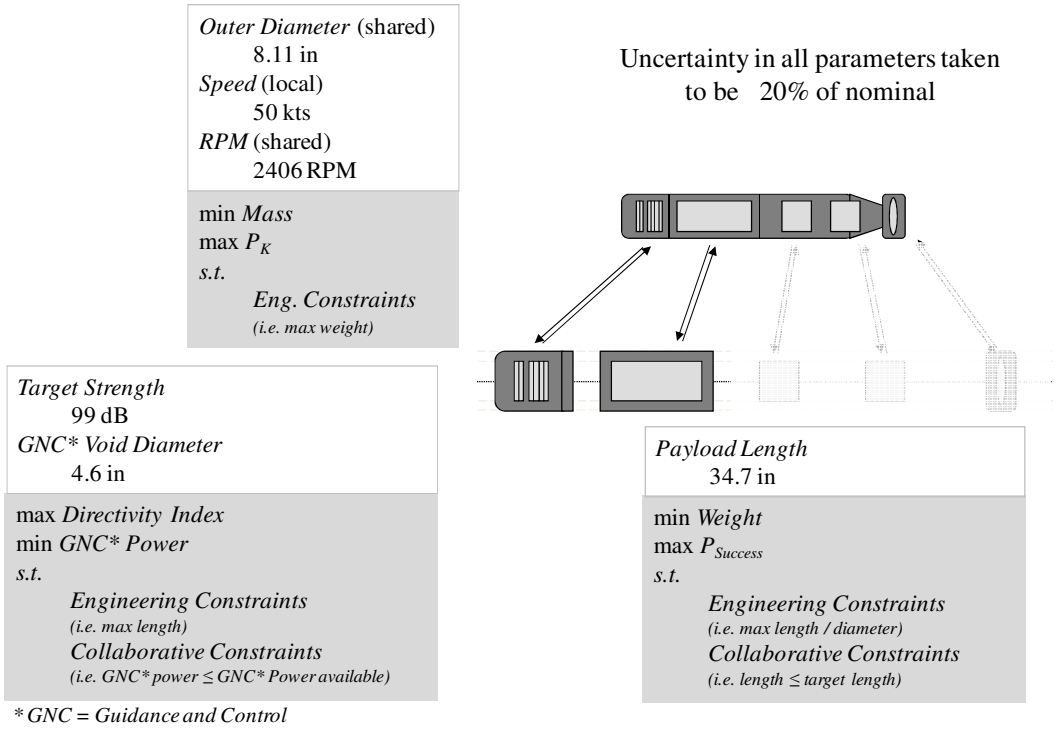

Figure 4.6: UUV MICOSA Example

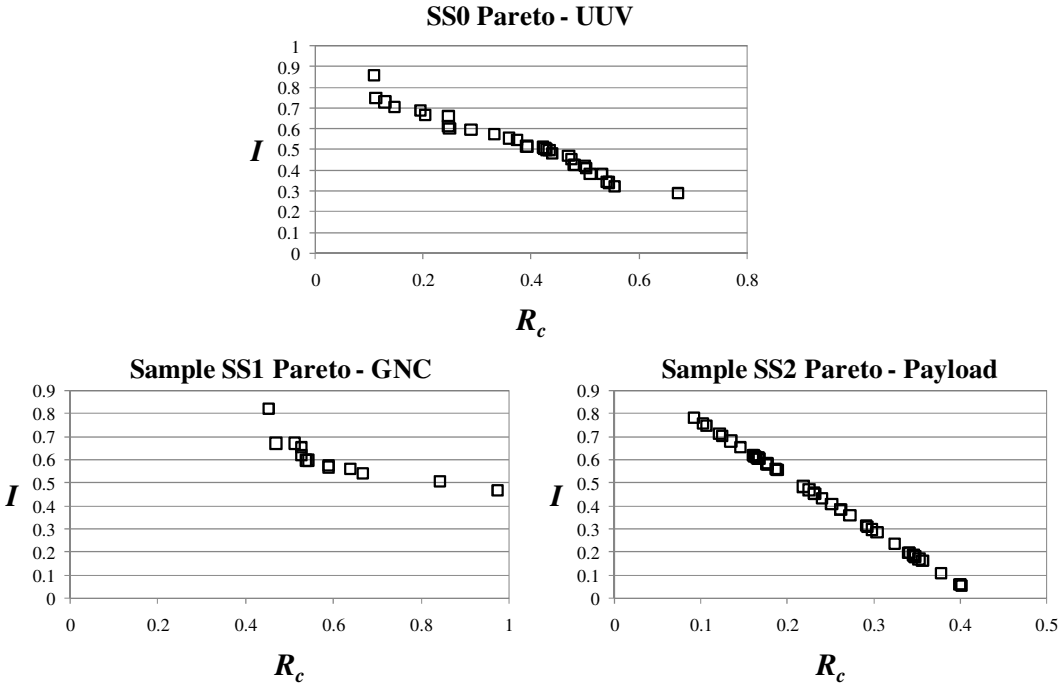

Figure 4.7: Sample UUV MICOSA Results

A few observations can be made from Figure 4.7. First, it is clear that MICOSA approach produces results that are very similar in nature to those provided by MIMOSA. These results provide designers with insight into how best to allocate limited resources in an effort to improve the performance of the overall system. Furthermore, MICOSA also is capable of determining the relative importance of different sub-systems when considering both objective function variations and engineering feasibility. Note that the sample payload sub-system results show a wide range of potential solutions ranging from very low to very high I values, indicating that a designer is free to select the uncertainty reduction levels for that sub-system based purely on the desired R_c value. Conversely for the SS1, the Guidance and Control (GNC) sub-system, a minimum I value of ≈ 0.5 is required for all solutions. This suggests that there is a minimum level of investment required for this system just to achieve feasibility ($R_g < 1$) under uncertainty, and that any

additional investment of resources (I greater than ≈ 0.5) can then result in reduced output function variations (i.e. better performance). These results suggests that the MICOSA approach is capable of ensuring that resources are first supplied to ensuring that the system will not fail prior to applying any uncertainty reduction resources to reducing other output performance variations.

4.5 SUMMARY OF RESEARCH THRUST 2

This chapter detailed the MICOSA approach, a simple extension to the MIMOSA approach presented in Chapter 3. This approach possesses all the same capabilities as MIMOSA, with the added benefit of also considering engineering feasibility. The capabilities of this new approach were demonstrated through two example problems that highlighted the key improvements of MICOSA over MIMOSA. The single disciplinary example was used to demonstrate the necessity of the R_g constraint to the formulation of the COSA approach. By solving the single disciplinary example problem two times, once with the constraint on R_g and once without, the capability of the COSA formulation to ensure feasibility under uncertainty was clearly demonstrated. The multi-disciplinary example problem demonstrated the full capability of the MIMOSA approach. First this example showed that MICOSA produced results comparable to those produced by MIMOSA, which was to be expected. Additionally, the second example problem demonstrated the value of using R_c as the objective function (as opposed to R_f or R_g) as it forces the approach to apply limited uncertainty reduction resources limiting the more critical output function variations (either objectives or constraints) first, which is an intuitive way to approach the use of limited resources.

However, it may not always be possible for uncertainty reduction alone to ensure feasibility, as demonstrated in this chapter. Many design solutions for various system may only be feasible when uncertainty is completely eliminated, which will most likely not be possible to accomplish since virtually all physical systems possess some level of uncertainty. Clearly in those cases the MICOSA approach, while certainly very capable, will be insufficient for mitigating the effect of input parameter uncertainty. The following chapter addresses this shortcoming of the MICOSA approach.

CHAPTER 5: DESIGN IMPROVEMENT BY SENSITIVITY ANALYSIS (DISA)

5.1 INTRODUCTION TO RESEARCH THRUST 3

As first stated in Chapter 1, much of the current research in engineering design (including the first two research thrusts presented in Chapters 3 and 4 of this dissertation) is driven by the fact that all real-world engineering systems are comprised of uncertain input parameters [Martin and Simpson, 2006; Schueller and Jensen, 2008; Moeller and Beer, 2008; Lee and Chen, 2009]. Understanding and managing uncertainty levels during an engineering design process is of particular importance when uncertainty can lead to the failure, or infeasibility, of an engineering system. In the previous chapter of this dissertation the MICOSA approach was presented which focused on mitigating the effects of uncertainty on a system's feasibility through the use of uncertainty reduction. That approach was proven to be capable of ensuring feasibility, but only in those cases where uncertainty reduction alone was sufficient, which may not always be the case. This chapter presents a more general approach to that problem for single disciplinary engineering systems.

As with the previous two chapters, the work presented in this chapter focuses on interval input uncertainty to engineering system analysis models and assumes that the uncertain intervals are reducible. Furthermore the work presented in this chapter has approach the problem of design under uncertainty from a sensitivity analysis (SA) point of view, as opposed to a robust optimization point of view, due to the fact that SA is better suited to uncertainty reduction decision making. The motivation and background details for these decisions were presented in detail in Chapter 1 of this dissertation.

It should be noted that some robust approaches have been used successfully to explore opportunities for uncertainty reduction (as opposed to simply considering all uncertainty as irreducible) in various ways. For example, there are RBDO methods reported in the literature that use Bayesian techniques [Wang et al., 2009], methods that sequentially perform RBDO and consider uncertainty reduction [Qu et al., 2003], and methods that simultaneously consider RBDO and uncertainty reduction options [Kale and Haftka, 2008]. These approaches are not limited to irreducible uncertainty as is traditionally the case for robust approaches, but like most robust approaches they consider many drastically different potential designs in an effort to design a system under uncertainty. In many cases a designer may already have a design in mind and may not wish to consider drastically different design alternatives. As previously discussed in Chapter 1, in those cases an SA approach is often preferable to a robust approach due to the unique capabilities of sensitivity analysis.

The MOSA approach [Li et al., 2009a] that was first presented in Chapter 2 and then extended in Chapters 3 and 4, is an SA based approach for uncertainty reduction. As previously discussed, MOSA (and MIMOSA for that matter) assume that uncertainty reduction is always possible and that any design under consideration will always be feasible given any combination of uncertain inputs. Furthermore, the MICOSA approach presented in Chapter 4 assumes that if a design is not feasible under nominal uncertainty, its feasibility can be guaranteed through uncertainty reduction. These assumptions may not hold for a design that is on or near the limits of a problem's feasible domain and may become infeasible due to uncertainty, regardless of how much uncertainty levels are reduced. Efforts were made by Li et al. to address this shortcoming by combining the

MOSA algorithm with robust optimization techniques in an effort to produce design solutions that are insensitive to irreducible uncertainty while simultaneously finding optimal levels of uncertainty reduction for all reducible uncertainty [Li et al., 2009c]. However, since this approach [Li et al., 2009c] is a robust approach, it considers many potential designs in addition to finding optimal uncertainty reduction opportunities. This multi-layered strategy adds potentially unnecessary computational expense and will also produce solutions that may be very different from a preferred preexisting design, as previously discussed. The work presented in the previous chapter attempted to address this shortcoming as well, but only for those cases where uncertainty reduction alone could be assured of guaranteeing feasibility, which is not always the case.

A method that has the ability to improve a preexisting design and simultaneously prevent its infeasibility through a better understanding of the effects of uncertainty would be very useful. A preexisting design in this sense refers to either: a) a design that is already in use but need to be slightly redesigned (adjusted) due to significant changes to input parameter values or uncertainty levels; or b) a deterministic design solution generated using a conceptual design procedure, such as one produced by a deterministic design optimization procedure. In either of the above cases the effect of uncertainty has to be accounted for carefully. Typically safety factors would be assigned to the critical aspects of the design, which could necessarily lead to some adjustments to the preexisting design's parameters. It would be preferable in many cases to instead utilize information from a sensitivity analysis approach to produce feasible designs under uncertainty in a systematic fashion without the need to arbitrarily guess or assume safety factor values.

The work presented in this research thrust seeks to provide just such a capability by proposing a new sensitivity analysis based approach, called Design Improvement by Sensitivity Analysis (DISA). This new approach is capable of first finding optimal uncertainty reduction options for a given design and then suggesting required small changes (or adjustments) to the original design to ensure the feasibility of the system when necessary, provided uncertainty reduction alone is insufficient. Small adjustments are defined in this work as changes to the nominal values of any uncertain parameter of an engineering system within the original uncertainty interval for a given parameter.

Additionally, this work will show that, if desired, the DISA approach is capable of suggesting those required small adjustments with very little (if any) additional information about the engineering system. This is accomplished by retaining system information obtained during an initial uncertainty reduction SA procedure and then using meta-modeling [Srivastava et al., 2004; Martin and Simpson, 2005; Wang and Shan, 2007; Allaire and Willcox, 2008; Ju and Lee, 2008; Shan and Wang, 2008] to approximate the system response for determining the required design adjustments. As a result, this new approach is no more computationally expensive than the MOSA approach [Li et al., 2009a], but is also capable of ensuring the engineering feasibility of a preexisting design without the need for feasibility robust optimization.

The basic capability of the DISA approach can be summarized with the following simple example. Suppose a design engineer would like to use a 2 inch diameter pin to fit into a 2 inch diameter hole based on certain requirements, as shown on the top half of Figure 5.1, but knows that the diameter of the pin (D_0) will undoubtedly possess some level of uncertainty. Clearly no amount of uncertainty reduction would be capable of

ensuring that the pin would always fit into the 2 inch diameter hole in this scenario. However, if the nominal diameter of the pin was reduced (or adjusted) to a value slightly less than 2 inches, that adjustment coupled with some small amount of uncertainty reduction could then guarantee that the pin would always fit into the required hole.

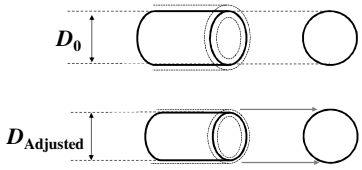

Figure 5.1: Simple Example

The DISA approach is capable of solving just such a problem involving numerous design variables, multiple design objectives and many constraints for a system possessing interval uncertainty in an efficient manner. Section 5.2 outlines specific background and terminology applicable to this new approach. Section 5.3 provides the formulation of the approach and the general results it is capable of producing. Section 5.4 shows two engineering examples of varying degrees of difficulty to demonstrate the applicability of this new approach. Section 5.5 contains some concluding remarks.

5.2 BACKGROUND AND TERMINOLOGY

In this section some necessary background, terminology and concepts will be introduced. Note that all these concepts are applicable to multi-dimensional problems but for simplicity two-dimensional illustrations are used. The approach presented in this chapter is an extension of the MIMOSA approach and thus builds on the concepts presented in Chapters 3 and 4.

Recall that SA approaches assume that a predetermined design already exists for a system of interest. Following this assumption all predetermined inputs into an engineering system can simply considered as fixed design parameters $\boldsymbol{p}$. Thus hereafter in this chapter the vector $\boldsymbol{p_0}$, as with the previous two chapters, is used to denote the nominal values for all inputs into a system for which a solution, or design, already exists. Furthermore this design $\boldsymbol{p_0}$ will be called a candidate design. As a result, the nominal objective and constraint functions values for a candidate design may be thought of simply as functions of the nominal values $\boldsymbol{p_0}$.

The work presented in this chapter focuses on how changes to the parameters contained in the vector $\boldsymbol{p_0}$, both in terms of nominal values and uncertainty level, affect the performance of the design described by the functions $\boldsymbol{f_0}$ and $\boldsymbol{g_0}$. As with the work presented in the previous chapters, if the uncertainty associated with a system's input parameters (bounded by the interval $[\boldsymbol{p_0} - \boldsymbol{\Delta p}, \boldsymbol{p_0} + \boldsymbol{\Delta p}]$) are reducible, then the uncertainty reduction vector $\boldsymbol{\alpha}$ can again be used to quantify the reduction in the uncertainty of those parameters. When the uncertainty in any of the input parameters to a system are reduced by decreasing the values for one or more elements in $\boldsymbol{\alpha}$, the range of output function variation will also inevitably be changed. This propagation of uncertainty from input parameters to output function values can be represented by a set of resulting uncertain objective and constraint function values:

$$\begin{aligned} & f_i(\boldsymbol{p}_v) \quad i = 1,\ldots,I \\ & g_j(\boldsymbol{p}_v) \quad j = 1,\ldots,J \\ & \textit{for all } \boldsymbol{p}_v \\ & \textit{where} \quad \boldsymbol{p}_0 - \boldsymbol{\alpha} \circ \boldsymbol{\Delta p} \le \boldsymbol{p}_v \le \boldsymbol{p}_0 + \boldsymbol{\alpha} \circ \boldsymbol{\Delta p} \end{aligned} \tag{5.1}$$

As shown in Eqn. (5.1), uncertainty propagation is a function of the nominal parameter values $\boldsymbol{p}_0$, the original uncertainty intervals $\Delta\boldsymbol{p}$, and uncertainty reduction vector $\boldsymbol{\alpha}$. In Eqn. (5.1) the vector $\boldsymbol{p}_v$ is again used (as in the previous chapter), which represents a single realization of the uncertain values $\boldsymbol{p}$ bounded by the retained uncertain interval $[\boldsymbol{p}_0 - \boldsymbol{\alpha} \circ \Delta\boldsymbol{p}, \boldsymbol{p}_0 + \boldsymbol{\alpha} \circ \Delta\boldsymbol{p}]$, and will be used throughout the chapter as a decision variable when attempting to quantify the effect of uncertainty. Figure 5.2 depicts the impact that different uncertainty reduction values could have on output function variations when nominal parameter values $\boldsymbol{p}_0$ remain unchanged.

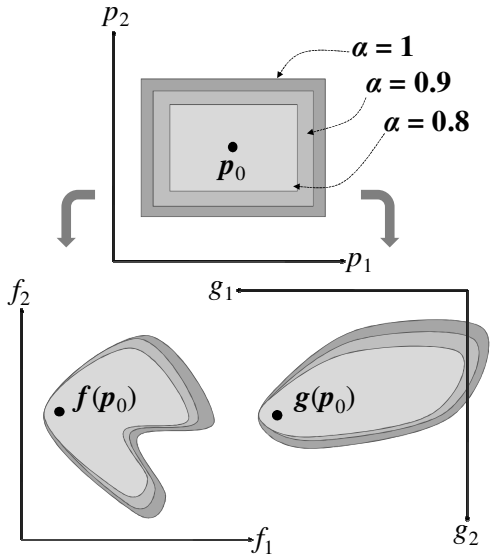

Figure 5.2: Parameter Uncertainty Mapping for Various α Values

5.2.1 Design Adjustment Vector

Small adjustments to the nominal values of the parameter vector $\boldsymbol{p}_0$, as discussed in Section 5.1, provide an obvious means for ensuring the feasibility of a design that cannot become feasible through uncertainty reduction alone. In this work the exact magnitude of the adjustment is controlled by a proposed design adjustment vector $\boldsymbol{\beta}$. This vector is a

set of scaling factors, much like $\boldsymbol{\alpha}$, that can be selected to make small adjustments to the nominal parameter values $\boldsymbol{p}_0$ of a candidate solution. One element of the design adjustment vector $\boldsymbol{\beta}$ is established for each element in the vector $\boldsymbol{p}_0$, yielding $\boldsymbol{\beta} = \{\beta_1,\ldots,\beta_k,\ldots,\beta_K\}$ with $-1 \leq \beta_k \leq 1$.

As with the $\boldsymbol{\alpha}$ vector, the values for $\boldsymbol{\beta}$ are typically taken to be continuous. If only discrete adjustments are possible for the k^{th} parameter of a system the corresponding β_k can be limited to discrete options. For each parameter p_k, the associated β_k value scales the predetermined maximum allowable adjustment in that parameter δp_k. $\boldsymbol{\delta p}$ is a vector of values specified by the designer based on specific system limitations and should be of the same order of magnitude as the original uncertainty levels in $\boldsymbol{\Delta p}$. For example, one parameter of a notional power tool design may be the thickness of wire used to connect the tool's electrical supply to its motor. For a candidate design under consideration the designer may specify 10 AWG wire (American Wire Gage, approximately 0.1 inches in thickness). However, the designer may know that the choice to use 10 AWG wire was arbitrarily made based on other factors and may suspect that the nominal wire thickness could actually be adjusted by ±0.01 inches without affecting the electrical system of the tool, which would amount to using 9 AWG (0.11 in) or 11 AWG (0.09 in) wire. As such the designer would then select δp_{wire} to be 0.01 inches. In this work δp_k is simply taken to be ten or twenty percent of its nominal value $p_{0,k}$ (depending on the engineering system of interest), but any assumed max adjustment is acceptable provided the max range of the adjustment is sufficiently small, as discussed previously.

When considering uncertain parameters whose nominal values are adjustable, the effects of those parameters on a system's outputs depends on the nominal parameter

values $\boldsymbol{p_0}$, the $\boldsymbol{\beta}$ values associated with each parameter, the assumed maximum adjustment values $\delta\boldsymbol{p}$ and a given level of parameter uncertainty as described in Eqn. (5.2). Again the vector $\boldsymbol{p_v}$ is used to denote a specific realization of the uncertainty in $\boldsymbol{p}$, this time bounded by the uncertain interval defined by $\boldsymbol{\Delta p}$, $\boldsymbol{\beta}$ and $\boldsymbol{\delta p}$ as shown in Eqn. (5.2):

$$\begin{aligned} & f_i(\boldsymbol{p}_v) \quad i = 1,\ldots, I \\ & g_j(\boldsymbol{p}_v) \quad j = 1,\ldots, J \\ & \textit{for all } \boldsymbol{p}_v \\ & \textit{where } \quad ((\boldsymbol{p}_0 + \boldsymbol{\beta} \circ \boldsymbol{\delta p}) - \boldsymbol{\Delta p}) \le \boldsymbol{p}_v \le ((\boldsymbol{p}_0 + \boldsymbol{\beta} \circ \boldsymbol{\delta p}) + \boldsymbol{\Delta p}) \end{aligned} \tag{5.2}$$

It can be seen in Figure 5.3 that small changes to nominal parameter values can ensure the feasibility of a candidate design for a given level of parameter uncertainty.

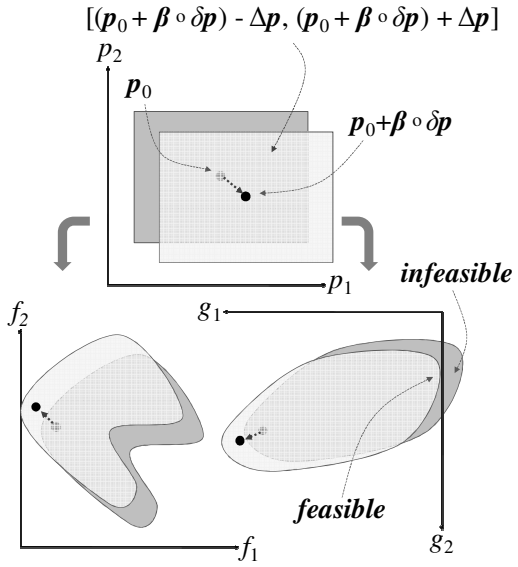

Figure 5.3: Parameter Adjustment Mapping

There is the possibility that for some problems no combination of uncertainty reduction or small adjustments on nominal parameter values will be sufficient to ensure feasibility. This possibility is highly problem dependent and in those cases a designer can enlarge the elements of the maximum allowable adjustment vector $\boldsymbol{\delta p}$.

5.2.2 Objective and Constraint Uncertainty Mapping

As discussed generally in Chapter 2, in order to effectively manage input uncertainty in an effort to improve output function performance (i.e., to reduce the variation in the outputs), it is necessary to measure and quantify objective and constraint function variations separately as a function of $\boldsymbol{\alpha}$ and $\boldsymbol{\beta}$. In order to do this, Li et al.'s work [2009a] is extended here to include both objective functions f_i as well as constraint functions g_j and to include the effects of parameter adjustments in addition to parameter uncertainty reduction. Two metrics, R_f and R_g, are used for measuring the variations in objective and constraint functions respectively in this chapter. The formulation of these metrics is slightly different then used in the previous chapter due to the inclusion of the $\boldsymbol{\beta}$ vector, which was not considered in MICOSA.

$$
\begin{aligned}
& R_f = \max_{\boldsymbol{p}_v} \left\| \Delta \boldsymbol{f} \right\|_2 \\
& \textit{where} \quad \Delta f_i = \frac{f_i(\boldsymbol{p}_v) - f_{0,i}}{f_{0,i}} \quad i = 1,\ldots,\ I \\
& \qquad \left((\boldsymbol{p}_0 + \boldsymbol{\beta} \circ \delta \boldsymbol{p}) - \boldsymbol{\alpha} \circ \Delta \boldsymbol{p}\right) \le \boldsymbol{p}_v \le \left((\boldsymbol{p}_0 + \boldsymbol{\beta} \circ \delta \boldsymbol{p}) + \boldsymbol{\alpha} \circ \Delta \boldsymbol{p}\right)
\end{aligned}
\tag{5.3}
$$

$$
\begin{aligned}
& R_g = \max_{\boldsymbol{p}_v} \left(\max_j \ \Delta \boldsymbol{g} \right) \\
& \textit{where} \quad \Delta g_j = \frac{g_j(\boldsymbol{p}_v)}{\left| g_{0,j} \right|} \quad j = 1,\ldots,\ J \\
& \qquad \left((\boldsymbol{p}_0 + \boldsymbol{\beta} \circ \delta \boldsymbol{p}) - \boldsymbol{\alpha} \circ \Delta \boldsymbol{p}\right) \le \boldsymbol{p}_v \le \left((\boldsymbol{p}_0 + \boldsymbol{\beta} \circ \delta \boldsymbol{p}) + \boldsymbol{\alpha} \circ \Delta \boldsymbol{p}\right)
\end{aligned}
\tag{5.4}
$$

As shown in Eqn. (5.3) objective function variations are normalized by the nominal design's objective function values and then the largest variation is found using a $\|.\|_2$ norm; however a $\|.\|_\infty$ norm is also acceptable if desired. In Eqn. (5.4) R_g is calculated as the maximum value of all constraint function values, normalized by the candidate design's nominal constraint function values. A simple maximization is used in Eqn. (5.4) to find the largest constraint deviation from the nominal and ensures that any positive R_g

value will indicate an infeasible input uncertainty interval [$(\boldsymbol{p}_0 + \boldsymbol{\beta} \circ \delta\boldsymbol{p}) - \boldsymbol{\alpha} \circ \Delta\boldsymbol{p}$, $(\boldsymbol{p}_0 + \boldsymbol{\beta} \circ \delta\boldsymbol{p}) + \boldsymbol{\alpha} \circ \Delta\boldsymbol{p}$]. Since the R_f and R_g metrics measure output variations given input uncertainty levels, both $\boldsymbol{\alpha}$ and $\boldsymbol{\beta}$ values must be specified for the system of interest prior to evaluating Eqns. (5.3) and (5.4). Once $\boldsymbol{\alpha}$ and $\boldsymbol{\beta}$ values are given, R_f and R_g values in Eqns. (5.3) and (5.4) can then be calculated by performing a single objective optimization to find the worst case variation in the system's objectives (R_f) and/or constraints (R_g). The decision variables in each of these optimizations are the values for the system's input parameters (denoted by $\boldsymbol{p}_v$) bounded by a predetermined level of uncertainty in each of those parameters (specified by $\boldsymbol{\alpha}$ and $\boldsymbol{\beta}$ values). In this work, R_f and R_g are mathematical metrics that quantify the resulting variations in multiple system outputs as a single scalar value for either the system's objectives (R_f) or constraints (R_g). Figure 5.4 depicts this relationship between changes in $\boldsymbol{\alpha}$ and R_f and R_g for demonstration purposes. A similar figure can be drawn for R_f and R_g as a function of $\boldsymbol{\beta}$ only, or both $\boldsymbol{\alpha}$ and $\boldsymbol{\beta}$ simultaneously.

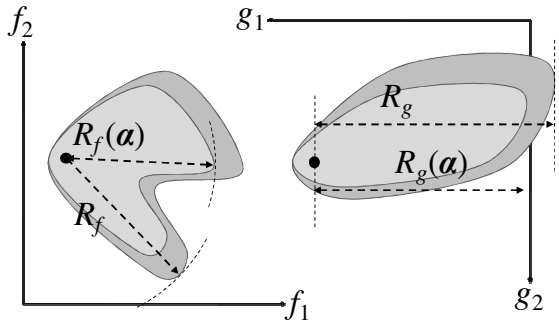

Figure 5.4: Graphical Depiction of $R_f(\boldsymbol{\alpha})$ and $R_g(\boldsymbol{\alpha})$

For many engineering systems it is possible that uncertainty reduction and/or design adjustments may not be possible for one or more of nominal parameters. Such limitations can be addressed by adjusting the upper and/or lower bounds of the corresponding elements of $\boldsymbol{\alpha}$ and $\boldsymbol{\beta}$.

5.2.3 Parameter Adjustment Cost Metric

In most engineering systems uncertainty reduction and/or small design adjustments are not always possible without additional penalty, cost, or investment. For example, a better machining process could produce a more accurate (less uncertain) dimension for a part, but only if a designer or manager were willing to make the cost investment required to purchase better equipment. Similarly, changing the nominal design parameters for a candidate design may not be completely desirable as small changes may require other related parts or complementary sub-systems to be redesigned as well, incurring more time and costs. In order to deal with these realities the following generic formulation for quantifying these costs is provided in Eqn. (5.5). This metric I (short for investment) is an extension of the *Investment* metric developed by Li et al. [2009a] and used in the last two research thrusts, modified here to measure both the uncertainty reduction requirements and design adjustments.

$$I = \frac{\sum_{k}\left(w_1\left(1-\alpha_k\right)+w_2\left|\beta_k\right|\right)}{k} \quad k=1,\ldots,K$$
$$\text{where } \mathbf{0} \le (w_1, w_2) \le 1 \text{ and } w_1 + w_2 = 1 \tag{5.5}$$

I can be used as a measure of the cost associated with those changes made to a nominal solution in the absences of any actual cost information for a given system. The two weighting factors in Eqn. (5.5), w_1 and w_2, can be used to adjust the relative costs associated with uncertainty reduction and nominal design adjustment in accordance with the designer's preferences. For this work w_1 = 0.75 and w_2 = 0.25 are chosen, corresponding to an arbitrarily determined preference for design adjustment over uncertainty reduction (accomplished by placing a greater weight, or penalty, on uncertainty reduction).

5.3 DISA APPROACH

In this section the Design Improvement by Sensitivity Analysis (DISA) approach is formulated. DISA seeks to efficiently determine the optimal combination of uncertainty reductions and/or small design adjustments required in order to produce the best possible reduction in objective function variation while ensuring the feasibility of a design under uncertainty. This is accomplished by solving two bi-objective optimization problems in a sequential fashion. The first optimization determines a Pareto set of uncertainty reduction ($\boldsymbol{\alpha}$) options in an effort to reduce objective function variation first. In the context of this approach uncertainty reduction is preferable since it does not require changes to the nominal parameter values of the predetermined candidate design. Then, if necessary, a second optimization problem is solved repeatedly, once for each Pareto solution of interest produced during the first stage optimization, in an effort to determine the optimal design adjustment ($\boldsymbol{\beta}$) required to ensure feasibility. If desired, this second stage optimization can be performed using a set of meta-models (one for each system output) created using system data retained during the first stage optimization problem.

The decision to formulate the DISA approach using a sequential algorithm (as opposed to the seemingly more intuitive all-at-once approach where both $\boldsymbol{\alpha}$ and $\boldsymbol{\beta}$ would be optimized simultaneously) was made for a specific set of reasons. Indeed DISA intentionally does not attempt to obtain solutions that are optimal with regard to both $\boldsymbol{\alpha}$ and $\boldsymbol{\beta}$ simultaneously, accepting the possibility of producing inferior solutions in order to provide an approach that has the following three important advantages over the all-at-once approach. First, it is possible that uncertainty reduction procedure alone could be enough to ensure feasibility. These types of solutions could be very attractive to some

designers but may potentially be suppressed (and therefore missed) in an all-at-once approach. Secondly, a two-stage approach allows a designer to only perform the second stage optimization on a subset of uncertainty reduction solutions obtained in the first-stage optimization that are of interest, providing the designer with further control over the approach and the type of results that it produces. The third and most compelling reason for formulating DISA in this way is to allow for greater computational efficiency. Solving DISA using two sequential stages makes it possible to use analysis data obtained in the first stage optimization to perform the second stage optimizations (recall that the second stage optimization may be solved repeatedly) using surrogate approximations as opposed to additional function calls. In this chapter a function call is defined as the evaluation of one specific input parameter vector $\boldsymbol{p}_v$ for its output function (i.e., $\boldsymbol{f}$ and $\boldsymbol{g}$) values obtained from a computational analysis or simulation model. See Chapter 2 for details on surrogate approximation.

To take advantage of the efficiency gains mentioned above all uncertain inputs to the system must be sufficiently sampled over their ranges of uncertainty during the first stage of the approach. This condition will be met in those cases when, after the first stage of the approach, all possible values for any uncertain parameters to be considered in the second stage are guaranteed to fall within the original maximum uncertain intervals for those parameters. This is because the first stage of the approach varies all uncertain input parameters over their maximum uncertain intervals in search of uncertainty reduction opportunities as shown in Eqns. (5.3) and (5.4), generating a wealth of function call (system outputs as a function of $\boldsymbol{p}_v$) information. Clearly, for many systems the parameter space may not be sufficiently sampled during the first stage of the algorithm as

discussed above and additional data will be required in order to build effective meta-models of the system's objective and constraint functions prior to searching for optimal adjustments to the nominal values of uncertain parameters. This does not preclude the use of the DISA approach and simply requires that any additional required function call information be obtained after the first stage problem but prior to building any meta-models for use in the second stage. This case will be addressed in detail in Section 5.3.2 and in Section 5.4 through the engineering examples.

Additionally, it should be pointed out that using meta-models within the second stage of the DISA approach is not without its own set of potential drawbacks which are well known and beyond the scope of this work. Prior to employing the meta-model assisted DISA approach the user should become familiar with the strengths and weaknesses associated with surrogate approximation by reviewing the literature for details (e.g., [Martin and Simpson, 2005]).

5.3.1 DISA Formulation

The DISA approach begins with a candidate design solution, defined by the parameter vector $\boldsymbol{p}_0$ for a system comprised of multiple objective functions $\boldsymbol{f}$ and constraint functions $\boldsymbol{g}$. The designer then determines which parameters have uncertainty and/or whose nominal values can be adjusted, including their associated uncertainty intervals and maximum design adjustments, $\Delta\boldsymbol{p}$ and $\delta\boldsymbol{p}$, respectively. A MOSA based unconstrained optimization problem (i.e., Eqn. (2.3) with *I* substituted for *Investment*) is then performed to minimize both the variation in objectives (R_f) and the metric *I* as defined in Eqn. (5.5). Recall that the decision variables in this first stage optimization problem are only the elements of the uncertainty reduction vector $\boldsymbol{\alpha}$, and since Eqn. 2.3

does not contain $\boldsymbol{\beta}$ (since MOSA does not consider design adjustments), $\boldsymbol{\beta}$ is taken to be a zero vector in the first stage. The optimization can be conducted using a population based optimizer, such as a Multi-Objective Genetic Algorithm (MOGA) [Deb, 2001] and during each generation all analysis data from the simulation model(s) are retained. Recall that this retained data is in the form of $f_i(\boldsymbol{p}_v)$ and $g_j(\boldsymbol{p}_v)$ data can be obtained when Eqn. (5.3) is solved within Eqn. (2.3), assuming that the $g_j(\boldsymbol{p}_v)$ constraint functions are also evaluated. Following the completion of the first stage optimization a Pareto set of Np optimal uncertainty reduction vector $\boldsymbol{\alpha}^*$ solutions will be obtained. Since this first stage optimization problem is performed in an unconstrained fashion (recall that MOSA is an unconstrained problem) the Pareto solutions produced cannot ensure the feasibility of the candidate design. Since uncertainty reduction alone may not be enough to ensure feasibility the second stage optimization is performed by solving Eqn. (5.6), once for each uncertainty reduction solution of interest obtained in the first stage problem.

$$\begin{aligned} &\min_{\boldsymbol{\beta}} \; R_f(\boldsymbol{\beta} \mid \boldsymbol{\alpha}_i^*) \\ &\min_{\boldsymbol{\beta}} \; I(\boldsymbol{\beta} \mid \boldsymbol{\alpha}_i^*) \\ &s.t. \\ &\quad R_g(\boldsymbol{\beta} \mid \boldsymbol{\alpha}_i^*) \le 0 \end{aligned} \tag{5.6}$$

The second stage is solved repeatedly, once for each Pareto $\boldsymbol{\alpha}_i^*$ solution of interest, $i = 1,\ldots, N_1$ ($N_1 \le Np$). A designer may wish to perform the second stage optimization procedure for all $\boldsymbol{\alpha}^*$ solutions obtained in the first stage if desired. It is also permissible to limit the number of $\boldsymbol{\alpha}^*$ solutions N_1 considered in the second stage optimization problem if a small subset of first stage solutions is more attractive. Selecting multiple solutions of interest will increase the range of possible feasible solutions produced by the approach,

providing the designer with a larger set of design adjustment options. In each of the second stage optimizations, $i = 1,\ldots, N_1$, the $\boldsymbol{\alpha}_i^*$ value of interest is held constant. As previously discussed, as long as R_g is less than or equal to 0 the corresponding combination of $\boldsymbol{\beta}$ and $\boldsymbol{\alpha}^*$ values will produce a feasible design. Simultaneously minimizing R_f and I again creates a natural tension, this time between objective function variation reduction due to design adjustments and the required magnitude of those design adjustments. It is important to note that the second stage solves for what is defined as $\boldsymbol{\beta}^*|\boldsymbol{\alpha}_i^*$ (i.e., $\boldsymbol{\beta}^*$ given $\boldsymbol{\alpha}_i^*$), not the more general independent $\boldsymbol{\beta}^*$, which is an important distinction. It is possible that for the i^{th} first stage solution considered in the second stage no combination of $\boldsymbol{\beta}^*|\boldsymbol{\alpha}_i^*$ can produce a feasible solution ($R_g \leq 0$) and as a result no Pareto solutions will be produced. In this case it is up to the designer to select an alternate $\boldsymbol{\alpha}_i^*$ solution from the first stage to investigate and further drives the need for the designer to select multiple $\boldsymbol{\alpha}_i^*$ solutions of interest.

If the DISA approach is solved in the manner described above using actual analysis functions to repeatedly solve Eqn. (5.6), the computational effort (in terms of the number of function calls) can become a problem if numerous $\boldsymbol{\beta}$ optimization problems have to be solved. In order to improve the computational efficiency of the DISA approach, Eqn. (5.6) is restated by using meta-models to obtain the values of R_f, R_g and I within the second stage optimization. The data for creating these meta-models comes from the data retained during the first stage uncertainty reduction optimization problem as previously discussed. Before beginning the optimization(s) to determine corresponding $\boldsymbol{\beta}$ values, meta-models for all functions f_i and g_j are created and then used in lieu of the actual simulation functions to determine approximated R_f, R_g and I values. Prior to building

those meta-models it is important to check the maximum and minimum $\boldsymbol{p}_v$ values retained during the first stage and compare them to the maximum and minimum $\boldsymbol{p}_v$ values that could be evaluated in the second stage (which can be determined based on $\boldsymbol{\alpha}_i^*$ and $\boldsymbol{\delta p}$). If there is any possibility that any of the second stage $\boldsymbol{p}_v$ value could fall outside the range of retained data, then additional function calls are needed and should be obtained and included in the meta-models. Eqn. (5.7) formulates this meta-model assisted second stage optimization to solve for $\boldsymbol{\beta}^* | \boldsymbol{\alpha}_i^*$ Pareto solutions. Recall that all $f_i(\boldsymbol{p}_v)$ and $g_j(\boldsymbol{p}_v)$ information generated during the first state procedure is retained, despite the fact that the first stage optimization does not check for constraint violation, making it possible to generate meta-models of the systems' constraint functions.

$$\begin{aligned} &\min_{\beta} \hat{R}_f(\boldsymbol{\beta} | \boldsymbol{\alpha}_i^*) \\ &\min_{\beta} \hat{I}(\boldsymbol{\beta} | \boldsymbol{\alpha}_i^*) \\ &s.t. \\ &\quad \hat{R}_g(\boldsymbol{\beta} | \boldsymbol{\alpha}_i^*) \le 0 \end{aligned} \tag{5.7}$$

Figure 5.5 depicts both formulations of the DISA approach for comparison purposes. Figure 5.5(a) depicts the general formulation which does not require meta-models of the system output functions and solves Eqn. (2.3) and (5.6) sequentially. Figure 5.5(b) shows the more efficient meta-model assisted DISA approach which involves solving Eqn. (2.3) and Eqn. (5.7).

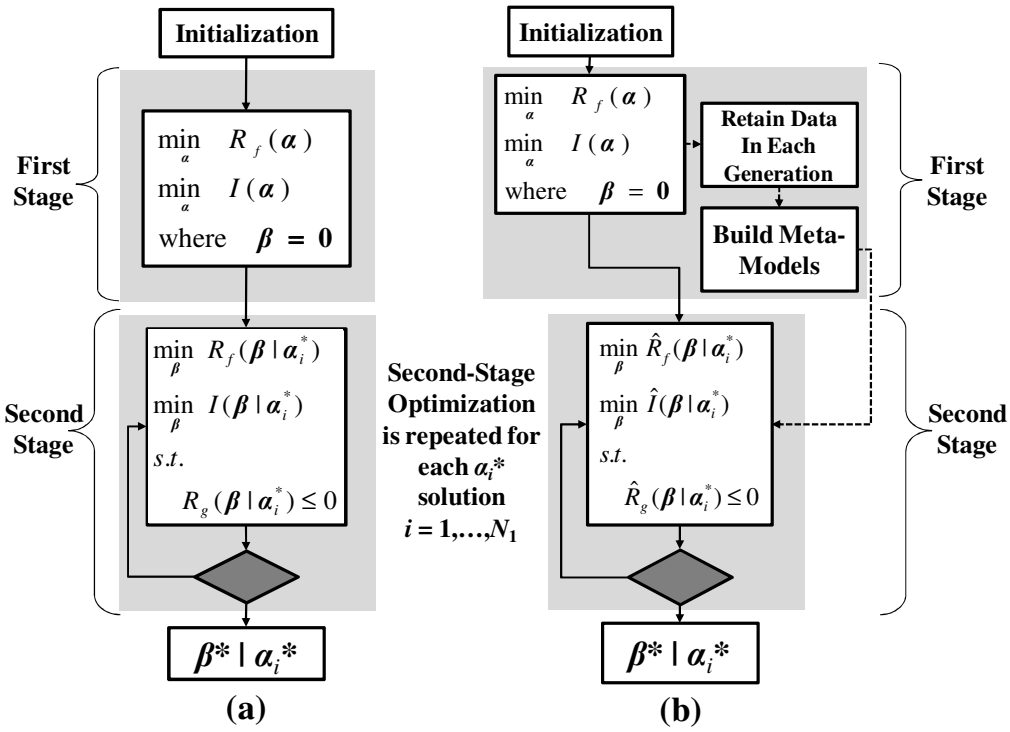

Figure 5.5: DISA Approach (a) Without Meta-Models and (b) With Meta-Models

5.3.2 DISA results

The DISA approach will produce solutions with the following properties, as shown in Figure 5.6. The first stage Pareto $\boldsymbol{\alpha}^*$ values will optimally reduce the uncertainty levels in the system. However, this first stage procedure will not necessarily ensure that the resulting design system will be feasible (note that in Figure 5.6 if only uncertainty reduction is considered the constraint g_1 is still violated). As a result the subsequent optimal selection of corresponding $\boldsymbol{\beta}^*$ values for each $\boldsymbol{\alpha}_i^*$ solution are needed to ensure feasibility of the design under uncertainty with a minimal change in objective performance.

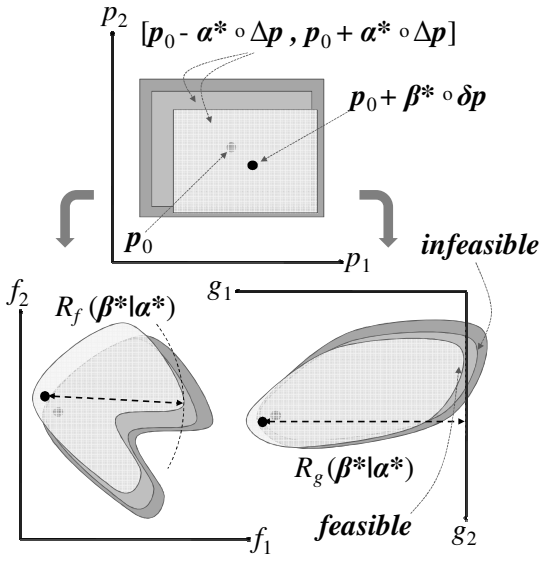

Figure 5.6: Sample DISA Results in Two Dimensions

Figure 5.7 depicts the cascading flow of information produced by this approach. As can be seen on the lower left side of the figure the first stage optimization finds a Pareto set of α^* solutions which optimally reduce uncertainty levels. Then, for each α^* solution of interest produced (one of which is depicted on the diagram) a second optimization is performed using meta-modeling (or actual analysis functions if desired) to produce an additional Pareto set of options, this time adjusting the nominal values of uncertain parameter in an effort to ensure feasibility given the predetermined optimal uncertainty reduction levels.

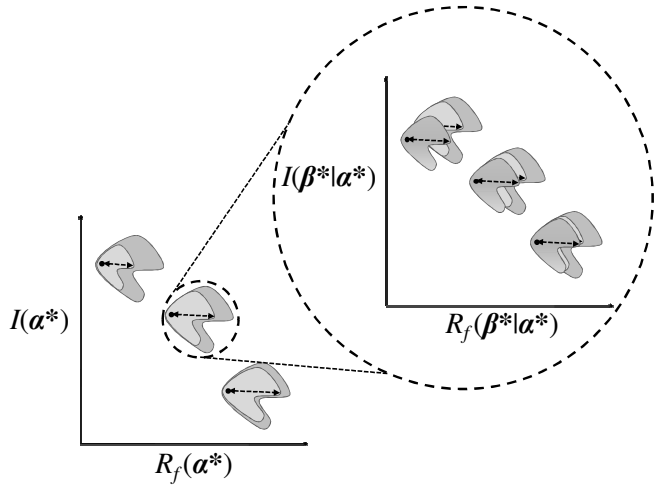

Figure 5.7: Sample Propagation of DISA Result

If analysis functions (or simulation models) are used for both stages of the DISA algorithm, as shown in Figure 5.5(a), the computational effort would be equal to the number of function calls required to solve the $\boldsymbol{\alpha}$ problem, M, times the number of function calls required to solve each $\boldsymbol{\beta}$ problem, N, times the number of times the $\boldsymbol{\beta}$ problem needs to be solved, N_1 in the worst case, resulting in a total computational effort of $O(MNN_1)$ calls. If meta-models are used to approximate the analysis function for all $\boldsymbol{\beta}$ problem optimizations performed, as shown in Figure 5.5(b), the computational savings would amount to the sum total of all function calls needed for all $\boldsymbol{\beta}$ problems required to be solved, or $O(NN_1)$ calls. Clearly this is a significant reduction in computational effort. However, when using the meta-model assisted approach it is important to verify that the parameter space is sufficiently sampled during the first stage optimization in order to produce valid meta-models over the entire range of potential design adjustments, as pointed out at the beginning of this section. If the range of permissible design adjustments for a specific problem is sufficiently smaller than the uncertainty levels presented in the system no additional information is required as the parameter space will

be sufficiently sampled during the first stage optimization. If the range of permissible design adjustments is larger than the area of the parameter space sampled during the first stage optimization then additional sampling data must be collected after the first stage optimization in order to construct valid meta-models, as previously discussed. In this case the computational effort would clearly increase by the number of function calls P required to adequately sample the neglected portion of the parameter space. In this case the resulting computational effort would be $O(M+P)$, which is still significantly less than the $O(MNN_1)$ function calls required if no meta-modeling is employed. This differentiation will be demonstrated in the next section via the first example. The exact number of function calls required in this case (P), however, should be determined by the designer based on the size of the parameter space that needs to be sampled.

5.4 EXAMPLES AND RESULTS

In order to demonstrate the capabilities and efficiency of the DISA approach, two engineering examples of varying complexity are presented. In both examples a single candidate design was obtained beforehand using a deterministic (no uncertainty considered) optimization procedure. The nominal parameter values for the candidate design were located on or near the boundaries of the corresponding system's feasible domain. As a result, the nominal designs will become infeasible if the input parameters are acknowledged to be uncertain. All parameter uncertainty intervals in these examples are considered to be reducible and all nominal parameter values considered are assumed to be adjustable by a small amount. In other words there will be associated selectable α_k and β_k values for each parameter considered. For the examples presented in this section the problems are solved twice in order to validate the capability of the meta-model

assisted DISA approach, first obtaining solutions using the DISA approach of Figure 5.5(a) and then again using the meta-model assisted DISA approach detailed in Figure 5.5(b).

5.4.1 Thin-Walled Tube Design

The first example presented is a simple two dimensional problem adapted from Arora [2004] to consider two objectives, chosen so that the solutions produced can be presented graphically. Figure 5.8 depicts the simple hollow tube system under consideration which is described by its length, *L*, radius, *R*, wall thickness, *t*, and the compression load it supports, *P*.

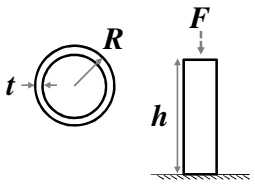

Figure 5.8: Tube Design Model

Determining the optimal dimensions for the parameters *R* and *t* without uncertainty can be accomplished by solving the following bi-objective optimization problem:

$$
\begin{aligned}
&\min_{R,t} f_1 = 2\rho h\pi Rt \\
&\min_{R,t} f_2 = \frac{R}{t} \\
&s.t. \\
&\quad g_1 \equiv \frac{F}{2\pi Rt} - \sigma_{\max} \le 0 \\
&\quad g_2 \equiv F - \frac{\pi^3 ER^3 t}{4h^2} \le 0 \\
&\quad R \ge 0,\ t \ge 0
\end{aligned}
\tag{5.8}
$$

The optimization problem in Eqn. (5.8) seeks to minimize the weight (f_1) and the radius to thickness ratio (f_2) of the tubular column subject to stress (g_1), buckling (g_2) and non-negativity constraints. Eqn. (5.8) contains the following constant parameters: ρ = 7833 kg/m^3 (material density), h = 5 m (tube length), F = 10,000 N (tube loading), σ_{max} = 248 MPa (max stress) and E = 207 GPa (Young's modulus). One deterministic optimal solution to this problem is R = 0.1558 (m) and t = 0.0412 (m), which for this problem can be obtained graphically. For this solution the nonlinear constraints g_1 and g_2 are both active. Based on this fact it is clear that if the input parameters R and t possess any uncertainty the only way to ensure the feasibility of the design would be to completely eliminate all uncertainty, which is usually not an option. As a result the DISA approach can be used for this problem to determine an optimal combination of uncertainty reduction and small design adjustments to ensure both feasibility and minimal performance variations with respect to the two original objective functions, f_1 and f_2 in Eqn. (5.8).

The uncertainty ranges $\boldsymbol{\Delta p}$ for each parameter (i.e., R and t) were set to be ±20% of each parameter's nominal value, as given above. Additionally each parameter was allowed to be adjustable ($\boldsymbol{\delta p}$) by ±10% from its nominal value. These values were determined intuitively for the purpose of demonstrating the capabilities of the approach, but for specific problems designers should set $\boldsymbol{\Delta p}$ and $\boldsymbol{\delta p}$ using system information. Based on these selected ranges for $\boldsymbol{\Delta p}$ and $\boldsymbol{\delta p}$ the allowable design adjustments will be guaranteed to be within the limits of the parameter uncertainty considered for each parameter provided at least 50% uncertainty reduction ($\boldsymbol{\alpha} \leq 0.5$) in the first stage problem. This is because a 50% reduction in uncertainty will result in a maximum retained

uncertainty of ±10% of the nominal parameter values, which will be guaranteed to fall within the original uncertain region (±20% of nominal) even if $\boldsymbol{\beta}$ adjusts $\boldsymbol{p_0}$ by the maximum 10% adjustment. The DISA approach was implemented using a MOGA optimizer and produced the results shown in Figures 5.9 and 5.10.

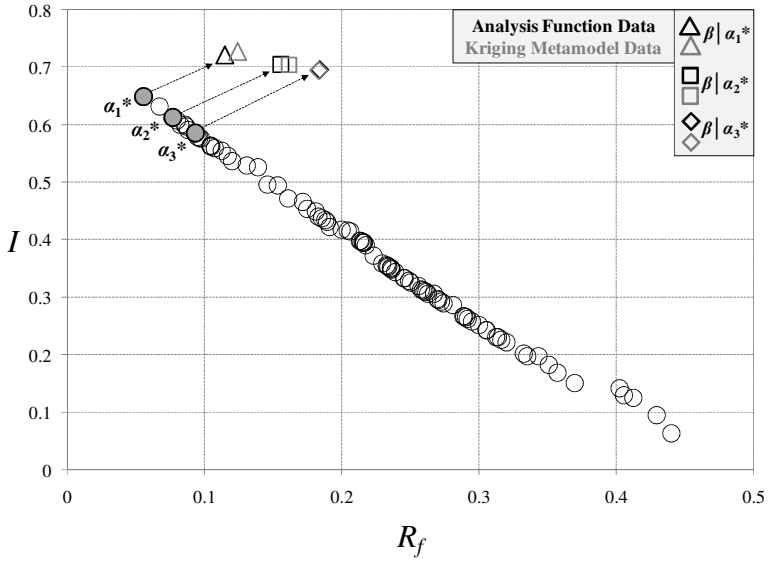

Figure 5.9: β Results for Three Sample α_i* Solutions

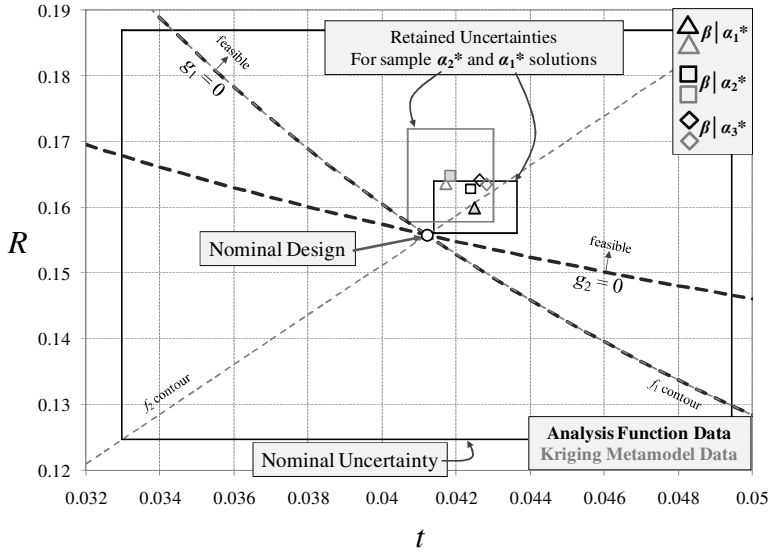

Figure 5.10: Adjusted Uncertain Solution in the Parameter Space

Figure 5.9 is an objective space (R_f vs. I) plot of the $\boldsymbol{\alpha}^*$ Pareto solutions, along with three sets of $\boldsymbol{\beta}$ Pareto solutions corresponding to three selected $\boldsymbol{\alpha}^*$ solutions (which have been highlighted in grey filled circles in Figure 5.9). Figure 5.10 is a plot of the same $\boldsymbol{\beta}$ Pareto solutions shown in Figure 5.9, but plotted in the parameter space of the tube design problem in order to show their relationship to the problem's objective and constraint function contours. In Figure 5.10 the nominal design's original input parameter uncertainty region and the retained uncertainty regions for two representative $\boldsymbol{\beta}$ solutions (called out with a grey fill) are plotted as rectangles around those solutions. This has been done to clearly show that the original candidate design is infeasible due to input parameter uncertainty and that the feasibility of the resulting solutions produced by the DISA approach is ensured. In both figures the solutions obtained with actual analysis function calls are shown in black outlines while those obtained using kriging meta-models of the analysis functions are shown in grey outlines. The geometric shapes of the solution point markers (triangles, squares, and diamonds) are the same for corresponding solutions in both Figures 5.9 and 5.10 for comparison purposes. For instance, the square shaped solutions in Figure 5.10 are the parameter space plots of the square shaped Pareto points in Figure 5.9. Recall that all $\boldsymbol{\alpha}$ solutions were obtained using actual analysis functions. In Figure 5.10 the original objective contours are depicted in black dashed lines (to show that the DISA approach does in fact minimize the variation in the original system objectives), the constraint function contours are depicted in bold and dashed black lines and the nominal design solution is depicted by a white filled circle. It should be noted that when both black and grey solution cannot be clearly distinguished on one of the corresponding figures it is because there is excellent agreement between the two

solution methods (actual analysis functions in black outlines and kriging meta-model assisted solutions in grey outlines).

As can be seen in Figure 5.9, each $\boldsymbol{\beta}$ Pareto solution set generated has larger R_f and I values than the $\boldsymbol{\alpha}^*$ solution used to generate those corresponding $\boldsymbol{\beta}$ solutions. This is because the parameter adjustments made to the candidate design in the second stage problem clearly increase both R_f and I when $\boldsymbol{\beta}$ values are nonzero, as seen in Eqn. (5.3) and Eqn. (5.5) respectively. This is the price of ensuring feasibility. The candidate design is clearly on two active constraint functions as shown in Figure 5.10. As a result all DISA solutions to this problem have been moved away from the constraint boundaries by some small amount, resulting in nonzero $\boldsymbol{\beta}$ values. The exact amount of parameter adjustments required is a function of the retained uncertainty in the system following the first stage problem. As the amount of retained uncertainty in the system increases, as shown by a decrease in I in the $\boldsymbol{\alpha}$ Pareto on Figure 5.9 (i.e., from $\boldsymbol{\alpha}_1^*$ to $\boldsymbol{\alpha}_2^*$), larger adjustments to the nominal parameter values are required. This can be seen in Figure 5.10 as the $\boldsymbol{\beta}$ solutions corresponding to $\boldsymbol{\alpha}_2^*$ are further away from the nominal solution than those corresponding to $\boldsymbol{\alpha}_1^*$, and the black outlined triangle $\boldsymbol{\beta}$ solution (corresponding to $\boldsymbol{\alpha}_1^*$) has a smaller retained uncertainty range than the grey outlined square point (corresponding to $\boldsymbol{\alpha}_2^*$).

As shown in Figures 5.9 and 5.10, for each of the solutions presented (i.e., from $\boldsymbol{\alpha}_1^*$ to $\boldsymbol{\alpha}_3^*$), the meta-model assisted $\boldsymbol{\beta}$ solutions do not match the analysis function results perfectly, but they do show general agreement, suggesting that any effective meta-modeling technique could produce solutions without the need for additional function calls after first solving the $\boldsymbol{\alpha}$ problem in this example. In this example the $\boldsymbol{\alpha}$ problem required

61,707 function calls while each of the three $\boldsymbol{\beta}$ problems solved using the DISA approach of Figure 5.5(a) required 178,120, 180,255 and 180,255 function calls respectively. Recalling that the meta-model assisted DISA solution, obtained using the approach formulation of Figure 5.5(b), did not require any additional function calls than what was previously obtained to solve the $\boldsymbol{\alpha}$ problem and thus it can be concluded that the meta-models assisted formulation leads to a total computational savings of 538,630 function calls.

If the above problem is restated using ±15% and ±20% of nominal as the ranges of parameter uncertainty $\Delta\boldsymbol{p}$ and maximum design adjustments $\delta\boldsymbol{p}$ respectively, clearly the range of potential design adjustments will fall outside of the region of the parameter space sampled during the first stage optimization. As a result, between the first and second stage optimizations the parameter space needs to be sampled a bit more to ensure adequate coverage in order to build valid meta-models for design adjustments. The DISA approach was applied to the problem again, this time using these new ranges. The computational effort for the $\boldsymbol{\alpha}$ and $\boldsymbol{\beta}$ problems was comparable to the original example, but this time an additional 1,017 function calls were used to sample the region of the parameter space not considered during the first stage optimization. For this case the results shown in Figures 5.11 and 5.12 are produced (which use the same notation as Figures 5.9 and 5.10 above).

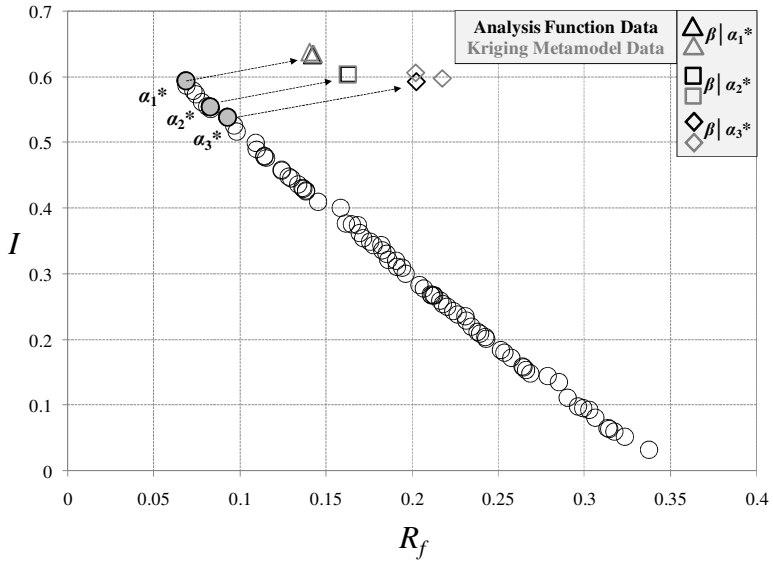

Figure 5.11: Alternate Problem Pareto Frontier

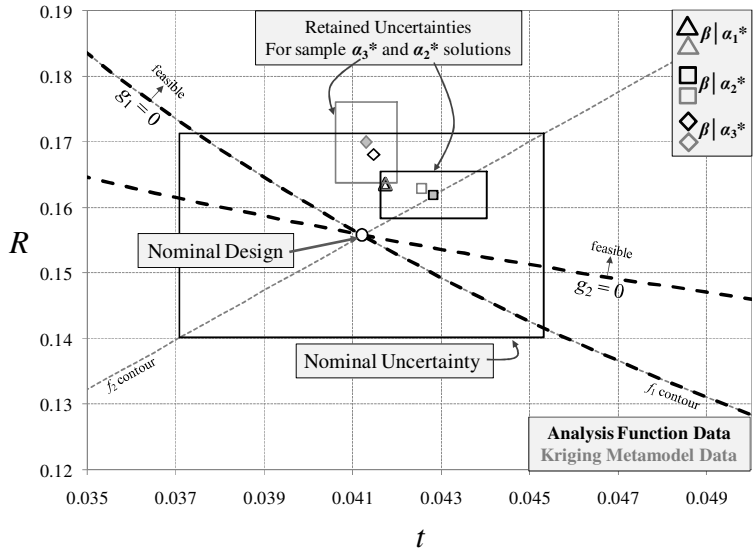

Figure 5.12: Alternate Problem Adjusted Uncertain Solutions

Notice that in Figure 5.12 the original nominal uncertain region is much smaller and that the retained uncertain regions for the solution points lie outside the original uncertain region. However, the produced results from kriging assisted DISA (Figure 5.5(b)) essentially agree with the results produced by the DISA approach using actual

analysis functions (Figure 5.5(a)). Clearly, a limited number of additional function calls can produce effective results in the cases where acceptable design adjustments fall outside of the region of the parameter space considered during the uncertainty reduction optimization problem.

5.4.2 Angle Grinder Design

To demonstrate the properties of the DISA approach with a more complex system, an angle grinder model used by Li et al. [2009a] (first presented by Williams et al. [2008] and used in the Chapter 3) was analyzed. As shown in Figure 5.13, the angle grinder system consists of a battery model, a motor model and a bevel gear model containing approximately 30 input parameters and numerous outputs. A deterministic optimal solution that produces a minimal grinder weight and a maximum available power was found using MOGA prior to employing the DISA approach to this system. Six of the model parameters were considered to have uncertainty in this example. For specific details on the grinder model see Williams et al. [2008].

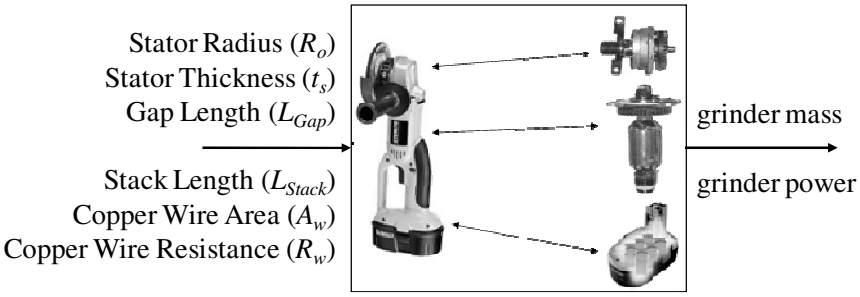

Figure 5.13: Angle Grinder System

Table 5.1 provides the settings used in the application of the DISA approach, while the nominal values for the 6 parameters considered in this application are shown below in Table 5.2 (all other inputs to grinder model were taken as deterministic constants).

Table 5.1: Grinder Problem Specifics

Objectives	2
Constraints	9
Parameters	6
Uncertainty	20% of nominal
Max Adjustment	10% of nominal

All of these parameters are critical elements of the design of the angle grinder's motor sub-system. These 6 parameters were analyzed by the DISA approach and were assumed to be both uncertain and adjustable in accordance with the limits given in Table 5.1. The nominal design was selected such that four constraints g_2, g_3 and g_4 were very close to being active. These constraints all represent limitations on the flux density of the stator, armature and air gap of the grinder's electric motor.

Table 5.2: Grinder Problem Nominal Parameters

Parameters	*Nominal Values*
Stator Radius (R_o)	0.0012 m
Stator Thickness (t_s)	0.0501 m
Gap Length (L_{Gap})	0.0006 m
Stack Length (L_{Stack})	0.0188 m
Copper Wire Area (A_w)	0.036 mm^2
Copper Wire Resistance (R_w)	0.504 Ω

Using the data in Tables 5.1 and 5.2 and the grinder analysis functions, a set of DISA results were obtained using a MOGA optimizer. Figure 5.14 displays three representative sets of $\boldsymbol{\beta}$ results for the grinder problem for three selected $\boldsymbol{\alpha}$ Pareto solutions. As with the previously presented two-dimensional example $\boldsymbol{\beta}$ solutions were determined in two ways: using actual analysis function model and using kriging meta-models. Figure 5.14 contains R_f vs. I plots for both the results of the first stage optimization and three sets of $\boldsymbol{\beta}^*|\boldsymbol{\alpha}_i^*$ Pareto solutions. In Figure 5.14, all $\boldsymbol{\alpha}$ Pareto solutions are presented in black circles. The $\boldsymbol{\alpha}_i^*$ solutions considered for each depicted $\boldsymbol{\beta}^*|\boldsymbol{\alpha}_i^*$ Pareto are called out by grey filled circles. The corresponding $\boldsymbol{\beta}$ Pareto solutions

obtained using the analysis function are presented in black outlines and the kriging meta-model assisted results are presented in grey outlines. As with the plots in the previous example, when a distinction between the black and grey solutions cannot be distinguished on the figure it is because the solutions obtained agree directly. Not all of the $\boldsymbol{\alpha}$ Pareto solutions for this example were infeasible following the first stage problem, indicating that for some cases (7 out of 15 $\boldsymbol{\alpha}$ Pareto solutions) the feasibility of the system could be achieved by uncertainty reduction alone and the second stage procedure was unnecessary. However, those solutions that were feasible after the first stage procedure also required a high level of investment (low $\boldsymbol{\alpha}$ values) which could potentially be undesirable to the designer. For those solutions that were infeasible (as indicated by positive R_g values) the second stage procedure of the DISA approach was necessary. Three $\boldsymbol{\alpha}_i$* solutions shown in Figure 5.14 were infeasible yet after the first stage procedure and thus need further adjustment to guarantee feasibility.

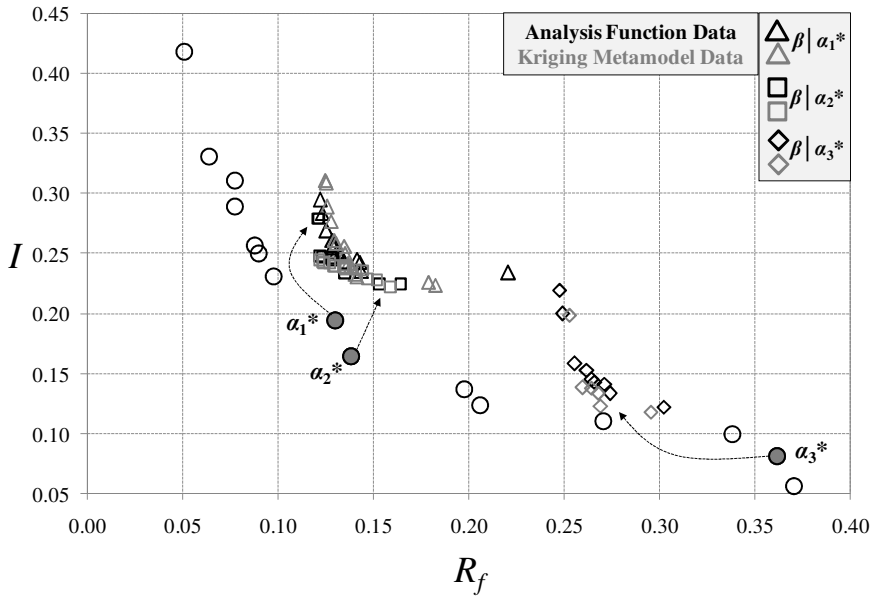

Figure 5.14: Grinder β Results for Various α_i* Solutions

As can be seen in Figure 5.14, the $\boldsymbol{\beta}$ solutions corresponding to two selected $\boldsymbol{\alpha}_1$* and $\boldsymbol{\alpha}_2$* overlap quite a bit. For this reason Figure 5.15 shows just the first stage solution $\boldsymbol{\alpha}_1$* and its corresponding $\boldsymbol{\beta}$ Pareto. Several observations can be made from Figures 5.14 and 5.15. First, in order to ensure feasibility additional cost is necessary as all $\boldsymbol{\beta}$ solutions have higher I values than $\boldsymbol{\alpha}_1$*. Secondly, the trade-off between I and R_f is very clear for the $\boldsymbol{\beta}$ solutions depicted, showing that more investment can lead to smaller variations in system objectives. The third and most interesting observation is that if the designer is willing to invest more it is possible to further reduce objective function variations (through adjusting the nominal values of parameters) than that achieved through uncertainty reduction alone. This result is demonstrated by the solutions with an R_f value being less than 0.13 in Figure 5.15**,** or the entire set of $\boldsymbol{\beta}$ solutions corresponding to $\boldsymbol{\alpha}_3$* in Figure 5.14.

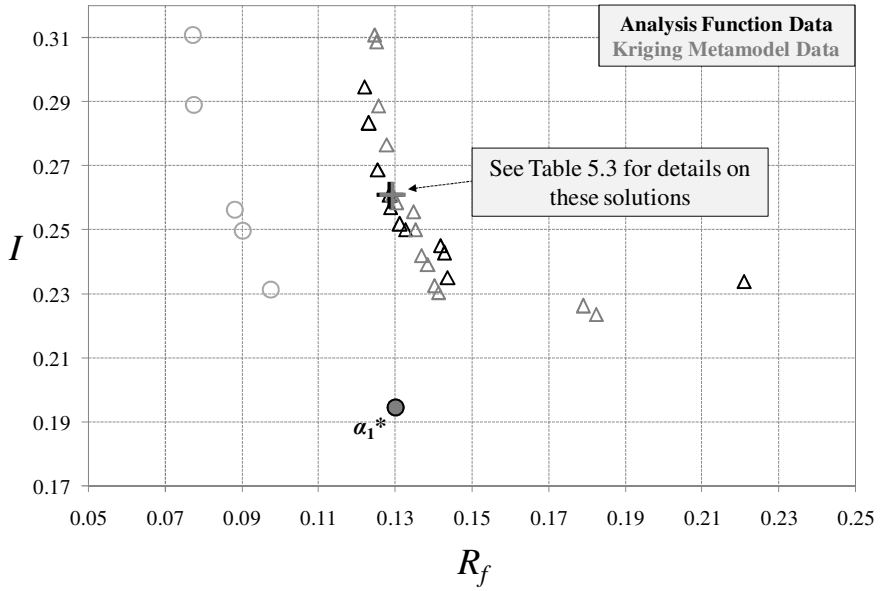

Figure 5.15: Grinder $\boldsymbol{\beta}$ Solutions for $\boldsymbol{\alpha}_1$*

As can be seen in the preceding figures there is actually a very good agreement between the two approaches for finding the corresponding $\boldsymbol{\beta}^*|\boldsymbol{\alpha}_i^*$ solutions suggesting again that the DISA approach can be made computationally efficient if legacy data from in the first stage uncertainty reduction problem is used to solve the subsequent design adjustment problem. To further demonstrate this fact and to describe a sample of the improvements to the nominal design suggested by the DISA approach in the case of the angle grinder, Table 5.3 is provided which contains a comparison of a single DISA $\boldsymbol{\beta}^*|\boldsymbol{\alpha}_i^*$ solution obtained through two different methods (the $\boldsymbol{\beta}^*|\boldsymbol{\alpha}_i^*$ solution point called out on Figure 5.15 with black and grey crosses, for the analysis function and kriging meta-model produced solutions, respectively).

Table 5.3: Sample Grinder Results Comparison

	First Stage ($\boldsymbol{\alpha}_1^*$)	***Analysis Functions***	***Kriging Metamodel***
R_f	0.138	0.129	0.129
I	0.165	0.261	0.261
R_g	0.394	-0.353	-0.354
	$\boldsymbol{\alpha}$	$\boldsymbol{\beta}_{Analysis}$	$\boldsymbol{\beta}_{Kriging}$
p_1 (R_o)	0.919	-0.279	0.292
p_2 (t_s)	0.103	-0.315	-0.136
p_3 (L_{Gap})	0.894	-0.718	-0.717
p_4 (L_{Stack})	0.918	0.514	0.410
p_5 (A_w)	0.889	-0.189	-0.508
p_6 (R_w)	0.960	-0.294	0.248

Table 5.3 also contains the corresponding R_f, I and R_g values of the first stage solution for comparison purposes. Note that the R_g value following the first stage procedure is greater than 0, indicating that the determined level of uncertainty reduction is incapable of guaranteeing feasibility which drives the need for the second stage procedure. Furthermore, Table 5.3 suggests that for this specific solution the copper wire area A_w needs only a small uncertainty reduction of 11% (α_5 = 0.889) and an equally

small nominal value adjustment of less than 2% (β_3 = -0.189, or 0.189×10% ≈ less than 2% of its nominal value in accordance with Tables 5.1 and Table 5.2), which suggests that the uncertainty in this parameter does have a large effect on the candidate design's performance and feasibility. Conversely this DISA solution suggests that the uncertainty in the mass of the stator thickness (t_s) is far too uncertain (α_2 = 0.103), and additionally needs to have its nominal value reduced as well by (β_2 = -0.315). This suggests that the uncertainty in the stator thickness parameter is far more important to the overall design and should be addressed more carefully. These conclusions make sense given that the original design objectives are to maximize grinder power and minimize grinder weight. Better control of the critical parameters of the grinder's motor design will clearly impact the overall grinder power in a positive fashion. Keep in mind that this analysis focuses on just one potential solution for this problem and the DISA approach produces numerous options just like this one for the designer to consider.

In terms of computational effort the first stage $\boldsymbol{\alpha}$ problem required approximately 2,640,000 function calls. An additional 931 function calls were required following the first stage procedure in order to sample regions of the parameter space not adequately sampled during the first stage optimization, as discussed in Section 5.3. Each of the $\boldsymbol{\beta}$ problems solved using the framework shown in Figure 5.5(a) required additional 3,400,000 function calls, on average. As before, solving the second stage problem using the formulation shown in Figure 5.5(b) required practically no additional function calls (save for the 931 extra calls required for meta-model refinement prior to beginning any second stage optimizations), which demonstrates the capability of the meta-model assisted DISA approach to produce a rather large total savings in function calls.

5.5 SUMMARY OF RESEARCH THRUST 3

A new sensitivity analysis based approach using a sequential two stage approach, DISA, has been presented for use in managing uncertainty in engineering design. For a candidate design containing interval parameter uncertainty this approach has the ability to determine the optimal combination of uncertainty reduction in the first stage optimization. If necessary, the DISA approach is then capable of determining the optimal combination of design adjustments required to minimize system objective function variations while simultaneously ensuring feasibility under the system's retained uncertainty in the second stage optimization problem. Most importantly, by using a two-stage optimization framework, this approach arrives at those solutions without searching the entire design space of the problem and in the process ensures that new design alternatives are as similar to the candidate design as possible.

This approach has been shown to be effective on engineering problems of varying difficulty and additionally has been shown to be capable of doing so rather efficiently using a meta-model assisted framework. It was shown in both examples that given various levels of optimal uncertainty reduction this new DISA approach is capable of taking an infeasible design and moving that design away from the nominally active constraint surfaces by a small amount in order to ensure feasibility while maintaining performance effectively. In the more complex engineering example a specific study was performed on a single candidate solution produced by the DISA approach to demonstrate the ability of the new method for showing a designer which specifics elements of an engineering system are the most critical to both the feasibility and performance of the design. More importantly, it was also shown that the DISA approach also is capable of

suggesting to a designer how best to use available investment through uncertainty reduction and/or small design adjustments.

The DISA approach, like the other approaches presented in this dissertation (and the MOSA approach which it was extended from), does require a significant level of *a priori* information to employ. The DISA approach is only applicable when a candidate design already exists and then assumes that the uncertainty in that candidate design can be reduced about the nominal parameter values for the candidate design. There may be many design problems for which a nominal or candidate design does not yet exist, but for which a designer must have a means for considering numerous sources of reducible uncertainty. The next chapter of this dissertation attempts to address this type of problem and thus provide a more general approach for the design of engineering systems under reducible interval uncertainty.

CHAPTER 6: REDUCIBLE UNCERTAIN INTERVAL DESIGN (RUID)

6.1 INTRODUCTION TO RESEARCH THRUST 4

In the previous three chapters new sensitivity analysis based approaches for the design of systems under reducible interval uncertainty were presented. These approaches have been shown to be effective at improving the performance of a preexisting candidate design by making changes to the known nominal uncertain intervals and/or making small adjustments to the predetermined nominal parameter values themselves. However, the underlying assumption for all these approaches has been that the nominal parameter values and nominal uncertain intervals are known, which may often not be the case. The work presented in this chapter provides designers with an approach for the design of engineering systems under reducible interval uncertainty without the need for a preexisting candidate designs and/or known uncertainty levels, thus relaxing the limiting assumptions required by the previous three research thrusts.

Many of the current approaches for design under uncertainty possess limitations. Some methods require large and difficult to obtain data requirements for statistical uncertainty quantification [Lui et al., 2006; Youn and Wang, 2008; Benanzer et al., 2009]. Other methods approximate or estimate unknown statistical information with evidence theory or possibility theory, resulting in a decrease in accuracy when compared to probabilistic methods [Mourelatos and Zhou, 2006; Zhou and Mourelatos, 2008]. Still other methods forgo statistics altogether in lieu of interval analysis but require designers assume nominal values and uncertain intervals for the uncertain parameters [Liao and Chiou, 2008; Hamel et al., 2010; Li et al., 2009a]. All of these approaches have distinct

strengths and weaknesses that a designer must consider when determining how and when to consider uncertainty in the design process. Statistical uncertainty quantification is certainly desirable but requires large amounts of information that is not always available. When that is the case, should a designer invest in obtaining that information? Does it always make sense to approximate unknown statistical information with lower fidelity estimations? If obtaining statistical information is not feasible or desired, what uncertain intervals should the designer assume or estimate for uncertain parameters? Does it even make sense to assume a nominal value for an uncertain parameter that by its very nature is uncertain, as required by numerous current approaches (e.g. [Liao and Chiou, 2008; Hamel et al., 2010; Li et al., 2009a])? These are the types of questions that a designer must be able to answer when deciding how to consider reducible sources of input uncertainty and the answers are not always clear. Furthermore, these questions may be particularly difficult to answer early in the design process when very little (if any) information is available about the types and sources of uncertainty that may exist within the system being designed.

When dealing with irreducible uncertainty the sources uncertainty becomes a known limiting factor in the system and must simply be designed around (e.g. robust optimization as discussed in Chapter 1). However, when faced with reducible uncertainty the problem becomes more complicated, as previously stated. A designer must evaluate how much uncertainty is acceptable and must consider if the system's performance could be improved through costly investments such as more information, better equipment or tighter control of tolerances; all of which will require additional resources or capital. RBDO approaches have been developed that allow for the inclusion of additional

statistical information should it become available as a means for considering reducible uncertainty [Gunawan and Papalambros, 2006; Youn and Wang, 2008]. Other approaches combine uncertainty reduction mechanisms with RBDO techniques, either through sequentially performing RBDO followed by uncertainty reduction [Qu et al., 2003], or through simultaneously considering reliability and uncertainty reduction mechanisms during the design process [Kale and Haftka, 2008]. There are also approaches presented in the literature that suggest treating the variance in an uncertain parameter as a factor to control within an RBDO algorithm provided a designer has a means for producing lower variance in input parameters [Benanzer et al., 2009]. For the cases where statistical uncertainty quantification is not possible some recent approaches have suggested that the uncertain intervals for input parameters can be reduced around a known nominal value (in effect specifying tighter tolerances) in order to improve the performance of a design [Li et al., 2009a; Li et al., 2009b, Hamel et al., 2010].

All of the approaches discussed in the previous paragraph, and in Chapters 3-5 for that matter, are extremely effective when the appropriate information is available with which to quantify or describe any relevant uncertainty. Collecting additional statistical information or specifying tighter tolerances about a known nominal parameter value necessarily implies that the uncertainty in that parameter is known to some extent, either in the form of distributions or uncertain intervals about that known nominal value, which may not always be the case. There may often be situations where a system designer faced with reducible sources of uncertainty will know, based on his/her experience, that the input parameters of a design will possess tolerances and/or uncertainties, but may have no way of estimating or specifying those tolerances without making many needless,

arbitrary or perhaps even erroneous assumptions, especially at early stages in the design process when information is necessarily limited.

Currently there is no existing approach capable of including reducible input uncertainty within an optimization framework and able to consider the following factors: 1) multiple sources of controllable (or reducible) input interval uncertainty, 2) limited resources for controlling uncertainty, 3) computationally expensive simulation models, 4) no available statistical information about uncertainty, 5) unknown nominal values for uncertain parameters, and 6) no reliable means for estimating uncertain intervals. This chapter presents a new multi-objective optimization approach designed to meet these needs. This new approach, called Reducible Uncertain Interval Design (RUID), is inspired by SA approaches in that it relates input uncertainty to output variations, but does not require a designer to have or estimate any statistical information, uncertain intervals or nominal values for any uncertain parameters. The only values a designer must specify to use this approach are the extreme upper and lower bounds on any uncertain input parameters for which the uncertainty is reducible or controllable. The RUID approach is able to determine the optimal uncertain intervals (upper and lower bounds) for the reducible uncertain input parameters to a system that will: i) guarantee minimum variations in system outputs under uncertainty, ii) guarantee minimal required control over reducible uncertainty (recognizing that reducing uncertainty has an associated cost), iii) ensure that the system's feasibility is satisfied under uncertainty, and iv) produce design solutions with as close to the deterministic multi-objective optimal system performance as possible.

Simply put, the RUID approach provides designers with optimal uncertain intervals for all input parameters which possess reducible uncertainty. These intervals can then be used to specify tolerances, select manufacturing processes, purchase equipment and/or make any other uncertainty related design decision later in the design process. Figure 6.1 depicts the manner in which the optimal uncertain intervals produced by the RUID approach can be used. An uncertain interval, such as the one shown at the top part of Figure 6.1, will be specified for all input parameters considered by the RUID approach. Once those intervals are determined, as long as a designer specifies tolerances in the form of a nominal value and an uncertain interval (left side of the lower part of the figure) or selects processes with statistical uncertainty (right side of the lower part of the figure) within the RUID determined upper and lower bounds for all reducible uncertain parameters considered, the performance of the system under uncertainty will be guaranteed.

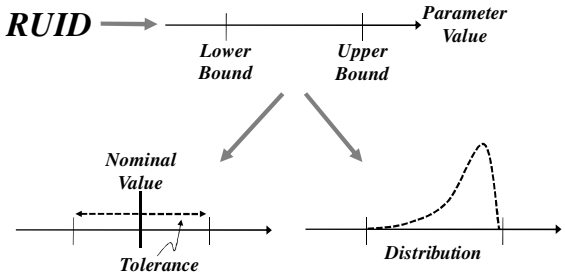

Figure 6.1: Unknown Uncertainty Quantification

RUID makes it possible to perform optimal design under reducible uncertainty without the need for limiting or degrading assumptions as previously discussed. It is formulated to handle design optimization problems possessing multiple objectives, multiple constraints and mixed continuous-discrete input parameters. Additionally the computational efficiency of the approach is improved through the use of a kriging meta-

modeling technique applied to system responses obtained early in the approach. This new approach does require an increase in the overall dimensionality of the problem due to fact that both the upper and lower bounds on the input parameters are determined. Additionally, while the use of meta-modeling techniques improves the efficiency of the approach, this improvement does create the potential for decreased accuracy. The strengths and weakness of this new approach will be detailed in the subsequent sections. Section 6.2 contains necessary background information and terminology. The formulation of the RUID approach is presented in Section 6.3. Section 6.4 presents the results obtained using the RUID approach on three example problems of varying difficulty. Section 6.5 contains some concluding remarks.

6.2 BACKGROUND AND TERMINOLOGY

This section contains the necessary background information and relevant terminology for the RUID approach that has not been previously presented in this dissertation.

6.2.1 Input Uncertainty Level Control

The set of uncertain intervals for a system can be depicted as an uncertain region in the parameter space for a problem, as seen in previous chapters of this dissertation. Recall that the term "parameter space" describes the set of all possible input parameter combinations for a system of interest, bounded by extreme upper and lower bounds $\boldsymbol{p}_{ub}$ and $\boldsymbol{p}_{lb}$. Figure 6.2 below depicts a two dimensional visualization of a general parameter space for a problem comprised of two inputs p_1 and p_2. Shown within the parameter space in Figure 6.2 is an input uncertainty region defined by the upper and lower bounds on

both parameters $\boldsymbol{p_U}$ and $\boldsymbol{p_L}$ (or the uncertain interval [$\boldsymbol{p_L}$, $\boldsymbol{p_U}$]) that a designer would like to determine. This figure is very similar to Figure 2.2 with the key difference that no nominal parameter value is depicted in Figure 6.2 since the assumption in this chapter is that nominal parameter values are unknown. Instead this figure depicts an uncertain region within the parameter space determined only by upper and lower bounds, $\boldsymbol{p_{lb}} \leq \boldsymbol{p_L} \leq \boldsymbol{p_U} \leq \boldsymbol{p_{ub}}$.

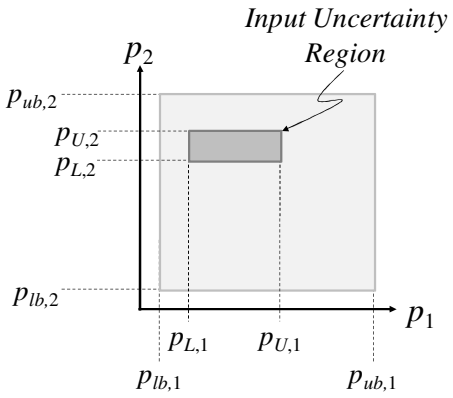

Figure 6.2: Input Uncertainty Region

As can be seen in Figure 6.2, the difference between the size of the input uncertainty region (the dark grey rectangle in Figure 6.2) and the region depicting all possible parameter combinations (light grey rectangle) can be thought of as the overall level of control over the reducible uncertain parameters in the system. The greater the difference in size between the two regions, the lower the level of input uncertainty the system will possess. Recall that the RUID approach will use optimization to select the upper ($\boldsymbol{p_U}$) and lower ($\boldsymbol{p_L}$) bounds for all input parameters to a system that possess reducible uncertainty. Eqn. (6.1), which is a function of $\boldsymbol{p_U}$ and $\boldsymbol{p_L}$, provides a formulation for describing the overall level of control over the reducible uncertainty in a system.

$$I_p = e^{-C\left(w_1\left(\frac{1}{N}\sum_k \Delta p_k\right)+w_2\left(\prod_k \Delta p_k\right)\right)}$$

$$where\ \Delta p_k = \frac{p_{U,k} - p_{L,k}}{p_{ub,k} - p_{lb,k}} \tag{6.1}$$

$$w_1 + w_2 = 1$$

This formulation is adapted from the *Investment* metric used in previous chapters and by Li et al. [2009a], but has eliminated the need for nominal parameter values and further penalizes extremely low uncertainty levels through the use of the exponential decay function. The metric I_p describes the overall control level over $k = 1,\ldots,K$ uncertain parameters, where Δp_k represents the uncertain interval in a single parameter normalized by the constant extreme upper and lower bounds on that parameter. As the elements of $\boldsymbol{\Delta p}$ approach zero when system uncertainty is decreased, the value for I_p will approach 1. High I_p indicates the need for greater control over uncertain parameters (e.g. lower tolerances or more uncertainty reduction), which will necessarily require a greater investment in resources and/or capital. The C in Eqn. (6.1) is a constant that can be selected by the designer in order to tune the relationship between uncertainty levels and the costs associated with reducing system uncertainty. The larger the value for C the more sensitive the value for I_p is to small changes in the values for Δp_k. When solving Eqn. (6.1) for I_p throughout this chapter the constant C is set to a value of 5. This value was selected based on empirical observations made during the development of this new approach and can obviously be adjusted as necessary to fit the needs of a particular design problem. Additionally a value of 0.5 is used for both w_1 and w_2 throughout this chapter, again based on empirical observations.

6.2.2 Worst Case Uncertainty Propagation

Uncertainty in the inputs to a system leads to a corresponding uncertainty, or variation, in the system's outputs. In the case of a system that a designer would like to optimize using Eqn. (2.2), uncertainty in $\boldsymbol{p}$ will lead to some level of variation in both $\boldsymbol{f}$ and $\boldsymbol{g}$ as shown in Figure 6.3. For visualization purposes Figure 6.3 depicts a notional system consisting of two uncertain parameters in the parameter space, the resulting variation of two objective functions in the objective or performance space, and the variation in two constraint functions shown in the constraint space. As with the parameter space defined previously, the objective and constraint spaces describe the set of all possible objective and constraint function combinations possible, respectively, for a particular level of input uncertainty.

Regardless of how a system's input uncertainty is quantified it is essential to understand the effect of that uncertainty on the performance of the system. If the input uncertainty to a system is quanified with upper and lower bounds, one means for quantifying the effect of that uncertainty is to search for the minimum and/or maximum values of all output functions of interest (i.e. objectives and constraints) using a simple single objective optimization procedure for each maximum and/or minimum output value. For example, if a designer is interested in the maximum possible value for an objective function (or the worst case value if the objective is to minimize function f_i) then the optimization problem given in Eqn. (6.2) should be solved. In Eqn. (6.2) the vector $\boldsymbol{p}_v$ is again used, which represents a single realization of the uncertain values of the vector $\boldsymbol{p}$ bounded by $\boldsymbol{p}_U$ and $\boldsymbol{p}_L$. This vector is again used as the decision variables when

attempting to quantify the effects of a set of known input uncertain intervals on a system's outputs.

$$f_{i,max} = \max_{p_v} f_i(\boldsymbol{p}_v) \quad \text{where } \boldsymbol{p}_L \le \boldsymbol{p}_v \le \boldsymbol{p}_U \tag{6.2}$$

If the minimum value for an objective function (or best possible performance) is desired, then the optimization problem in Eqn. (6.3) must be solved.

$$f_{i,min} = \min_{p_v} f_i(\boldsymbol{p}_v) \quad \text{where } \boldsymbol{p}_L \le \boldsymbol{p}_v \le \boldsymbol{p}_U \tag{6.3}$$

Lastly, if a designer is interested in the feasibility of a system, then it is important to know if any of the constraint functions will potentially have a value greater than 0. As such, in order to check the feasibility of a system under uncertainty it is necessary to check the maximum possible values for all constraint functions. This can potentially be accomplished by solving Eqn. (6.4) for each constraint function.

$$g_{j,max} = \max_{p_v} g_j(\boldsymbol{p}_v) \quad \text{where } \boldsymbol{p}_L \le \boldsymbol{p}_v \le \boldsymbol{p}_U \tag{6.4}$$

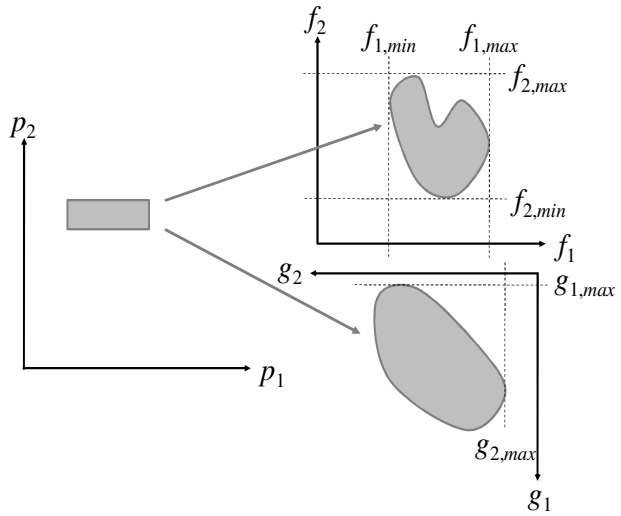

Figure 6.3: Uncertainty Propagation

If a designer is attempting to solve the multi-objective optimization problem given in Eqn. (2.2) for a system known to possess input parameter uncertainty, the worst case variation in the system's objective functions $\boldsymbol{f}$ can be quantified with a single value as shown in Eqn. (6.5).

$$V_f = \left\| \Delta \boldsymbol{f} \right\|_\infty$$
$$where \quad \Delta f_i = \frac{f_{i,max} - f_{i,min}}{f_{i,good} - f_{i,bad}} \tag{6.5}$$

In the above equation $f_{i,max}$ and $f_{i,min}$ are found using Eqn. (6.2) and Eqn. (6.3) respectively. Recall that solving Eqns. (6.2) and (6.3) for $f_{i,max}$ and $f_{i,min}$ requires that the values for $\boldsymbol{p}_U$ and $\boldsymbol{p}_L$ be specified. The top half of Figure 6.4 graphically shows V_f for a bi-objective system. The denominator of each Δf_i value in Eqn. (6.5) consists of two constant normalization factors $f_{i,good}$ and $f_{i,bad}$ which must be determined prior to evaluating Eqn. (6.5). These normalization or scaling factors should be selected to ensure that each Δf_i value considered is between 0 and 1, with 0 describing no variation and 1 describing maximum variation in the i^{th} system objective given a specified level of system uncertainty. This scaling makes it possible to compare multiple Δf_i values of drastically different orders of magnitude using a $\|.\|_\infty$ as given in Eqn. (6.5). The method for determining these scaling factors within the context of the RUID approach will be discussed in Section 6.3.

As stated previously, variation in $\boldsymbol{p}$ may very well lead to system failure, or infeasibility. Recall that in Eqn. (2.2) infeasibility results when at least one of the system's constraint functions has a value greater than 0. In order to check this, given a specified level of system input uncertainty, Eqn. (6.6) can be evaluated.

$$V_g = \max_{p_v}(\max_j g_j(\boldsymbol{p}_v))$$
$$where\ \boldsymbol{p}_L \le \boldsymbol{p}_v \le \boldsymbol{p}_U \tag{6.6}$$

As with Eqn. (6.5), Eqn. (6.6) is solved for specified values of $\boldsymbol{p_U}$ and $\boldsymbol{p_L}$. If the value for V_g is greater than 0 the system may become infeasible given the specified input uncertainty intervals. This formulation is used to find V_g in a single step in order to avoid the computational effort that could result from considering each constraint function independently through the use of Eqn. (6.4).

The bottom half of Figure 6.4 graphically depicts V_g for a two constraint system for two different levels of input uncertainty. In Figure 6.4 the dark grey uncertainty interval will result in a V_g value greater than 0 and an infeasible system. Also shown in Figure 6.4 is the correlation between I_p, or input uncertainty control, and V_f and V_g. If a designer can afford to place greater control over system uncertainty the most likely outcome will be lower variations in system outputs and in some cases will eliminate the potential for system failure.

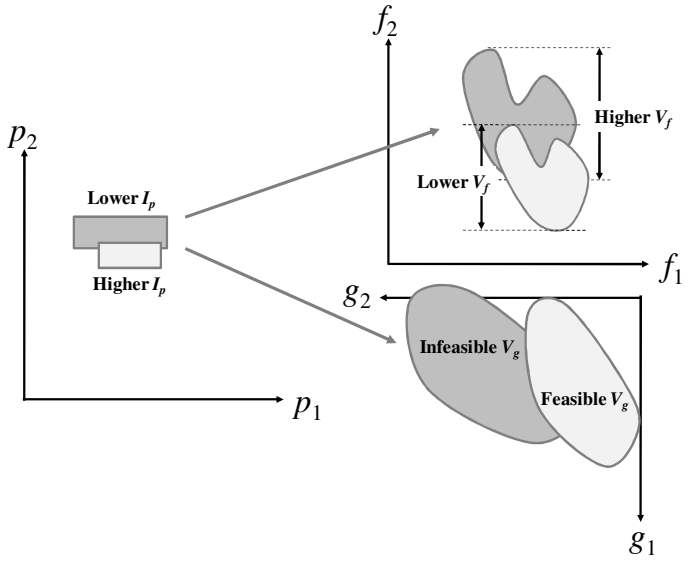

Figure 6.4: Propagated Uncertainty Comparison

6.2.3 Anchor points

If all the elements of the vector $\boldsymbol{p}$ are known with certainty (i.e., $\boldsymbol{p} = \boldsymbol{p}_U = \boldsymbol{p}_L$) then Eqn. (2.2) can be solved in a deterministic sense for the optimal values for $\boldsymbol{p}$. The set of Pareto optimal solutions that are produced describe the best performance attainable for the system in a multi-objective sense. Each of the determined Pareto optimal solutions corresponds to a different deterministic solution for the elements of the vector $\boldsymbol{p}$, assuming the values for $\boldsymbol{p}$ are known with certainty. However, as previously stated uncertainty in the input parameters for most systems is unavoidable. As a result, the values for $\boldsymbol{p}$ may very well possess some uncertainty and thus the performance of the obtained deterministic Pareto optimal solutions cannot be guaranteed. Figure 6.5 depicts this likely scenario in the parameter space for a two parameter system given a single objective function contour for simplicity.

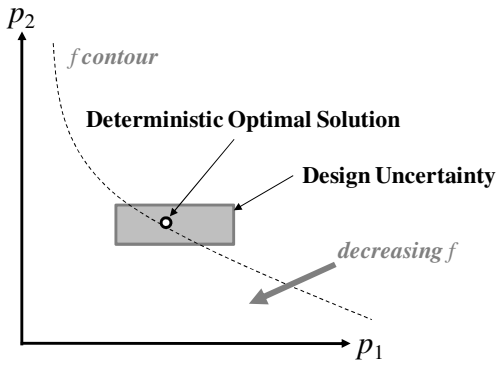

Figure 6.5: Variation from Deterministic Optima

As shown in Figure 6.5, for some realizations of $\boldsymbol{p}$ the performance of the system may improve (*f* may decrease), while for other realizations the performance may degrade and the designer cannot reliably know which of the two will occur. This relationship between input uncertainty and output variation is present in all outputs, including objectives and constraints, further exacerbating the issue. When optimizing a system

under uncertainty a designer must decide what realizations of $\boldsymbol{p}$ to focus on in the optimization problem as a result of these potential variations. As previously discussed, a designer of a system that possesses input uncertainty could optimize the expected value of the system's outputs in a statistical sense if data is available, or if data is not available the designer could optimize the system around an assumed nominal design. In either case the designer must make an assumption about the system and in extreme cases the system may perform very different from the expected or nominal performance, especially in multi-objective problems.

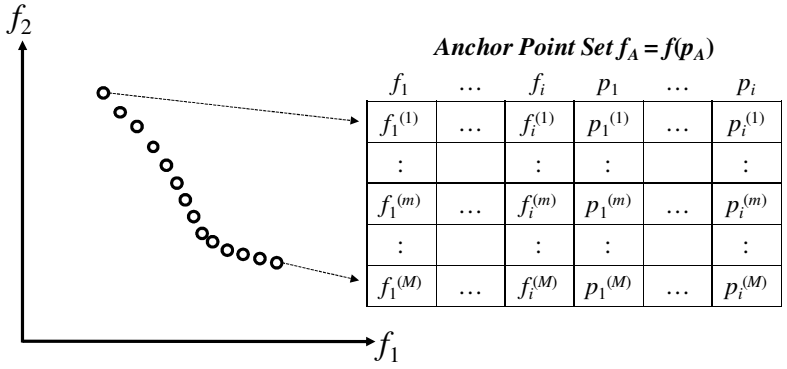

Figure 6.6: RUID Anchor Points

An alternate approach to the challenge of optimizing a design under uncertainty is to treat the deterministic Pareto optimal solution set for a system of interest as the ideal performance of the system. Using this approach a designer would like the system's performance under uncertainty to vary as little as possible from the deterministic optimal performance. To this end a Pareto optimal set of solutions for a system of interest, determined by solving Eqn. (2.2) for $\boldsymbol{p}$ in a deterministic sense, can be treated as target values, or anchor points, for a follow on optimization under uncertainty procedure, as shown in Figure 6.6.

6.2.4 Anchor Point Upper and Lower Bounds

Once a set of M anchor points $\boldsymbol{p_A}$ is obtained, as detailed in the previous section, the uncertainty associated with the m^{th} anchor point ($\boldsymbol{p_A^{(m)}}$) can be described by the distance from the anchor point to the upper/lower bounds on all uncertain parameters, as shown in Eqn. (6.7).

$$\begin{aligned} \boldsymbol{p_U} &= \boldsymbol{p_A^{(m)}} + \boldsymbol{d_U} \\ \boldsymbol{p_L} &= \boldsymbol{p_A^{(m)}} - \boldsymbol{d_L} \end{aligned} \tag{6.7}$$

The vectors $\boldsymbol{d_U}$ and $\boldsymbol{d_L}$ have the same number of elements as $\boldsymbol{p_A}$ and describe the uncertainty associated with the m^{th} anchor point as shown in Figure 6.7. The values for $\boldsymbol{d_U}$ and $\boldsymbol{d_L}$ should be limited to values between 0 and a designer specified maximum distance, which could typically be some percentage of the difference between the extreme upper and lower bounds ($\boldsymbol{p_{ub}}$ and $\boldsymbol{p_{lb}}$) on the system's inputs. The index of the anchor point m and the anchor point distances $\boldsymbol{d_U}$ and $\boldsymbol{d_L}$ associated with that anchor point will be selected systematically by the RUID approach thus defining the upper and lower bounds on the reducible uncertain parameters of a system.

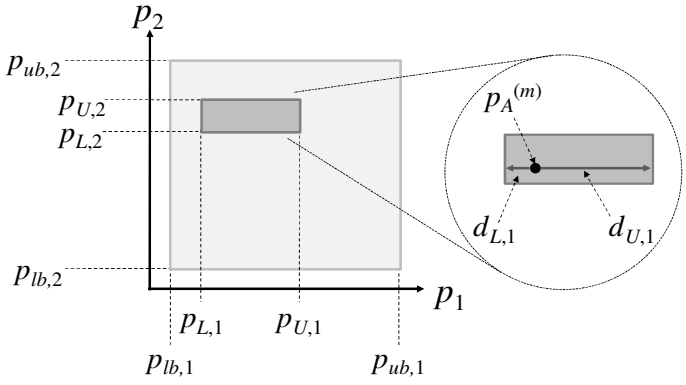

Figure 6.7: Uncertain Region for the m^{th} Anchor Point

6.3 REDUCIBLE UNCERTAIN INTERVAL DESIGN (RUID)

As previously stated the Reducible Uncertain Interval Design (RUID) approach determines the optimal upper and lower bounds for input parameters to a system that possesses reducible uncertainty. The resulting solutions will produce minimal variation from the deterministic Pareto optimal performance of the system provided a maximum level of input uncertainty in a multi-objective sense. This is accomplished by solving two different multi-objective optimization problems in sequence. First the system is optimized in a deterministic sense with respect to the engineering objectives $\boldsymbol{f}$ and the parameters of interest that possess reducible uncertainty $\boldsymbol{p}$ in order to provide a set of anchor points. Then a second bi-objective optimization problem is solved that seeks to maximize the reducible uncertainty in the system's inputs (minimum I_p value as given in Eqn. (6.1)) provided the solution contains a deterministic anchor point, while simultaneously minimizing the variations of the systems outputs. The computational efficiency of the approach is improved through the use of kriging meta-models built using function call data obtained during the deterministic optimization procedure and refined as necessary during the second optimization under uncertainty procedure.

6.3.1 RUID Formulation

As previously stated, the RUID approach involves sequentially solving two optimization problems. The first stage optimization problem optimizes the performance of the engineering system with respect to the uncertain parameters in a deterministic sense, thus providing a set of anchor points for use in the second stage of the approach. This is accomplished by solving Eqn. (2.2). The first stage optimization problem also generates a large amount of system information ($\boldsymbol{f}(\boldsymbol{p}_v)$ and $\boldsymbol{g}(\boldsymbol{p}_v)$ data) which is retained

and used to generate system output function scaling factors and kriging meta-models of the system output functions for use in the second stage optimization problem. The second stage problem then focuses on solving the optimization problem given in Eqn. (6.8).

$$\begin{aligned}
&\min_{m,\boldsymbol{d}_U,\boldsymbol{d}_L} V_f \\
&\min_{m,\boldsymbol{d}_U,\boldsymbol{d}_L} I_p \\
&s.t. \\
&\quad V_g \le 0 \\
&\quad V_f \le \varepsilon \;\; or \; I_p \le \varepsilon \quad (optional) \\
&where \\
&\quad m \in [1,...,M] \\
&\quad 0 \le d_U, d_L
\end{aligned} \tag{6.8}$$

The decision variables in Eqn. (6.8) are the index of the anchor point of interest m, along with the vectors $\boldsymbol{d_U}$ and $\boldsymbol{d_L}$ which describe the upper and lower bounds of the input uncertainty with respect to the m^{th} anchor point. When a set of M anchor points are known, the index m can be used to look up the values for $\boldsymbol{p_A}^{(m)}$ and then Eqn. (6.7) can be used to determine the upper and lower bounds $\boldsymbol{p_U}$ and $\boldsymbol{p_L}$ on all reducible input parameters given $\boldsymbol{d_U}$ and $\boldsymbol{d_L}$. This obviously represents an increase in the dimensionality of the original problem, but that increase allows for an extremely low number of *a priori* assumptions as listed in Section 6.1. Recall that V_f is determined by solving Eqn. (6.5) given $\boldsymbol{p_U}$ and $\boldsymbol{p_L}$. I_p also depends on $\boldsymbol{p_U}$ and $\boldsymbol{p_L}$ and is determined by solving Eqn. (6.1). Lastly V_g is determined by solving Eqn. (6.6), again given $\boldsymbol{p_U}$ and $\boldsymbol{p_L}$. The other two constraints listed in Eqn. (6.8) are optional and simply allow the designer to specify boundaries on V_f and/or I_p if desired. It is important to note that solving Eqns. (6.5) and (6.6) both involve solving single objective optimization problems. As a result, Eqn. (6.8)

is a two-level nested optimization problem. This nested structure can obviously result in high computational effort as is the case for many design optimization approaches that include parameter uncertainty as discussed in Section 6.1. The computational effort of the RUID approach is reduced through the use of kriging meta-models, as discussed in Chapter 2, built using the data retained during the first stage optimization problem. This process will be discussed in detail in the following sections.

Eqn. (6.8) uses a bi-objective optimization framework to place system objective function variations (V_f) in tension with the cost required to control (or reduce) system input uncertainty (I_p). These two competing objectives are formulated such that for a given decrease in output uncertainty, which is desirable, there is an associated increase in cost to the designer, which is unavoidable. Additionally, the use of an anchor point set and the vectors $\boldsymbol{d_U}$ and $\boldsymbol{d_L}$ as the decision variables in Eqn. (6.8) makes it possible for the RUID approach to guarantee that any uncertain solution produced by the approach (as defined by $\boldsymbol{p_U}$ and $\boldsymbol{p_L}$) will be as close to a deterministic Pareto optimal design for the system as possible. This is because any uncertain solution produced by Eqn. (6.8) will necessarily contain a deterministic Pareto optimal solution within the bounds of the uncertain intervals of that solution.

6.3.2 Steps of the RUID Approach

Figure 6.8 contains a flow chart for the overall RUID algorithm.

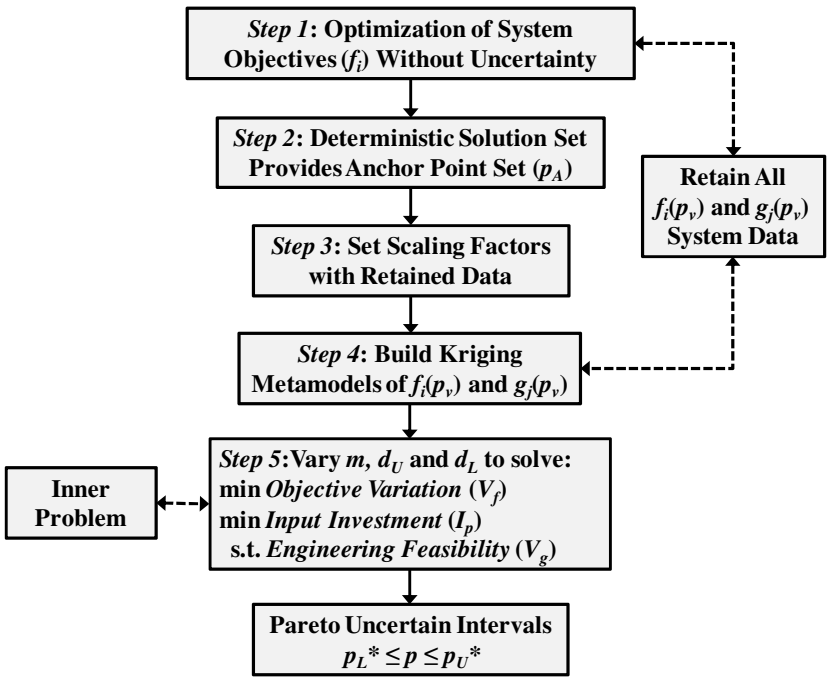

Figure 6.8: RUID Approach

The steps of the approach are as follows:

Step1: Solve Eqn. (2.2) for $\boldsymbol{p}^*$ (optimal $\boldsymbol{p}$) in a deterministic sense (i.e. no uncertainty). During this initial optimization problem retain all function call data.

Step 2: Deterministic Pareto optimal solutions obtained provides the set of anchor points $\boldsymbol{p}_A$.

Step 3: Search set of retained function call data for the maximum and minimum observed values for each of the f_i objectives functions. Set maximum and minimum observed values as $f_{i,good}$ and $f_{i,bad}$, respectively, for each objective function to serve as scaling factors in Eqn. (6.5). Recall that Eqn. (6.6) does not require scaling factors for calculating V_g, so scaling data for constraint functions is not required.

Step 4: Using retained function call data, build kriging meta-models of all system objective and constraint functions.

Step 5: Solve Eqn. (6.8) to determine Pareto optimal set of upper and lower bounds on all input parameters $\boldsymbol{p_U}$ and $\boldsymbol{p_L}$. Solving Eqn. (6.8) requires iteratively varying the selected anchor point index m and the variables $\boldsymbol{d_U}$ and $\boldsymbol{d_U}$ and then solving Eqns. (6.2), (6.3) and (6.6) to obtain V_f, I_p and V_g. This process is called the inner problem and consists of solving numerous single objective optimization problems focused on determining the maximum variations of all system output function given specified levels of input uncertainty. Figure 6.9 contains a flow chart of the inner problem.

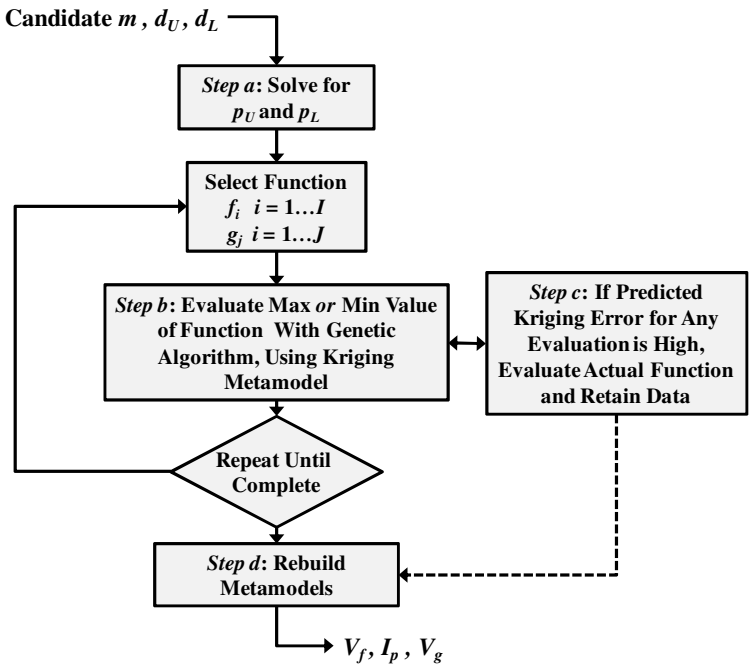

Figure 6.9: RUID Inner Problem

The steps of the inner problem are as follows:

Step a: Given m, $\boldsymbol{d_U}$ and $\boldsymbol{d_L}$ from optimizer, look up $\boldsymbol{p_A}^{(m)}$ from the anchor point set and evaluate Eqn. (6.7) to obtain $\boldsymbol{p_U}$ and $\boldsymbol{p_L}$.

Step b: Solve Eqns. (6.2), (6.3) and (6.6) for each system objective and/or the system constraint functions. For each function the meta-model built during *Step 4* is used in lieu of the actual system analysis models.

Step c: If the kriging error estimate for any evaluation is too high, the actual function is evaluated to ensure accuracy and the newly obtained function call is retained to refine meta-model(s).

Step d: Rebuild meta-model(s), if necessary.

6.3.3 RUID Computational Efficiency

The unique capability of the kriging interpolation technique makes it possible for the RUID approach to be more efficient. To solve a multi-objective optimization problem in a deterministic sense using MOGA requires G generations and H populations, resulting in a computation effort of the order $O(GH)$. Solving a multi-objective optimization problem that includes input uncertainty requires the use of an inner problem that consists of solving several optimization problems for each population point considered in each generation. In the case of the RUID approach the inner problem requires solving an additional set of single objective maximization problems, one for each of the I objective functions and one for all J constraint functions considered together. If each single objective inner optimization problem requires a total of U function calls, the resulting computational effort for RUID would be of the order $O(GH(2I+1)U)$. Since the RUID approach involves solving both a deterministic and uncertain optimization problem, the effort required by RUID in the absence of any surrogate approximation would be of the order $O(G_1H_1+G_2H_2(2I+1)U)$ in the worst case,

where the subscript 1 represents the deterministic first stage problem, while the subscript 2 denotes the second stage optimization problem.

Clearly this level of computational effort could quickly become unacceptable for any system that consists any more than a few objective and/or constraint functions. However, using meta-models built from the function call data generated by the first stage deterministic optimization procedure a significant savings is possible, even considering the additional V function calls required by the inner problem when the kriging predicted error [Martin and Simpson, 2005] is too high (as shown in Figure 6.9). The resulting meta-model assisted algorithm would have a computational effort of the order $O(G_1H_1+V)$, which yields a total savings of $G_2H_2(2I+1)U - V$ function calls. In this work a kriging predicted error of 1% of the function value was considered too high, but this value can be adjusted by a designer as appropriate. The accuracy of this technique will be demonstrated in the next section for each of the example problems.

6.4 EXAMPLES AND RESULTS

In this section the RUID approach is applied to one numerical and two engineering example problems of varying complexity, as presented in the first three subsections. The accuracy of the meta-modeling strategy used will be addressed in Section 6.4.4.

6.4.1 Numerical Example

The first example problem presented is a two-dimensional constrained multi-objective problem called TNK [Deb, 2001]. The formulation of TNK is provided in Eqn. (6.9).

$$
\begin{aligned}
&\min_{p} f_1 = p_1 \\
&\min_{p} f_2 = p_2 \\
&s.t. \\
&\quad g_1 \equiv (p_1 - 0.5)^2 + (p_2 - 0.5)^2 - 0.5 \\
&\quad g_2 \equiv -p_1^2 - p_2^2 + 1 + 0.1\cos\left(16\arctan\frac{p_1}{p_2}\right) \\
&\quad 0 \le p_1, p_2 \le \pi
\end{aligned}
\tag{6.9}
$$

Since TNK is a two dimensional problem where the two objectives are to minimize the two decision variables, the results can be visualized graphically. RUID was applied to the TNK problem using MOGA as the optimizer. A population size of 40 and 100 generations were used in the first stage and the total realized computational effort was 2,218 function calls. In the second stage optimization a population size of 80 and 100 generations was used and required only 4,657 additional function calls (required when the kriging predicted error was too high), vice the maximum of 40,000,000 calls that could have been required if meta-modeling had not been used. This maximum number was calculated by multiplying the number of generations (G = 100) by the population size (H = 80) by the sum of 2 times the number of objectives (I = 2) plus one (for the V_g optimization) times the number of function calls required for each inner problem optimization on average (U = 1000) using the procedure discussed in Section 6.3.3.

The second stage optimization produced the Pareto solutions provided in Figure 6.8, while the anchor points produced by the first stage optimization along with a set of four representative RUID solutions are depicted in the parameter space for the TNK problem in Figure 6.11. The V_f, I_p and determined upper and lower bounds for the four representative solutions are provided in Table 6.1 and are called out in Figure 6.10 with

grey fill for comparison purposes. To obtain these solutions V_f was constrained to be less than 0.1 (or 10% maximum variation in system objective(s)) and the maximum values for $\boldsymbol{d_U}$ and $\boldsymbol{d_L}$ were both limited to 10% of the maximum values for $\boldsymbol{p}$ as shown in Eqn. (6.9).

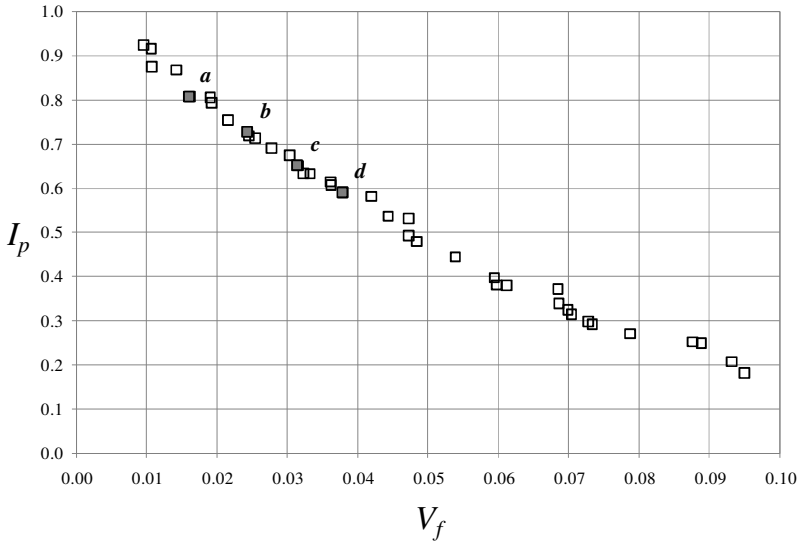

Figure 6.10: RUID Pareto Solutions for TNK Problem

Table 6.1: Select RUID Pareto Points for TNK Problem

	V_f	I_p	$p_{U,1}$	$p_{L,1}$	$p_{U,2}$	$p_{L,2}$
a	0.016	0.807	0.519	0.495	0.867	0.843
b	0.024	0.727	0.832	0.796	0.561	0.529
c	0.031	0.651	0.640	0.594	0.820	0.778
d	0.038	0.590	1.050	0.994	0.151	0.101

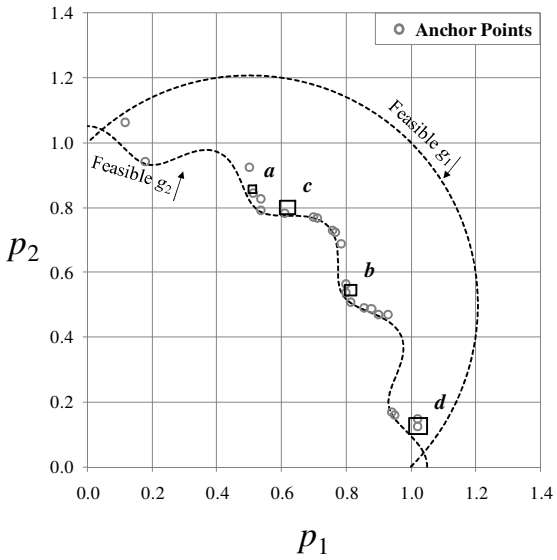

Figure 6.11: TNK Problem Parameter Space

Figures 6.10 and 6.11 clearly show the capability of the RUID approach to provide a designer with a set of design alternatives for the upper and lower bounds on the system's two inputs, leaving the designer with the freedom to choose the level of acceptable output variations based on required input uncertainty control (or reduction). For example, solution *a* has an extremely low V_f value, but achieves that low output variation through tight control over the uncertainty in p_1 and p_2, as demonstrated by the extremely high I_p value and the extremely small region of uncertainty associated with that solution in Figure 6.11. This example problem is a difficult bi-objective optimization problem and shows the capability of the RUID approach to find uncertain solutions that do not violate any constraints while simultaneously achieving as close to deterministic Pareto optimal performance as possible given the specified level of input uncertainty.

6.4.2 Simple Engineering Design Problem

The second example problem presented is a simple two-dimensional engineering optimization problem from Arora [2004], previous used in Chapter 5. This problem was

chosen again in order to again present the obtained uncertain interval results graphically thus clearly demonstrating the capabilities of the RUID approach further. Figure 6.12 depicts the system graphically while Eqn. (6.10) formulates the corresponding optimization problem.

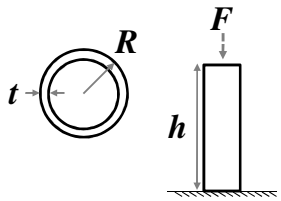

Figure 6.12: Tube Design Problem

$$
\begin{aligned}
&\min_{R,t} f_1 = 2\rho h\pi Rt \\
&\min_{R,t} f_2 = \frac{R}{t} \\
&s.t. \\
&\quad g_1 \equiv \frac{F}{2\pi Rt} - \sigma_{\max} \le 0 \\
&\quad g_2 \equiv F - \frac{\pi^3 ER^3 t}{4h^2} \le 0 \\
&\quad 0.10 \le R \le 0.30 \\
&\quad 0.02 \le t \le 0.10
\end{aligned}
\tag{6.10}
$$

Eqn. (6.10) was first solved in a deterministic sense using a population size of 40 and 100 generations and required 1,591 function calls. As before this procedure produced a set of deterministic Pareto optimal points, which again served as the anchor points for the second stage of the RUID approach. Next, Eqn. (6.8) was solved by MOGA using a population size of 80 and 100 generations. For this problem, as with the previous example, the maximum possible number of required function calls that would have been required if kriging had not used was 40,000,000. In reality the second stage actually only required an additional 4,922 function calls, resulting in a total function call

savings of almost 100%. This savings was calculated by subtracting the total additional function calls required from the maximum total possible, and then dividing that number by the maximum possible function calls. The population size was increased from 40 to 80 in the second stage optimization procedure in order to better converge given the increased dimensionality of the second stage of the RUID problem. Recall that a deterministic optimization procedure determines the values for each of the elements of the vector $\boldsymbol{p}$, while the second stage optimization in the RUID approach solves for both the upper and lower bound on each of the elements of the vector $\boldsymbol{p}$. As before V_f was again limited to a maximum of 0.1 and for this problem the anchor point distance vectors ($\boldsymbol{d}_U$ and $\boldsymbol{d}_L$) were varied between 0 and 10% of the difference between the extreme upper and lower bounds for R and t provided in Eqn. (6.10).

Figure 6.13 shows the Pareto optimal frontier obtained by solving Eqn. (6.8) for the tube design problem shown in Eqn. (6.10). Each solution on the Pareto frontier depicts an optimal option for the upper and lower bounds on the two input parameter for the tube design problem, the radius of the tube R and the thickness of the tube t. The entire Pareto frontier is shown on Figure 6.13, while four representative solutions have been called out with grey fill as with the previous example. The values for the RUID determined upper and lower bounds $\boldsymbol{p}_U$ and $\boldsymbol{p}_L$, along with the corresponding V_f and I_p values for each of the four representative solutions are provided in Table 6.2. Lastly the optimal uncertain regions for each of the four representative solutions have been plotted in the parameter space for the tube design problem in Figure 6.14, along with the deterministic Pareto optimal solutions which served as the anchor points for the RUID

algorithm. Figure 6.14 also includes constraint function contours to define the feasible domain of the problem, along with objective function contours for comparison purposes.

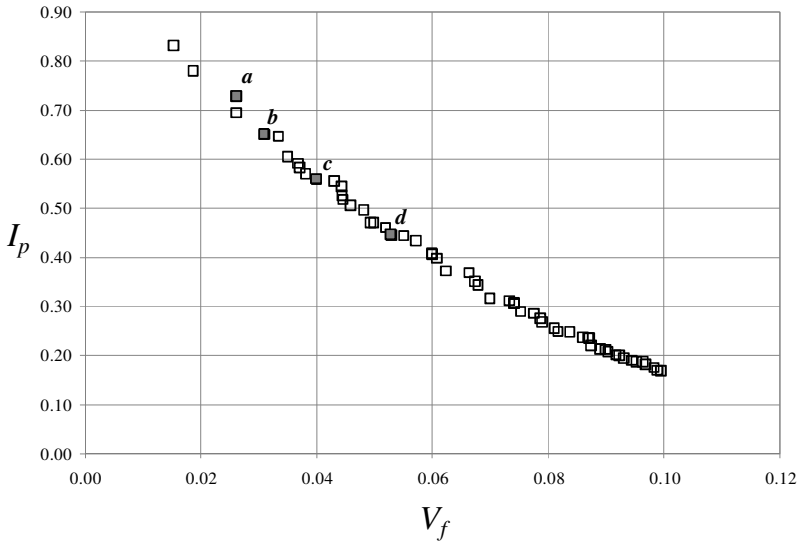

Figure 6.13: RUID Pareto Solutions for Tube Problem

Table 6.2: Select RUID Pareto Points for Tube Problem

	V_f	I_p	$p_{U,t}$	$p_{L,t}$	$p_{U,R}$	$p_{L,R}$
a	0.026	0.728	0.068	0.066	0.139	0.134
b	0.031	0.650	0.064	0.062	0.140	0.136
c	0.040	0.559	0.052	0.049	0.153	0.148
d	0.053	0.446	0.058	0.054	0.149	0.143

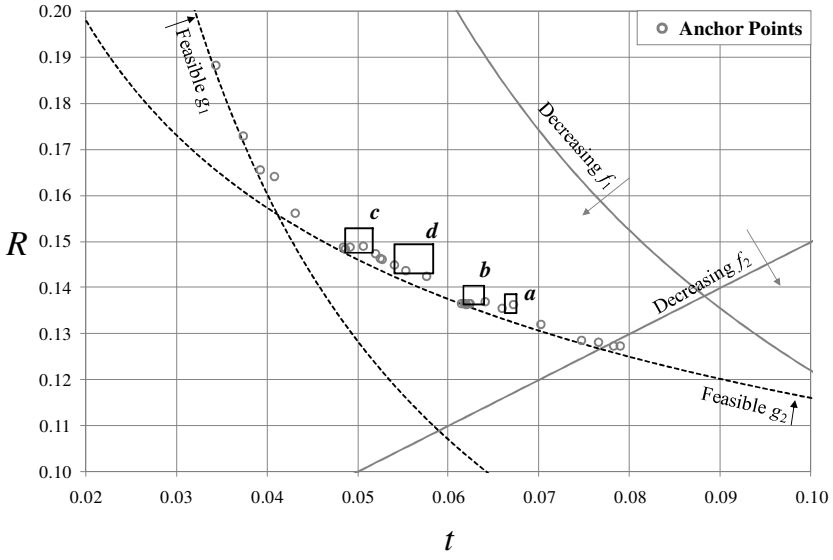

Figure 6.14: Tube Problem Parameter Space

Solution *a* in Table 6.2 and Figure 6.13 and 6.14 has extremely low variation in the system's objective functions, but in order to achieve that low variation tight control over the input parameters is necessary, including only 0.005 m of uncertainty in R and only 0.002 m of uncertainty in t. Solution *d* on the other hand has significantly more variation in the objective (higher V_f) but is also much cheaper to obtain in that it has a correspondingly low I_p value. If the designer of the tube system is happy with the variation level associated with solution *d*, then that design can be achieved with much lower tolerances on R and t. However, if it is extremely important that the variation in the performance of the tube design be as low as possible, then the designer can select the further reduced uncertainty in R and t as specified by solution *a*. The RUID approach provides designers with a suite of options and tradeoff, such as those discussed above, to aide in determining input parameter tolerances and potential uncertainty reductions without making any *a priori* assumptions about the statistical, expected or nominal values of the parameters. It is also important to note that in Figure 6.14 all the solutions depicted contain a deterministic optimal anchor point within the uncertain regions determined by the RUID approach based on the formulation of the approach and thus guarantee as close to deterministic Pareto optimal performance as possible under uncertainty.

6.4.3 Heat Exchanger Design Problem

In order to demonstrate the RUID approach on a more complicated system, a thermal-fluid problem taken from Magrab et al. [2005], was adapted into the bi-objective optimization problem given in Eqn. (6.11) and depicted graphically in Figure 6.15. This problem is concerned with the design of a shell and tube heat exchanger that uses a flow

of cold water to remove heat from a flow of hot water. One fluid flows through a set of small tubes mounted inside a larger shell, while the other fluid flows over the smaller tubes within the shell. The overall system objectives are to maximize the heat transfer rate of the heat exchanger (a measure of how much energy is moved from the cold fluid to the hot fluid) while simultaneously minimizing the length of the heat exchanger. The system consists of 6 input parameters (including 1 discrete parameter), 2 objectives and multiple thermal-fluid, performance and geometric constraints, as shown in Eqn. (6.11). For details on this system see Magrab et al. [2005].

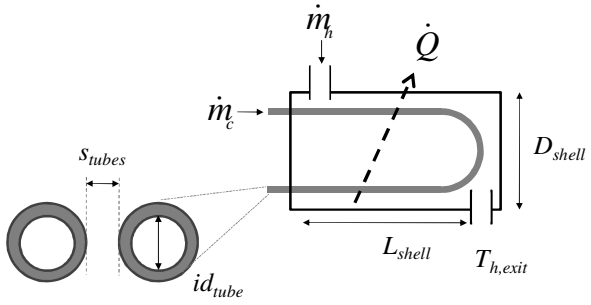

Figure 6.15: Shell and Tube Heat Exchanger Problem

$$
\begin{aligned}
&\min_{\boldsymbol{p}} \; f_1 = -\dot{Q} \\
&\min_{\boldsymbol{p}} \; f_2 = L_{shell} \\
&s.t. \\
&\quad g_1 \equiv \Delta P_h \le 5000Pa \\
&\quad g_2 \equiv \Delta P_c \le 5000Pa \\
&\quad g_3 \equiv \dot{Q} \ge 800kW \\
&\quad g_4 \equiv T_{h,exit} \le 60^{\circ}C \\
&\quad Geometric\ Limits \\
&where \\
&\quad \boldsymbol{p} \equiv [\dot{m}_h, \dot{m}_c, D_{shell}, id_{tube}, n_{tubes}, s_{tubes}] \\
&\quad n_{tube} \in \text{int}
\end{aligned}
\tag{6.11}
$$

The heat exchanger problem was solved using the procedure described in Section 6.3 just as with the previous two example problems. The Pareto set of uncertain solutions produced are shown in Figure 6.16 and as with before a set of 4 representative solutions have been called out with dark grey fill and the details for these 4 solutions are shown in Table 6.3. As with the previous examples both the first stage and second stage problems were solved with MOGA using 100 generations in each stage. When considering both the function calls required by the first stage optimization and the additional function calls required by the inner problem of the second stage problem for the cases when the meta-model predicted error was too high, an overall computational savings of about 100% was again observed when compared to the worst case as described in Section 6.3.3, despite the increased dimensionality and increased number of constraint functions in this problem.

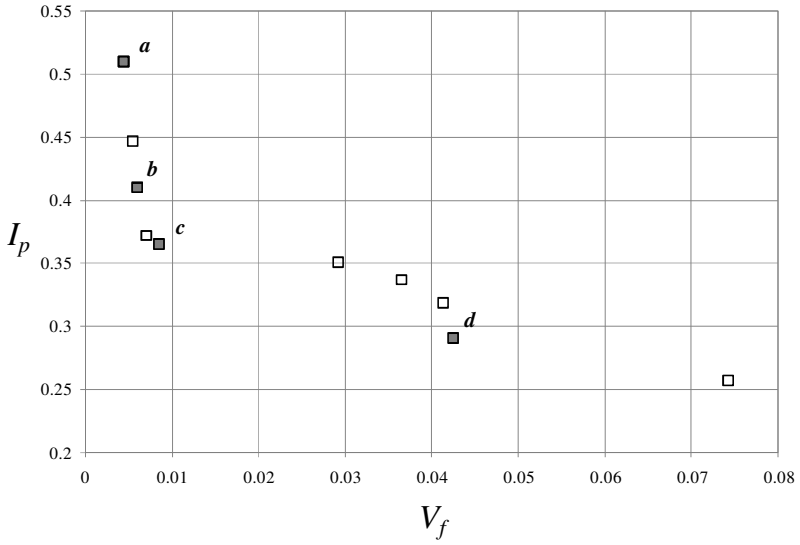

Figure 6.16: RUID Pareto Solutions for Heat Exchanger

Table 6.3: Select RUID Pareto Points for Heat Exchanger Problem

	V_f	I_p		$\dot{m}_h$	$\dot{m}_c$	D_s	id_{tube}	s_{tubes}	n_{tubes}
a	0.004	0.51	$\boldsymbol{p_U}$	19.84	11.68	0.32	0.11	0.03	149
			$\boldsymbol{p_L}$	19.73	11.63	0.28	0.10	0.03	145
b	0.006	0.41	$\boldsymbol{p_U}$	19.54	11.10	0.33	0.12	0.03	146
			$\boldsymbol{p_L}$	18.89	11.04	0.29	0.10	0.03	140
c	0.008	0.36	$\boldsymbol{p_U}$	19.90	11.68	0.32	0.13	0.03	148
			$\boldsymbol{p_L}$	19.36	11.60	0.26	0.10	0.03	142
d	0.043	0.29	$\boldsymbol{p_U}$	19.73	10.96	0.33	0.13	0.03	150
			$\boldsymbol{p_L}$	18.81	10.53	0.30	0.10	0.03	142

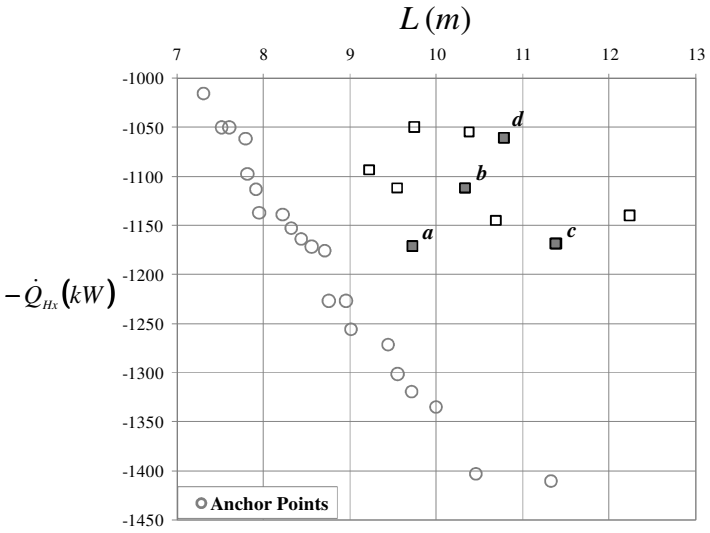

Figure 6.17: Heat Exchanger System Performance

Based on Table 6.3 it can be concluded that it is most important to tightly control the cold fluid flow rate through the heat exchanger given that the optimal uncertain intervals for those two parameters are all less than 4%, determined by dividing the uncertain interval for each parameter by the maximum parameter value. It is also clear that the spacing between the tubes is more important in ensuring low variation in the system's objectives (maximum heat transfer rate and minimum heat exchanger length) than is the diameter of the shell or even number of tubes in the shell and tube heat exchanger. These results not exactly intuitive and could be used by a designer going

forward in the process of developing the heat exchanger by focusing more attention and resources on pumps (to control flow rate) and interior geometry (to control tube space).

As with the previous example, these solutions are as close to the deterministic Pareto optimal performance as possible given the level of uncertainty associated with each solution. Since the design space for this problem cannot be visualized to demonstrate this fact the worst case objective function values for of the RUID optimal solutions included in Table 6.3 have been plotted over the deterministic optimal solutions in the objective space for the problem in Figure 6.17. In the figure the four representative solutions provided in Table 6.3 are called out with grey fill for emphasis. The RUID solutions are shown with square markers, while the anchor points are shown with circles. As expected, the RUID solutions are all reasonably close to the deterministic Pareto frontier, suggesting that even in the worst case the uncertain solutions found using the RUID approach will provide objective performance that is very close to the deterministic optimal performance for the system.

6.4.4 Meta-Model Accuracy

In order to demonstrate the accuracy of the meta-model assisted inner problem used by the RUID approach, each of the obtained Pareto optimal solutions for the first two example problems were verified by recalculating the V_f and V_g values for each optimal $\boldsymbol{p}_{\mathbf{U}}$ and $\boldsymbol{p}_{\mathbf{L}}$ solution obtained using actual function calls vice the kriging meta-models. The results obtained were then compared and a percent error value was calculated assuming the function call obtained solution was the true solution. The average percent error values (μ) along with the standard deviation (σ) of those percent error values are provided in Table 6.4, which clearly show that the meta-model assisted

RUID approach is capable of accurately representing the objective and constraint functions of the example problems presented in this chapter.

Table 6.4: Meta-Model Accuracy Statistics

	V_f Percent Error		V_g Percent Error	
	μ	σ	μ	σ
TNK	-3.2e-16	1.9e-15	0	0
Tube Design	7.6e-17	7.2e-16	0	0

6.5 SUMMARY OF RESEARCH THRUST 4

A new approach for optimal design under uncertainty, called Reducible Uncertain Interval Design (RUID), has been presented. This approach is focused on determining the appropriate level of uncertainty for reducible sources of system uncertainty. RUID does not require statistical quantification of uncertainty, which may be difficult to obtain or unavailable, and relaxes many of the assumptions required by other current approaches. RUID places minimizing objective function variation in tension with the cost of producing that minimal variation in a bi-objective optimization framework. Furthermore the RUID approach forces the worst case objective performance of an uncertain design, in a multi-objective sense, to be as close as possible to the deterministic Pareto optimal performance of the system. The efficiency of this new approach is significantly improved through the use of kriging meta-models within the inner problem of the RUID algorithm. The kriging meta-models used are built using data obtained early in the algorithm and continually refined throughout the algorithm in order to ensure accuracy. This process makes it possible to conduct optimization under uncertainty for only a slightly higher computational effort than is required to complete a deterministic optimization of the system. The capabilities and efficiency of the of the RUID approach

were demonstrated through three example problems of varying difficulty. These example problems showed how the RUID approach can be used to determine optimal uncertain intervals for reducible input parameters that will ensure as close to deterministic Pareto optimal performance as possible. The results produced by the RUID approach can then be used by designers to specify tolerances, materials and/or manufacturing processes. Additionally the RUID results can also be used to gain a better insight into a system's uncertain parameter and then focus attention and resources on those uncertainties that are the most important to control in order to ensure minimal variations in the system's overall performance.

The RUID approach makes it possible for designer to consider reducible, or controllable, uncertainty in an optimization framework in an efficient manner without the need for potentially erroneous or degrading *a priori* assumptions about system uncertainty levels. This capability makes it possible for uncertainty to be considered earlier in the design process and with less available parameter information. The results produced by this new approach are compelling, especially given the fact that the approach requires virtually no parameter uncertainty information. However, this new approach is not without its own limitations and weaknesses. First and foremost this approach requires an overall increase in the dimensionality of the problem as it determines upper and lower bounds on all parameter values. The approach also requires that two optimization procedures be performed in sequence with the second stage optimization containing a set of nested inner optimization problems. Both the increase in dimensionality and the nested structure have the potential to cause extreme computational issues for many problems, including the second example presented in this chapter.

Kriging meta-models were used in the approach in an effort to reduce this computational burden, but meta-modeling in general is difficult to employ effectively for some systems and possesses its own drawbacks including decreased accuracy. Obviously these issues must be considered before employing the RUID approach.

However, in spite of these drawbacks the new RUID approach is clearly a useful new method for optimization under reducible uncertainty that does not require a designer to supply numerous pieces of potentially unavailable information about the nature and quantification of a system's uncertain parameters. The RUID approach is capable of producing optimal solutions for a system that a designer can then use to specify materials, manufacturing process and/or tolerances. The solutions produced by this approach, in the form of upper and lower bounds on all uncertain system parameters, will assure a designer of minimal variations in a system's objectives for a minimal cost and provide as close to deterministic optimal performance as possible.

CHAPTER 7: CONCLUSIONS

This dissertation has presented four distinct strategies for understanding and optimally mitigating the degrading effects of reducible input uncertainty on both single and multi-disciplinary engineering systems. Chapter 1 discussed the motivation for this research, along with the specific focus and assumption of this work. Chapter 2 then established some necessary background information and terminology that was used through the dissertation. Chapters 3 through 6 outlined the details of the four interrelated research thrusts of this dissertation. Each research thrust built on or extended the work presented in the preceding thrust in an attempt to overcome inherent limitations or to add increased functionality. This final chapter is organized as follows: Section 7.1 summarizes the key conclusions of each research thrust, Section 7.2 details the main contributions of this work and Section 7.4 provides some directions for future research.

7.1 DISSERTATION SUMMARY

In this section each of the four research thrusts will be summarized and the key conclusions of each research thrust will be reviewed.

7.1.1 Research Thrust 1 Conclusions

In Chapter 3 a new global sensitivity analysis approach for fully coupled multi-disciplinary, multi-output engineering systems under uncertainty, called Multi-dIsciplinary Multi-Output Sensitivity Analysis (MIMOS) was presented. This approach extended the work of Li et al. [2009a] to multi-disciplinary systems and was built on the multi-disciplinary design optimization framework proposed by Aute and Azarm [2006].

This new approach assumes that input parameter uncertainty is quantified in the form of intervals about a set of predetermined nominal parameter values for a candidate design and that the interval uncertainty is reducible. The approach then solves for the optimal level of uncertainty reduction at both the system and sub-system level in a multi-objective sense. The competing objectives in this approach are the level of reduced variations in the system and sub-system outputs, here called *R*, placed in tension with the cost of achieving those reduced variations. This "cost" is a function of the required reduction in input uncertainty and is called *Investment* in this work.

The capabilities of the MIMOSA approach were demonstrated through two example problems, including a numerical example and an engineering example. MIMOSA was shown to be able to identify both critical parameters (the uncertain input parameters that have the greatest effect on system variations) and critical sub-systems (the sub-system(s) that have the greatest effect on the overall performance of the system as a whole under uncertainty). Both examples specifically present how the MIMOSA approach can identify the sub-system in a decomposed multiple sub-system problem that is the most sensitive to the uncertainty and has the greatest effect on the system level performance under uncertainty. The engineering example also demonstrates how MIMOSA is capable of isolating parameters whose uncertainty greatly influence system and sub-system outputs in contrast to those who do not.

The MIMOSA approach is very effective but not without its downsides. The approach does not consider engineering feasibility and thus in not effective in analyzing designs where input uncertainty levels may lead to potential engineering failure. Additionally MIMOSA requires that a designer possess a preexisting or preferred

candidate design in the form of nominal parameter values and known parameter uncertainties, which may not always be available. Furthermore, the MIMOSA approach nests a sensitivity analysis optimization problem within a multi-level MDO framework, resulting in a potentially high computational cost for many applications.

7.1.2 Research Thrust 2 Conclusions

The work presented in Chapter 4 simply extended the MIMOSA approach to also consider engineering feasibility, thus effectively overcoming one of MIMOSA's major shortcomings. This new sensitivity analysis approach for multidisciplinary systems under reducible interval input uncertainty is called Multi-dIciplinary multi-objective COmbined Sensitivity Analysis (MICOSA). In contrast to MIMOSA this approach differentiates between the objective function variations and constraint function variations for a candidate design. MICOSA then uses sensitivity analysis techniques to determine the optimal combination of uncertainty reductions at both the system and sub-system levels that will optimally reduce the variation in all system and sub-system outputs while simultaneously ensuring engineering feasibility.

This new approach was demonstrated through both a single disciplinary example (in the form of a UUV propulsor model) and a multi-disciplinary example (the entire UUV system in a decomposed fashion). The results obtained were shown to be very similar to those produced by the MIMOSA approach, with the key distinction of also being able to guarantee feasibility under any retained uncertainty. The single disciplinary propulsor model example specifically demonstrated the capability of the approach to ensure feasibility through a side by side comparison. The multi-disciplinary UUV example demonstrated the ability of the MICOSA approach to detect critical sub-systems.

Furthermore, the UUV example demonstrated the ability of the R_c metric to apply limited uncertainty reduction resources to critical constraint variations prior to using uncertainty reduction to reduce objective variations.

This new approach is a significant improvement over MIMOSA, but was very limited in its scope. MICOSA requires that uncertainty reduction alone will be sufficient to ensure engineering feasibility under retained uncertainty in all cases, which may not necessarily always be possible. For many designs no amount of uncertainty reduction may be sufficient to ensure feasibility. Additionally MICOSA also shares MIMOSA potential for high computational cost due to the nested structure of the approach.

7.1.3 Research Thrust 3 Conclusions

To overcome the key limitation of the MICOSA approach, its assumption that uncertainty reduction alone is sufficient to ensure feasibility under uncertainty, a new sensitivity analysis approach for single disciplinary systems was developed. This approach, called Design Improvement by Sensitivity Analysis (DISA) was again based on the work of Li et al., but it not limited to uncertainty reduction alone. Like MIMOSA and MICOSA it places reduced system output variations in tension with the cost to achieve those reduced variation in a multi-objective sense, but allows not just for uncertainty reduction but also for small changes to the nominal design of the system. Those small changes, called design adjustments, are the key to being able to ensure feasibility under uncertainty. The DISA approach is performed in two distinct stages. During the first stage the system is analyzed with respect to uncertainty reduction opportunities. Then in the second stage the nominal parameter values of the candidate design are adjusted as necessary (given some level of uncertainty reduction as determined

in the first stage) in an effort to produce design solutions that possess an optimal level of uncertainty reduction but are also guaranteed to be feasible. The two stage structure of the DISA approach also makes it possible to use system analysis information generated during the first stage to build surrogate models of the system for use in the second stage procedure, thus greatly increasing the computational efficiency of the approach.

The capabilities of the DISA approach were demonstrated through two example problems of varying complexity. The DISA approach was applied to a simple two-dimensional example problem and a more complex engineering example. The simple example clearly demonstrated the ability of the DISA approach to use small design adjustments to change the nominal parameter values of a candidate design in order to move the candidate design away from active constraints and ensure the feasibility of the design under uncertainty. With the complex example a specific study was performed on a single candidate solution produced by the DISA approach to demonstrate the ability of the new method for showing a designer which specifics elements of an engineering system are the most critical to both the feasibility and performance of the design. More importantly, it was also shown through both examples that the DISA approach is also capable of suggesting to a designer how best to use available investment through uncertainty reduction and/or small design adjustments.

The approach proved to be very capable at both ensuring feasibility and reducing system variations, in some cases to an even greater extent than would be possible through uncertainty reduction alone. However, the DISA approach like the MIMOSA and MICOSA approaches required a large amount of known or predetermined system information in the form of a candidate design and known parameter uncertainty intervals

about the nominal parameter values of the candidate design. These *a priori* requirements are limiting the cases where a designer is faced with sources of reducible system uncertainty, but does not yet have a system design in place to analyze. Furthermore, the DISA approach relies on surrogate approximation techniques (specifically kriging) to ensure a reasonable computational effort. Surrogate approximation techniques are not without their own specific sets of drawbacks and limitations [Shan and Wang, 2008]. Additionally, the DISA approach is currently only applicable to single disciplinary systems.

7.1.4 Research Thrust 4 Conclusions

As a result of the limiting requirements of the previous three research thrusts, a new more general approach for the design of multi-objective engineering systems under reducible interval uncertainty was developed. This approach, called Reducible Uncertain Interval Design (RUID) eliminates the need for candidate designs, known uncertain intervals and nominal parameter values. RUID simple searches the parameter space of a system in an effort to find the optimal upper and lower bounds for all system input parameters that are known to possess reducible uncertainty. The solutions produced are optimal in the sense that RUID places minimizing objective function variation in tension with the cost of producing that minimal variation in a bi-objective optimization framework. Furthermore the RUID approach forces the worst case objective performance of an uncertain design, in a multi-objective sense, to be as close as possible to the deterministic Pareto optimal performance of the system. The computational efficiency of the approach is again improved through the use of surrogate models which

are again developed using information obtained early in the approach and then refined over time as the approach converges to the optimal uncertain interval solutions.

The capabilities of the RUID approach were demonstrated through three example problems of varying complexity and the results produced were quite compelling. The first two example problems presented where both two-dimensional problems of varying complexity and both graphically demonstrated the capability of the approach to produce optimal upper and lower bounds for all reducible input parameter that guaranteed feasibility while simultaneously being as close to the deterministic Pareto frontier of the problem as possible. The complex engineering example further demonstrated the ability of the approach to draw a designer's attention to an engineering system's most critical uncertain input parameters.

The RUID approach is a sensitivity analysis inspired approach for the design of multi-objective systems under reducible systems that does not require statistical information or any other limiting *a priori* information about the system or its inputs. This makes the RUID approach useful to designers focused on answering uncertainty reduction questions much earlier in the design process and with much less required information and/or system knowledge. The main drawback of the RUID approach is the associated computational effort. Attempts were made to address this issue through the use of kriging meta-models, but as pointed out in the previous subsection meta-modeling is not without its own significant drawbacks. As with all the approaches presented in this dissertation, virtually all approach for design under uncertainty must determine the effects of uncertainty on any design solution considered within the approach. This assessment of the effects of uncertainty often involves an optimization procedure, which

necessarily then requires that the approach consists of solving nested optimization problems. This nested structure is what produces the high computational expense of the RUID approach, and many other approaches optimization under uncertainty approach for that matter. Furthermore, RUID is only presently applicable to single disciplinary systems.

7.2 MAIN CONTRIBUTIONS

Several new and novel sensitivity analysis based approaches for optimally mitigating the effects of reducible interval uncertainty on single- and multi-disciplinary systems have been presented in this dissertation. The specific key contributions of this work to the design research community are outlined in the following paragraphs.

The MIMOSA approach presented in Chapter 3 provided a new framework for analyzing the effect of reducible interval uncertainty on fully coupled multi-disciplinary, multi-output systems. As previously stated this approach is capable of determining the relative importance of different uncertain inputs and of different sub-system with regards to their impact on the overall performance of the system as a whole. Furthermore the MIMOSA approach provides designer with the combination of uncertainty reduction required to optimally mitigate the effect of uncertainty on the system and sub-system designs. The MISMOSA approach was presented in part in Li et al. [2009b].

The DISA approach presented in Chapter 5 provides a sensitivity analysis based approach for optimally mitigating the effects of reducible input uncertainty on a preexisting candidate design that is capable of both ensuring engineering feasibility and also providing minimal objective function variations at a minimal require cost through

the use of uncertainty reduction mechanisms and small design adjustments. The DISA approach is capable of providing designers with solutions that suggest optimal combinations of uncertainty reduction and small nominal parameter value adjustments that will improve the overall performance of a candidate design with respect to both objective function variations and engineering feasibility under uncertainty. The DISA approach was presented in part in Hamel et al. [2010].

The RUID approach presented in Chapter 6 provides new multi-objective design under uncertainty approach, inspired by the previously developed SA approaches, that can produce optimal solutions in the form of upper and lower bounds (which specify uncertain intervals) for all input parameters to a system that possess reducible uncertainty. The solutions produced by this approach provide minimal variation in system objectives for a maximum allowed level of input uncertainty in a multi-objective sense and furthermore guarantee as close to deterministic Pareto optimal performance as possible with respect to the uncertain parameters. This approach requires a very limited amount of *a priori* information and/or assumptions and thus makes it much easier for designers to consider the degrading effects of reducible uncertainty much earlier in the design process. The RUID approach was presented in part in Hamel and Azarm [2010].

7.3 FUTURE RESEARCH DIRECTIONS

The final section of the dissertation outlines some directions for potential future research. These ideas either build on or extend the work presented in this dissertation or seek to overcome some of the shortcoming of the work presented.

7.3.1 Multi-Disciplinary Extension of the DISA and RUID Approaches

A clear next step, as alluded to earlier in this chapter, would be to develop multi-disciplinary extensions of the approaches presented in Chapter 5 and 6. These two new approaches are very capable and have many compelling attributes, but are thus far only applicable to single disciplinary systems. This fact limits their applicability to real-world engineering design challenges, which as discussed in Chapter 1 will often be multi-disciplinary in nature. The framework developed for the MIMOSA approach detailed in Chapter 3 could provide a good starting point for this work and multi-disciplinary extension of both the DISA and RUID approaches would be particularly useful.

7.3.2 Approaches for Mixed Reducible and Irreducible Uncertainties

All the work presented in this dissertation has focused on reducible uncertainty, which is clearly an important aspect of engineering design. However, irreducible uncertainty is also obviously a critical issue as evidenced by the numerous robust approaches that appear throughout the literature (see [Beyer and Senhoff, 2007]). As discussed earlier in this thesis a few recent approaches have attempted to combine irreducible sources of uncertainty and uncertainty reduction mechanisms in a few different ways (e.g. [Qu et al., 2003; Li et al., 2009c, Wang et al., 2009]). This area of research deserves more attention and would be useful to real-world design efforts. The distinction between reducible and irreducible uncertainties is somewhat subjective and thus distinguishing between these two ways of looking at uncertainty is limiting. It is extremely likely that a designer may not be able to classify various sources of uncertainty as either purely reducible or strictly irreducible, especially in the early stages of a design process. Careful work should be undertaken to develop new approaches that can reliably

consider both reducible and irreducible sources of uncertainty and that allow designer with freedom to change the way uncertainty is classified should better information become available.

7.3.3 More Efficient Nested Optimization Algorithms

Chapter 1 clearly motivates the need for more efficient strategies for solving nested optimization problems. Most current SA and design under uncertainty approaches rely heavily on multi-disciplinary optimization and decomposition techniques. As previously discussed, there are numerous MDO approaches currently reported in the literature, but the work that has been done up to this point in the area has proved to be relatively inefficient from a computational effort standpoint. Current decomposition techniques, such as Collaborative Optimization and Analytical Target Cascading, involve nesting sub-system design algorithms inside a coordinating or system-level design algorithm at a high computational expense [Balling and Sobieszczanski-Sobieski, 1996; Aute and Azarm, 2006; Kokkolaras et al., 2006; Yi et al., 2007]. As seen throughout this dissertation, nested optimization techniques are frequently used when solving sensitivity analysis problems and the work presented in this dissertation was repeatedly impacted by the high computational effort of those techniques. Clearly more work is needed in this area before SA approaches and become more efficient and useful to practicing design engineers. Thus far the only real answer to these efficiency issues have been to use meta-modeling techniques to approximate expensive analysis models (such as CFD codes) with less expensive analytical functions [Martin and Simpson, 2005; Wang and Shan, 2007; Shan and Wang, 2008]. Meta-models can be used to reduce the underlying computational expense associated with the analysis functions of a design system quite

effectively, as demonstrated in Chapters 5 and 6, but their use does nothing to lessen the efficiency issues associated with the nested algorithms currently used to solve multidisciplinary problems. Clearly other means for improving the efficiency of multi-disciplinary algorithms are needed, particularly for problems that already use meta-modeling but are still too computationally expensive to solve efficiently. Perhaps new applications and/or extensions of other classical decomposition techniques, such as Bender's Decomposition [e.g. Conejo et al., 2006], could provide the answer to this very real and challenging problem that must be addressed in the near future.

REFERENCES

[1] Acar, E., Haftka, R. T., and Johnson, T. F., 2007, "Tradeoff of Uncertainty Reduction Mechanisms for Reducing Weight of Composite Laminates," *Journal of Mechanical Design*, 129(3), pp. 266-274.

[2] Allaire, D., and Willcox, K., 2008, "Surrogate Modeling for Uncertainty Assessment with Application to Aviation Environmental System Models," *Proceedings of the 12th AIAA/ISSMO Conference*, Victoria, BC, Canada.

[3] Apley, D. W., Liu, J., and Chen, W., 2006, "Understanding the Effects of Model Uncertainty in Robust Design with Computer Experiments," *Journal of Mechanical Design*, 128(4), pp. 945-958.

[4] Arora, J. S., 2004, *Introduction to Optimum Design, 2nd Edition*, Elsevier Academic Press, San Diego, CA.

[5] Aute, V., and Azarm, S., 2006, "A Genetic Algorithms Based Approach for Multi-Disciplinary Multi-objective Collaborative Optimization," AIAA-2006-6953, *Proceedings of the 11th AIAA/ISSMO Conference*, Portsmouth, Virginia.

[6] Balling, R.J., and J. Sobieszczanski-Sobieski, 1996, "Optimization of Coupled Systems: A Critical Overview of Approaches," *AIAA Journal*, 34(1), pp. 6-17.

[7] Barron, H., and C. P. Schmidt, 1988, "Sensitivity Analysis of Additive Multiattribute Value Models," *Operations Research*, 36(1), pp. 122-127.

[8] Benanzer, T.W., R.V. Grandhi and W.P. Krol, 2009, "Reliability-Based Optimization of Design Variance to Identify Critical Tolerances," *Advances in Engineering Software*, 40, pp. 305-311.

[9] Beyer, H., and Sendhoff, B., 2007, "Robust Optimization - A Comprehensive Survey," *Computer Methods in Applied Mechanics and Engineering*, 196(33-34), pp. 3190-3218.

[10] Castillo, E., Minguez, R., and Castillo, C., 2008, "Sensitivity Analysis in Optimization and Reliability Problems," *Reliability Engineering & System Safety*, 93(12), pp. 1788-1800.

[11] Chen, W., Jin, R., and Sudjianto, A., 2005, "Analytical Variance-Based Global Sensitivity Analysis in Simulation-Based Design under Uncertainty," *Journal of Mechanical Design*, 127(5), pp. 875-886.

[12] Chiralaksanakul, A. and Mahadevan, S., 2007, "Decoupled approach to multi-disciplinary design optimization under uncertainty," *Optimization and Engineering*, 8(1), pp. 21-42.

[13] Conejo, A. J., E. Castillo, R. Minguez and R. Garcia-Bertrand, 2006, *Decomposition Techniques in Mathematical Programming*, Springer-Verlag, Berlin.

[14] Crespo, L. G., Giesy, D. P., and Kenny, S. P., 2008, "Robustness Analysis and Robust Design of Uncertain Systems," *AIAA Journal*, 46(2), pp. 388-396.

[15] Deb, K., 2001, *Multi-Objective Optimization Using Evolutionary Algorithms*, John Wiley and Sons, New York, NY.

[16] Du, L., and Choi, K. K., 2006, "An Inverse Analysis Method for Design Optimization with both Statistical and Fuzzy Uncertainties," *Proceedings of ASME IDETC/CIE Conference*, Philadelphia, Pennsylvania, DETC2006-99731.

[17] Du, X. and Chen, W., 2002, "Efficient Uncertainty Analysis Methods for Multi-Disciplinary Robust Design," *AIAA Journal*, 40(3), pp. 545-552.

[18] Du, X. and Chen, W., 2005, "Collaborative Reliability Analysis under the Framework of Multi-Disciplinary Systems Design," *Optimization and Engineering*, 6(1), pp 63-84.

[19] Du, X., 2007, "Interval Reliability Analysis," *Proceedings of ASME IDETC/CIE Conference*, Las Vegas, Nevada, DETC2007-34582.

[20] Du, X., 2008, "Unified Uncertainty Analysis by the First Order Reliability Method," *Journal of Mechanical Design*, 130(9), pp. 091401/1 - 091401/10.

[21] Fiacco, A. V., 1983, *Introduction to Sensitivity and Stability Analysis in Nonlinear Programming*, Academic Press, New York, NY.

[22] Frey, H. C., and S. R. Patil, 2002, "Identification and Review of Sensitivity Analysis Methods," *Risk Analysis*, 22(3), pp. 553-578.

[23] Greenland, S., 2001, "Sensitivity Analysis, Monte Carlo Risk Analysis, and Bayesian Uncertainty Assessment," *Risk Analysis*, 21(4), pp. 579-584.

[24] Gu, X., Renaud, J. E., and Batill, S. M., 1998, "Investigation of Multi-Disciplinary Design Subject to Uncertainties," AIAA Paper 1998-4747, *Proceedings of the 7th AIAA/ISSMO Conference*, St. Louis, MO.

[25] Gu, X., Renaud, J. E., and Penninger, C. L., 2006, "Implicit Uncertainty Propagation for Robust Collaborative Optimization," *Journal of Mechanical Design*, 128(4), pp. 1001-1013.

[26] Gunawan, S., and Azarm, S., 2005, "A Feasibility Robust Optimization Method using Sensitivity Region Concept," *Journal of Mechanical Design*, 127(5), pp. 858-865.

[27] Gunawan, S. and Papalambros, P. Y., 2006, "A Bayesian Approach to Reliability-Based Optimization with Incomplete Information," *Journal of Mechanical Design*, 128(4), pp. 909-918.

[28] Gunawan, S., and Papalambros, P. Y., 2007, "Reliability Optimization with Mixed Continuous-Discrete Random Variables and Parameters," *Journal of Mechanical Design*, 129(2), pp. 158-165.

[29] Guo, J., and Du, X., 2007, "Sensitivity Analysis with Mixture of Epistemic and Aleatory Uncertainties," *AIAA Journal*, 45(9), pp. 2337-2349.

[30] Hamby, D. M., 1994, "Review of Techniques for Parameter Sensitivity Analysis of Environmental Models," *Environmental Monitoring and Assessment*, 32(2), 1994, pp. 135-154.

[31] Hamel, J., Li, M., and Azarm, S., 2009, "Multi-Disciplinary Sensitivity Analysis and Optimization of Undersea Systems under Uncertainty," ONR Multi-Disciplinary Systems Design and Optimization Workshop, June 16-17, 2009.

[32] Hamel, J. and Azarm, S., 2010, "Reducible Uncertain Interval Design (RUID) by Kriging Meta-Model Assisted Multi-Objective Optimization," *Proceedings of ASME IDETC/CIE Conference*, Montreal, Canada. (To Appear)

[33] Hamel, J., Li, M., and Azarm, S., 2010, "Design Improvement By Sensitivity Analysis (DISA) Under Interval Uncertainty Using Multi-Objective Optimization," *Journal of Mechanical Design* (To Appear).

[34] Helton, J. C., and Davis, F. J., 2003, "Latin Hypercube Sampling and the Propagation of Uncertainty in Analyses of Complex Systems," *Reliability Engineering & Systems Safety*, 81(1), pp. 23-69.

[35] Iman R. L. and Helton, J. C., 1988, "An Investigation of Uncertainty and Sensitivity Analysis Techniques for Computer Models," *Risk Analysis*, 8(1), pp. 71-90.

[36] Ju, B. H., and Lee, B. C., 2008, "Reliability-Based Design Optimization using a Moment Method and a Kriging Metamodel," *Engineering Optimization*, 40(5), pp. 421-438.

[37] Jung, D. H., and Lee, B.C., 2002, "Development of a Simple and Efficient Method for Robust Optimization," *International Journal for Numerical Methods in Engineering*, 23, pp. 2201-2215.

[38] Kale, A.A, and Haftka, R.T., 2008, "Tradeoff of Weight and Inspection Cost in Reliability-Based Structural Optimization," *Journal of Aircraft*, 45 (1): 77-85..

[39] Kern, D., Du, X., and Sudjianto, A., 2003, "Forecasting Manufacturing Quality During Design Using Process Capability Data," *Proceedings of the IMECE/ASME International Mechanical Engineering Congress and RD&D Expo*, Washington, DC.

[40] Kokkolaras, M., Mourelatos, Z. P., and Papalambros, P. Y., 2006, "Design Optimization of Hierarchically Decomposed Multilevel Systems under Uncertainty," *Journal of Mechanical Design*, 128(2), pp. 503-508.

[41] Lee, S. H., and Chen, W., 2009, "A Comparative Study of Uncertainty Propagation Methods for Black-Box-Type Problems," *Structural and Multidisciplinary Optimization*, 37(3), pp. 239-253.

[42] Lee, T. W., 2006, "A Study for Robustness of Objective Function and Constraints in Robust Design Optimization," *Journal of Mechanical Science and Technology*, 20(10), pp. 1662-1669.

[43] Li, M., and Azarm, S., 2008, "Multiobjective Collaborative Robust Optimization with Interval Uncertainty and Interdisciplinary Uncertainty Propagation," *Journal of Mechanical Design*, 130(8), pp. 081402/1 - 081402/11.

[44] Li, M., Williams, N., and Azarm, S., 2009a, "Interval Uncertainty Reduction and Sensitivity Analysis with Multi-Objective Design Optimization," *Journal of Mechanical Design*, 131(3), pp. 031007/1 - 031007/11.

[45] Li, M., Hamel, J., and Azarm, S., 2009b, "Optimal Uncertainty Reduction for Multi-Disciplinary Multi-Output Systems Using Sensitivity Analysis," *Structural and Multidisciplinary Optimization*, DOI: 10.1007/s00158-009-0372-6.

[46] Li, M., Williams, N., Azarm, S., Al Hashimi, S., Almansoori, A., and Al Qasas, N., 2009c, "Integrated Multi-Objective Robust Optimization and Sensitivity Analysis with Irreducible and Reducible Interval Uncertainty," *Engineering Optimization*, 41(10), pp. 889-908.

[47] Liu, H., Chen, W., and Sudjianto, A., 2006, "Relative Entropy Based Method for Global and Regional Sensitivity Analysis in Probabilistic Design," *Journal of Mechanical Design*, 128(2), pp. 1-11.

[48] Liao, Y.S. and Chiou, C.Y., 2008, "Robust Optimum Designs of Fibre-Reinforced Composites with Design-Variable and Non-Design-Variable Uncertainties," *Journal of Materials: Design and Applications*, 222(2), pp, 111-121.

[49] Magrab, E.B., Azarm, S., Balachandran, B., Duncan, J.H., Herold, K.E., and Walsh, G.C., 2005, *An Engineer's Guide to MATLAB, 2nd Edition*, Prentice-Hall, Upper Saddle River, NJ.

[50] Martin, J. D., and Simpson, T. W., 2005, "Use of Kriging Models to Approximate Deterministic Computer Models," *AIAA Journal*, 43(4), pp. 853-863.

[51] Martin, J. D., and Simpson, T. W., 2006, "A Methodology to Manage System-Level Uncertainty during Conceptual Design," *Journal of Mechanical Design*, 128(4), pp. 959-968.

[52] Miettinen, K., 1999, *Nonlinear Multi-Objective Optimization*, Kluwer Academic Publishers, Norwell, MA.

[53] Moeller, B., and Beer, M., 2008, "Engineering Computation under Uncertainty - Capabilities of Non-Traditional Models," *Computers & Structures*, 86(10), pp. 1024-1041.

[54] Moore, R. E. 1966, *Interval Analysis*, Prentice-Hall, Englewood Cliffs, NJ.

[55] Mourelatos, Z.P. and Zhou, J., 2006, "A Design Optimization Method Using Evidence Theory," *Journal of Mechanical Design*, 128(4), pp. 901-908.

[56] Noh, Y., Choi, K. K., and Lee, I., 2008, "MPP-Based Dimension Reduction Method for RBDO Problems with Correlated Input Variables," *Proceedings of the 12th AIAA/ISSMO Conference*, Victoria, BC, Canada.

[57] Noor, A. K., Starnes, J. H., and Peters, J. M., 2000, "Uncertainty Analysis of Composite Structures," *Computer Methods in Applied Mechanics and Engineering*, 185(2-4), pp. 413-432.

[58] Padula, S. L., Gumbert, C. R., and Li, W., 2006, "Aerospace Applications of Optimization under Uncertainty," *Optimization and Engineering*, 7(3), pp. 317-328.

[59] Qiu, Z., Hu, J., Yang, J., and Qishao, L., 2008, "Exact Bounds for the Sensitivity Analysis of Structures with Uncertain-But-Bounded Parameters," *Applied Mathematical Modeling*, 32(6), pp. 1143-1157.

[60] Qu, X., Haftka, R.T., Venkataraman, S., and Johnson, T.F., 2003, "Deterministic and Reliability-Based Optimization of Composite Laminates for Cryogenic Environments," *AIAA Journal*, 41(10), pp. 2029-2036.

[61] Rao, S. S., and Cao, L. T., 2002, "Optimum Design of Mechanical Systems Involving Interval Parameters," *Journal of Mechanical Design*, 124(3), pp. 465-472.

[62] Saltelli, A., Chan, K., and Scott, E. M., 2000, *Sensitivity Analysis*, John Wiley & Sons, New York, NY.

[63] Saltelli, A., Ratto, M., Andres, T., Campolongo, F., Cariboni, J., Gatelli, D., Saisana, M., and Tarantola, S., 2008, *Global Sensitivity Analysis: The Primer*, John Wiley & Sons, New York, NY.

[64] Schueller, G. I., and Jensen, H. A., 2008, "Computational Methods in Optimization Considering Uncertainties - an Overview," *Computer Methods in Applied Mechanics and Engineering*, 198(1), pp. 2-13.

[65] Shan, S. and Wang, G. G., 2008, "Survey of Modeling and Optimization Strategies for High-Dimensional Design Problems," *Proceedings of the 12th AIAA/ISSMO Conference*, Victoria, BC, Canada.

[66] Smith, N., and Mahadevan, S., 2005, "Integrating System-Level and Component-Level Designs under Uncertainty," *Journal of Spacecraft and Rockets*, 42, pp. 752-760.

[67] Sobieszczanski-Sobieski, J., 1990, "Sensitivity of Complex, Internally Coupled Systems," *AIAA Journal*, 28(1), pp.153-160.

[68] Sobieszczanski-Sobieski, J., Bloebaum, C., and Hajela, P., 1991, "Sensitivity of Control-Augmented Structure Obtained by a System Decomposition Method," *AIAA Journal*, 29(2), pp. 264-270.

[69] Sobol, I. M., 2001, "Global Sensitivity Indices for Nonlinear Mathematical Models and Their Monte Carlo Estimates," *Mathematics and Computers in Simulation*, 55(1-3), pp. 271-280.

[70] Srivastava, A., Hacker, K., and Lewis, K., 2004, "A Method for using Legacy Data for Metamodel-Based Design of Large-Scale Systems," *Structural and Multidisciplinary Optimization*, 28(2-3), pp. 146-155.

[71] Wang, G. G., and Shan, S., 2007, "Review of Metamodeling Techniques in Support of Engineering Design Optimization," *Journal of Mechanical Design*, 129(4), pp. 370-380.

[72] Wang, P., Youn, B. D., Xi, Z., and Kloess, A., 2009, "Bayesian Reliability with Evolving, Insufficient, and Subjective Data Sets," *Journal of Mechanical Design*, 131(11), pp. 111008/1-111008/11.

[73] Wehrhahn, E., 1991, "Hierarchical Sensitivity Analysis of Circuits," *IEEE International Symposium on Circuits and Systems*, pp. 864-867.

[74] Williams, N., Azarm, S., and Kannan, P. K., 2008, "Engineering Product Design Optimization for Retail Channel Acceptance," *Journal of Mechanical Design*, 130(6) pp. 061402/1-061402/10.

[75] Wu, W. D., and Rao, S. S., 2007, "Uncertainty Analysis and Allocation of Joint Tolerances in Robot Manipulators Based on Interval Analysis," *Reliability Engineering & System Safety*, 92(1), pp. 54-64.

[76] Yi, S. I, Shin, J. K., and Park, G. J., 2007, "Comparison of MDO methods with mathematical examples," *Structural and Multidisciplinary Optimization*, 35(5), pp. 391-402.

[77] Yin, X., and Chen, W., 2008, "A Hierarchical Statistical Sensitivity Analysis Method for Complex Engineering Systems Design," *Journal of Mechanical Design*, 130(7), 071402.

[78] Youn, B. D., and Wang, P., 2008, "Bayesian Reliability-Based Design Optimization using Eigenvector Dimension Reduction (EDR) Method," *Structural and Multidisciplinary Optimization*, 36(2), pp. 107-123.

[79] Yu, J. C., and Ishii, K., 1998, "Design for Robustness Based on Manufacturing Variation Patterns," *Journal of Mechanical Design*, 120, pp. 196-202.

[80] Zhang W. H., 2003, "On the Pareto Optimum Sensitivity Analysis in Multicriteria Optimization," *International Journal for Numerical Methods in Engineering*, 58(6), pp. 955-977.

[81] Zhou, J. and Mourelatos, Z.P., 2008, "A Sequential Algorithm for Possibility-Based Design Optimization," *Journal of Mechanical Design*, 130(1), pp. 011001/1-011001/10.